

Using Genetically Modified Mutant Mice to Model Autism Spectrum Disorder and Determine Its

Developmental Pathogenesis

by

Samuel William Hulbert

Department of Neurobiology  
Duke University

Date: \_\_\_\_\_

Approved:

\_\_\_\_\_  
Yong-hui Jiang, Supervisor

\_\_\_\_\_  
James McNamara

\_\_\_\_\_  
Fan Wang

\_\_\_\_\_  
Cagla Eroglu

Dissertation submitted in partial fulfillment of  
the requirements for the degree of Doctor  
of Philosophy in the Department of  
Neurobiology in the Graduate School  
of Duke University

2019

ABSTRACT

Using Genetically Modified Mutant Mice to Model Autism Spectrum Disorder and Determine Its

Developmental Pathogenesis

by

Samuel William Hulbert

Department of Neurobiology  
Duke University

Date: \_\_\_\_\_

Approved:

\_\_\_\_\_  
Yong-hui Jiang, Supervisor

\_\_\_\_\_  
James McNamara

\_\_\_\_\_  
Fan Wang

\_\_\_\_\_  
Cagla Eroglu

An abstract of a dissertation submitted in partial fulfillment of the requirements for the degree of Doctor of Philosophy in the Department of Neurobiology in the Graduate School of Duke University

2019

Copyright by  
Samuel William Hulbert  
2019

## Abstract

Numerous mouse models of autism spectrum disorder (ASD) have been generated to determine the molecular and circuit mechanisms underlying the condition. In this dissertation, I characterize the behavior of two mouse models mimicking some of the most common mutations found in human patients, which is an important step in establishing them as models.

One important application of mouse models is our ability to use them to test specific treatments in a preclinical setting. These treatments are primarily pharmacological in nature, but some work has also been done to test the effects of the environment on the presentation of phenotypes. In particular, environmental enrichment has been shown to prevent the manifestation of ASD-like behaviors in several different mouse models of the disorder. In this dissertation, I tested the effects of environmental enrichment on our *Shank3* mouse model of ASD and found that it did not rescue any of the behavioral phenotypes we previously observed, but rather exacerbated some common comorbidities.

More recently, methods have been developed to manipulate gene expression in mice over space and time and have been utilized to gain a clearer picture of the cell types, circuits, brain regions, and developmental time periods involved in autism spectrum disorder. I utilized conditional knockout technology to test whether behavioral phenotypes associated with ASD could be induced by deleting *Shank3* in adult and developing mice. We found that *Shank3* may play a role in development and that inducing mutations in adult mice is insufficient to cause ASD-like behaviors. Unfortunately, technical concerns limit our interpretation of the data, and this study adds to the growing concern of the limitations inherent in this technology.

## **Dedication**

This dissertation is dedicated to my brother, Jefferson Gregory Hulbert, who has a mild form of autism spectrum disorder, which helped start my interest in the topic. This dissertation is also dedicated to patients who have much more severe forms of the disorder, for which these studies are intended to benefit.

# Contents

Abstract .....	iv
List of Tables .....	xi
List of Figures .....	xii
Acknowledgements .....	xv
1. Introduction: Modeling autism spectrum disorder (ASD) in mice.....	1
1.1 Introduction to autism spectrum disorder .....	1
1.2 What constitutes a valid model for ASD? .....	6
1.3 Monogenic mouse models: common mechanisms and missing links .....	7
1.3.1 Epigenetic and transcriptional regulators .....	14
1.3.1.1 <i>Mecp2</i> (Rett syndrome) .....	14
1.3.1.2 <i>Chd8</i> (non-syndromic ASD) .....	17
1.3.2 Post-transcriptional protein modifiers and regulators .....	18
1.3.2.1 <i>Fmr1</i> (fragile X syndrome) .....	18
1.3.2.2 <i>Tsc1/Tsc2</i> (tuberous sclerosis complex) .....	21
1.3.2.3 <i>Pten</i> (PTEN hamartoma tumor syndromes and non-syndromic ASD) .....	23
1.3.2.4 <i>Ube3a</i> (Angelman syndrome and non-syndromic ASD) .....	25
1.3.3 Synaptic organizing and scaffolding .....	28
1.3.3.1 <i>Shanks</i> (Phelan-McDermid syndrome and non-syndromic ASD) .....	28
1.3.3.2 <i>Neurexins/Neuroligins</i> (non-syndromic ASD) .....	33
1.3.4 Convergent molecular pathways and mechanisms .....	37
1.4 Temporospacial manipulation of ASD-causing mutations and behavior.....	39
1.4.1 Assays for ASD-related behaviors .....	40

1.4.1.1 Tests to assess social communication .....	42
1.4.1.2 Tests to assess repetitive behavior .....	43
1.4.2 Tools to manipulate gene expression .....	44
1.4.3 The roles of excitatory and inhibitory neurons in ASD .....	46
1.4.3.1 Excitatory (glutamatergic) neurons .....	46
1.4.3.2 Inhibitory (GABA-ergic) neurons .....	48
1.4.4 Other neurotransmitter systems .....	50
1.4.5 The role of the cerebellum in ASD .....	52
1.4.6 Developmental time points implicated through inducible mutations and rescues .....	54
1.4.7 Conclusions from temporospatial manipulation of ASD-causing mutations .....	56
1.5 Attribution of work within this dissertation .....	67
2. Behavioral characterization of <i>Shank3</i> and <i>Chd8</i> conventional mutant mice .....	68
2.1 Introduction .....	68
2.2 Methods .....	69
2.2.1 Generation of mutant lines .....	69
2.2.2 Behavioral phenotyping .....	71
2.2.2.1 Cohorts for behavioral assays .....	71
2.2.2.2 Three chamber test for sociability and social novelty .....	73
2.2.2.3 Social dyadic .....	74
2.2.2.4 Adult ultrasonic vocalizations .....	74
2.2.2.5 Pup ultrasonic vocalizations .....	75
2.2.2.6 Neonatal nest preference .....	75
2.2.2.7 Self-grooming .....	75
2.2.2.8 Hole-board .....	76

2.2.2.9 Elevated zero maze .....	76
2.2.2.10 Dark-light emergence .....	76
2.2.2.11 Rotarod .....	76
2.2.2.12 Open field locomotion .....	77
2.2.2.13 Operant conditioning .....	77
2.3 Results .....	78
2.3.1 <i>Shank3</i> $\Delta e4-22^{-/-}$ mice have impaired social communication .....	78
2.3.2 The <i>Shank3</i> $\Delta e4-22^{+/+}$ phenotype is independent of parental origin.....	80
2.3.3 <i>Chd8</i> mutant mice present with alterations in USVs and motor function .....	86
2.4 Conclusions .....	102
3. Environmental enrichment has minimal effects on behavior in <i>Shank3</i> $\Delta e4-22^{-/-}$ mice.....	104
3.1 Introduction .....	104
3.2 Methods .....	105
3.2.1 Animals .....	105
3.2.2 Rearing conditions .....	105
3.2.3 Behavioral testing .....	106
3.2.4 Statistical analysis .....	108
3.3 Results .....	108
3.3.1 <i>Shank3</i> $\Delta e4-22^{-/-}$ display repetitive behaviors which are not ameliorated by early environmental enrichment .....	108
3.3.2 Early environmental enrichment does not affect spontaneous motor activity, but increases anxiety-like behavior irrespective of genotype .....	110
3.3.3 Early environmental enrichment has a negative impact on motor performance which is specific to wildtype mice .....	113
3.4 Conclusions .....	114

4. Incompletely disrupting Shank3 expression postnatally is insufficient to produce phenotypes associated with germline deficiency .....	126
4.1 Introduction .....	126
4.2 Methods .....	127
4.2.1 Animals .....	127
4.2.2 Tamoxifen Administration .....	128
4.2.3 Isolation of striatal postsynaptic density fractions .....	129
4.2.4 Quantitative immunoblot analysis .....	129
4.2.5 Antibodies .....	130
4.2.6 Behavioral phenotyping .....	130
4.2.6.1 Cohorts for behavioral assays .....	130
4.2.6.2 Open field locomotion .....	131
4.2.6.3 Self-grooming .....	131
4.2.6.4 Rotarod .....	131
4.2.6.5 Operant conditioning .....	131
4.2.6.6 Adult ultrasonic vocalizations .....	132
4.3 Results .....	132
4.3.1 Shank3 expression can be depleted in adult mice with limited efficiency .....	132
4.3.2 Adult knockout mice do not present with behavioral phenotypes that have been observed in germline knockout mice .....	133
4.3.3 Shank3 expression can be disrupted in developing mice with variable efficiency..	141
4.3.4 Disrupting Shank3 expression during an earlier period in development has minimal effects on behaviors associated with germline deficiency .....	143
4.4 Conclusions .....	150
5. Conclusion: Discussion and future directions .....	153

5.1 Different mouse models of ASD present with widely varying behavioral phenotypes...	153
5.2 Environmental enrichment can improve behavioral in some, but not all, mouse models of ASD .....	154
5.3 Limitations inherent in conditional knockout technology caution its future use .....	154
References .....	156
Biography .....	187

## List of Tables

Table 1: List of genes with strong evidence for syndromic and non-syndromic ASD.....	4
Table 2: Summary of cellular, molecular, and electrophysiological findings from monogenic mouse models of ASD.....	8
Table 3: Summary of behavioral assays.....	41
Table 4: Summary of transgenic mouse lines used for the temporospatial manipulation of ASD genes in the mouse brain.....	57
Table 5: Cohorts and order of behavior testing for <i>Shank3</i> and <i>Chd8</i> mutant mice.....	72
Table 6: Summary of behavioral phenotyping of <i>Chd8</i> mutant lines.....	87
Table 7: Representation of significant findings from <i>Chd8</i> behavioral phenotyping.....	92
Table 8: Order of behavioral tests for environmental enrichment cohorts and number of mice per group.....	107
Table 9: Summary of key findings from previous studies utilizing environmental enrichment and rodent models of ASD.....	115

## List of Figures

Figure 1: Generation of <i>Chd8</i> mutant mice.....	70
Figure 2: <i>Chd8</i> mutant mice are haploinsufficient for CHD8.....	71
Figure 3: <i>Shank3</i> $\Delta e4-22^{-/-}$ mice show abnormal social interaction in the social dyadic test.....	79
Figure 4: <i>Shank3</i> $\Delta e4-22^{-/-}$ mice show impairments in ultrasonic vocalizations.....	80
Figure 5: Heterozygous <i>Shank3</i> $\Delta e4-22$ mice show mild hypoactivity in the open field, regardless of the parental origin of the mutation.....	82
Figure 6: Parental origin of <i>Shank3</i> $\Delta e4-22$ mutation does not affect the lack of thigmotaxis phenotype in heterozygous mice.....	83
Figure 7: Parental origin of <i>Shank3</i> $\Delta e4-22$ mutation does not influence the tendency to spend more time in the open areas of the elevated zero maze.....	84
Figure 8: Parental origin of <i>Shank3</i> $\Delta e4-22$ mutation does not influence the neonatal nest preference test.....	85
Figure 9: Parental origin of <i>Shank3</i> $\Delta e4-22$ mutation does not influence performance on the accelerating rotarod.....	86
Figure 10: <i>Chd8</i> mutant mice are similar in body weights to their sex-matched wildtype littermates.....	93
Figure 11: <i>Chd8</i> mutant mice show normal levels of activity in the open field.....	94
Figure 12: <i>Chd8</i> mutant mice and their wildtype littermates spend similar amounts of time in the center of the open field.....	95
Figure 13: <i>Chd8</i> mutant mice do not show significant differences in the light-dark emergence task.....	96
Figure 14: <i>Chd8</i> mutant mice and their wildtype littermates spend similar amounts of time in the open areas of the elevated zero maze.....	97
Figure 15: <i>Chd8</i> mutant mice show altered ultrasonic vocalizations in adulthood.....	98
Figure 16: <i>Chd8</i> mutant mice show altered ultrasonic vocalizations as pups.....	99
Figure 17: <i>Chd8</i> mutant mice show normal rates of self-grooming behavior.....	100
Figure 18: <i>Chd8</i> mutant mice have improved performance on the rotarod.....	101

Figure 19: <i>Chd8</i> mutant mice show no deficits in the 3-chamber test.....	102
Figure 20: Grooming in <i>Shank3</i> $\Delta e4-22^{-/-}$ mice is elevated whether they are reared in standard or enriched environments.....	109
Figure 21: Back-to-back pokes on the hole-board test are increased in <i>Shank3</i> $\Delta e4-22^{-/-}$ mice, but there is no effect of environment.....	110
Figure 22: <i>Shank3</i> $\Delta e4-22^{-/-}$ mice display reduced spontaneous motor activity which is unaffected by rearing condition.....	111
Figure 23: Environmental enrichment decreases time spent in the center of the open field regardless of genotype.....	112
Figure 24: Environmental enrichment does not affect time spent in the open areas of the elevated zero maze.....	113
Figure 25: Environmental enrichment impairs performance on the accelerating rotarod specifically in wildtype mice.....	114
Figure 26: Quantification of Shank3 protein levels in adult knockout (AKO) mice.....	133
Figure 27: Self-grooming rates of Shank3 adult knockout, germline knockout, and control groups.....	134
Figure 28: Cumulative duration of ultrasonic vocalizations in Shank3 adult knockout, germline knockout, and control groups.....	135
Figure 29: Total distance traveled in the open field in Shank3 adult knockout, germline knockout, and control groups.....	136
Figure 30: Time spent in the center of the open field in Shank3 adult knockout, germline knockout, and control groups.....	137
Figure 31: Latency to fall off of the accelerating rotarod over four trials for Shank3 adult knockout, germline knockout, and control groups.....	138
Figure 32: Average latency to fall off of the accelerating rotarod over four trials for Shank3 adult knockout, germline knockout, and control groups.....	139
Figure 33: Lever presses per minute during a reward learning task over seven trials for Shank3 adult knockout, germline knockout, and control groups.....	140
Figure 34: Average lever presses per minute during a reward learning task over seven trials for Shank3 adult knockout, germline knockout, and control groups .....	141
Figure 35: Quantification of Shank3 protein levels in early postnatal knockout (EPKO) mice...142	

Figure 36: Self-grooming rates of Shank3 early postnatal knockout, germline knockout, and control groups.....	143
Figure 37: Cumulative duration of ultrasonic vocalizations in Shank3 early postnatal knockout, germline knockout, and control groups.....	144
Figure 38: Total distance traveled in the open field in Shank3 early postnatal knockout, germline knockout, and control groups.....	145
Figure 39: Time spent in the center of the open field in Shank3 early postnatal knockout, germline knockout, and control groups.....	146
Figure 40: Latency to fall off of the accelerating rotarod over four trials for Shank3 early postnatal knockout, germline knockout, and control groups.....	147
Figure 41: Average latency to fall off of the accelerating rotarod over four trials for Shank3 early postnatal knockout, germline knockout, and control groups.....	148
Figure 42: Lever presses per minute during a reward learning task over seven trials for Shank3 early postnatal knockout, germline knockout, and control groups.....	149
Figure 43: Average lever presses per minute during a reward learning task over seven trials for Shank3 early postnatal knockout, germline knockout, and control groups.....	150

## **Acknowledgements**

I would like to thank the past and present members of the Jiang laboratory for their support.

# **1. Introduction: Modeling autism spectrum disorder in mice**

Transgenic mice carrying mutations that cause autism spectrum disorder continue to be valuable for determining the molecular underpinnings of the disorder. Recently, researchers have taken advantage of such models combined with *Cre-loxP* and similar systems to manipulate gene expression over space and time. Thus, a clearer picture is starting to emerge of the cell types, circuits, brain regions, and developmental time periods underlying ASD. ASD-causing mutations have been restricted to or rescued specifically in excitatory or inhibitory neurons, different neurotransmitter systems, and cells specific to the forebrain, cerebellum, or striatum. In addition, mutations have been induced or corrected in adult mice, providing some evidence for the plasticity and reversibility of core ASD symptoms.

## ***1.1 Introduction to autism spectrum disorder***

Autism spectrum disorder (ASD) is primarily characterized by impairments in social communication and engagement in restricted, repetitive behaviors [1]. Common comorbidities include intellectual disability, epilepsy, anxiety, sleep disturbances, abnormal sensory processing, motor impairments, and gastrointestinal complaints [2]. ASD is heterogeneous in nature, as patients display a wide range of symptom severity and prognosis [3, 4], which is mirrored by hundreds of identified causal or potentially causal genetic variants [5, 6]. Unfortunately, most genetic mutations are rare or private (i.e. observed only in a single family). Both the phenotypic and genetic heterogeneity present significant obstacles to understanding the disorders and attempts to associate phenotypic severity with genetic differences have had mixed results [7, 8].

While genetics undoubtedly play a substantial role in ASD pathophysiology, the inexplicable phenotypic heterogeneity and incomplete concordance rates between monozygotic twins [9], suggest that non-genetic factors may also contribute to the etiology.

A recent survey indicates that 1 in 68 children in the United States are diagnosed with ASD, a drastic increase from previous estimates over the last few decades [10]. While there is considerable debate regarding the degree to which the increase in prevalence can be explained by broadened diagnostic criteria [11], increased awareness [12], or changes in environmental factors [13], there is nevertheless an ever-increasing urgency to determine the underlying pathophysiology and develop safe, cost-effective interventions for ASD to improve patient outcomes. Regardless of the source of the rising prevalence, it is an issue of great public health concern, as the lifetime cost of ASD-related care ranges from approximately \$1.4 million to \$2.2 million per individual [14].

Studies in human clinical populations have been and continue to be critical for understanding the genetic and non-genetic contributions to ASD [5]. However, animal models are needed determine the mechanisms leading to abnormal functioning. Although human brain imaging techniques have identified regions and circuits involved in the disorders [15], animal models provide opportunities for direct manipulation of these brain regions and circuits to test their precise functions. In current clinical practice, ASD is defined by behavioral symptoms that are uniquely human and there is no singular neuropathological hallmark identified so far that is pathognomonic, so it is challenging to determine the validity of an animal model of autism.

Nevertheless, recent successes in identifying genes implicated in ASD have paved the way to explore the neurobiology underlying the disorders using animal models.

Substantial progress has been made to understand the genetic causes of ASD. Genes implicated in syndromic forms of autism were first identified in the 1990s. Subsequent genomic copy number variant (CNV) analysis in the 2000s generated a list of rare but highly penetrant CNVs associated with ASD. Pathogenic CNVs are estimated to account for ~10% of non-syndromic ASD [16]. Most recently, whole exome and whole genome sequencing techniques have been utilized to identify rare de novo and inherited sequence variants in hundreds of genes from ASD subjects. Despite the inability to establish a causal role for the majority of these sequence variants, a subset of new genes have emerged as strongly causal because de novo loss-of-function and likely-gene-disrupting mutations are found in multiple affected patients and are absent in a large number of controls (Table 1). In other cases, mutations that likely disrupt protein function are found in genes that are implicated in other neuropsychiatric disorders. Functional annotation of these genes suggests the following molecular categories: 1) neuronal ion channels and receptors; 2) synapse-related cytoskeleton and scaffolding proteins; 3) epigenetic and transcriptional regulators; 4) post-translational protein modifiers and regulators. An important question is whether or not mutations in these genes share a common molecular and/or circuit-level mechanism underlying the pathophysiology of ASD. Modeling these mutations in animal models is essential to address this question.

**Table 1: List of genes with strong evidence for syndromic and non-syndromic ASD**

Syndromic ASD		Non-Syndromic ASD	
<u>Gene Name</u>	<u>Locus</u>	<u>Gene Name</u>	<u>Locus</u>
<a href="#">ADNP</a>	20q13.13	<a href="#">ASH1L</a>	1q22
<a href="#">ADSL</a>	22q13	<a href="#">ASXL3</a>	18q11
<a href="#">AHI1</a>	6q23.3	<a href="#">CACNA1H</a>	16p13.3
<a href="#">ALDH5A1</a>	6p22	<a href="#">CACNA2D3</a>	3p21.1
<a href="#">ANKRD11</a>	16q24.3	<a href="#">CHD2</a>	15q26
<a href="#">ARID1B</a>	6q25.1	<a href="#">CHD8</a>	14q11.2
<a href="#">ARX</a>	Xp22.	<a href="#">CNTN4</a>	3p26
<a href="#">ASXL3</a>	18q11	<a href="#">CNTNAP2</a>	7q35
<a href="#">CACNA1C</a>	12p13.3	<a href="#">CUL3</a>	2q36.2
<a href="#">CDKL5</a>	Xp22	<a href="#">DEAF1</a>	11p15.5
<a href="#">CHD2</a>	15q26	<a href="#">DSCAM</a>	21q22.2
<a href="#">CHD7</a>	8q12.2	<a href="#">DYRK1A</a>	21q22.13
<a href="#">CNTNAP2</a>	7q35-q36	<a href="#">GABRB3</a>	15q12
<a href="#">DHCR7</a>	11q13	<a href="#">GRIN2B</a>	12p12
<a href="#">DYRK1A</a>	21q22.13	<a href="#">GRIP1</a>	12q14.3
<a href="#">EHMT1</a>	9q34.3	<a href="#">KATNAL2</a>	18q21.1
<a href="#">FMR1</a>	Xq27.3	<a href="#">KDM5B</a>	1q32.1

Syndromic ASD		Non-Syndromic ASD	
<u>Gene Name</u>	<u>Locus</u>	<u>Gene Name</u>	<u>Locus</u>
<a href="#">HDAC4</a>	2q37.3	<a href="#">KMT2A</a>	11q23
<a href="#">KMT2A</a>	11q23	<a href="#">KMT2C</a>	7q36.1
<a href="#">MECP2</a>	Xq28	<a href="#">MED13L</a>	12q24.21
<a href="#">NIPBL</a>	5p13.2	<a href="#">MET</a>	7q31
<a href="#">PTEN</a>	10q23.3	<a href="#">MSNP1AS</a>	5p14.1
<a href="#">RAI1</a>	17p11.2	<a href="#">MYT1L</a>	2p25.3
<a href="#">SCN1A</a>	2q24.3	<a href="#">NRXN1</a>	2p16.3
<a href="#">SYNGAP1</a>	6p21.3	<a href="#">POGZ</a>	1q21.3
<a href="#">TSC1</a>	9q34	<a href="#">PTCHD1</a>	Xp22.11
<a href="#">TSC2</a>	16p13.3	<a href="#">RELN</a>	7q22
<a href="#">UBE3A</a>	15q11.2	<a href="#">SCN2A</a>	2q23
<a href="#">VPS13B</a>	8q22.2	<a href="#">SETD5</a>	3p25.3
		<a href="#">SHANK2</a>	11q13.3
		<a href="#">SHANK3</a>	22q13.3
		<a href="#">SUV420H1</a>	11q13.2
		<a href="#">SYNGAP1</a>	6p21.3
		<a href="#">TBR1</a>	2q24

## ***1.2 What constitutes a valid model for ASD?***

Animal models of psychiatric disorders have classically been evaluated on three criteria, which were first applied to mouse models of depression: construct, face, and predictive validity [17]. Ever since these criteria were articulated, they have been interpreted in a variety of ways [18], making it worth elaborating on their precise meanings and their relationships to animal models of ASD.

Construct validity, for our purposes, refers to the rationale behind the creation of the model and its ability to recapitulate the etiology of the disorder. For instance, a model of ASD with high construct validity mimics a genetic mutation that has been observed in affected human individuals, or at least has the same molecular consequences; this can perhaps more accurately be described as pathogenic validity [18]. The determination of construct validity is difficult for genes that have a complex structure at transcriptional level.

Face validity refers to the model's resemblance to the clinical features of the disorder, both in terms of behavioral symptoms and physiological biomarkers; this definition of face validity can be separated into ethological validity and biomarker validity [18]. Currently, ASD is diagnosed based solely on behavioral assessments, limiting discussion of face validity to the behavioral realm.

Finally, predictive validity refers to the model's ability to determine the effectiveness that interventions will have on a clinical population. A model of ASD with high predictive validity will respond (e.g. with a reduction in repetitive behaviors) to pharmaceuticals in a similar manner

to the patients they are intended to model. This is particularly challenging in autism models because there are no established treatment paradigms for the core symptoms in human autism clinics currently. Conceptually, interventions are not necessarily limited to drugs, but it is more difficult to assess the translational value of non-pharmacological therapies, such as environmental enrichment. Predictive validity can also refer to the penetrance of specific phenotypes, given a specific genetic mutation or other trigger [18], but these data are seldom reported.

### ***1.3 Monogenic mouse models: common mechanisms and missing links***

By far the most common animals used to model ASD are mice because of the well-established techniques to manipulate their genome and study brain function at several levels of analysis. As mammals, mice are genetically and biologically similar to humans, but their rapid reproduction and accelerated development allow for the testing of large numbers of animals at a relatively low cost. Various assays have been developed to test mice for behaviors that resemble the core features of autism [19], allowing researchers to determine the face validity of their models, but the translatability of these assays to humans is unknown.

Much of what we know about the underlying mechanism of ASD comes from detailed analysis of mouse models of syndromic autism, for which a genetic cause is clearly defined. Unfortunately, while patients with these disorders frequently meet the diagnostic criteria for ASD, autism is not always present and there are a variety of other symptoms related to abnormal brain function, making the results of these studies not necessarily generalizable to all ASD. Nevertheless, careful review of common findings in these models contributes to a basic understanding of the pathophysiology contributing to autistic behaviors. It should be noted that

there are other types of mouse models, including inbred strains, chromosomal CNVs, and environmentally induced models, but the biological mechanisms in these models are currently less understood. The models I selected to review are grouped by the reported function of the disrupted protein and the findings are summarized in Table 2.

**Table 2: Summary of Cellular, Molecular, and Electrophysiological Findings From Monogenic Mouse Models of ASD**

Gene	Molecular Changes	Cellular and Spine Morphology	Electrophysiology
<i>Mecp2</i>	↓BDNF, ↓RNA splicing	<p><i>Mecp2</i><sup>tm1.1Bird</sup> CTX: ↓spine density, ↓dendritic complexity</p> <p><i>Mecp2</i><sup>tm1.1Jae</sup> CTX: ↓spine density</p> <p><i>Mecp2</i><sup>tm1.1Jae</sup> CA1: ↓cell size</p> <p><i>Mecp2</i><sup>tm1.1Jae</sup> p7 CA1: ↓spine density</p> <p><i>Mecp2</i><sup>tm1.1Jae</sup> SCX: ↑spine stability (p25-p26)</p> <p><i>Mecp2</i><sup>tm1.1Bird</sup> PNC: ↓glutamatergic synapses</p>	<p><i>Mecp2</i><sup>tm1.1Bird</sup> CA1: ↓LTP, ↓NMDA LTD</p> <p><i>Mecp2</i><sup>tm1.1Bird</sup> PNC: ↓mEPSC freq, ↓eEPSC amp</p> <p><i>Mecp2</i><sup>tm1.1Jae</sup> CA1: ↓LTP, ↓NMDA LTD</p> <p><i>Mecp2</i><sup>tm1.1Jae</sup> SCX: ↓mEPSC amp</p> <p><i>Mecp2</i><sup>tm1.Hzo</sup> CA1: ↓LTP, ↓NMDA LTD</p> <p><i>Mecp2</i><sup>tm1.Hzo</sup> SCX: ↓LTP</p> <p><i>Mecp2</i><sup>tm1.Hzo</sup> PMC: ↓LTP</p>
<i>Chd8</i>	↑Wnt signaling, ↑REST	IUE KD: ↓Axonal and dendritic growth	<p>exon 1 7nt del MSNs NAc: ↑sEPSC freq, ↑sEPSC amp, ↓mIPSC amp</p> <p><i>Chd8</i><sup>+N2373K</sup> CA1: ↓mIPSC amp, ↑mIPSC freq (females only), ↓mIPSC freq (males only)</p>
<i>Fmr1</i>	↑mGluR5 signaling, ↑mRNA translation, ↓NLGN1, ↑Shank1	<p>SCX: ↑spine density, ↓spine stability (p10-p12), ↓mature spines</p> <p>CA1: ↓mature spines</p>	<p>SCX: ↓LTP</p> <p>CA1: ↓LTP, ↑mGluR LTD</p> <p>p14 CA1: ↓AMPA/NMDA, ↑NMDA LTP</p> <p>PC: ↑mGluR LTD</p>

Gene	Molecular Changes	Cellular and Spine Morphology	Electrophysiology
<i>Tsc1/Tsc2</i>	↑mTORC1 signaling, ↑activated Rheb	<b>Tsc1/Tsc2 PNC KD:</b> ↓spine density, ↑spine size, ↑soma size <b>Tsc1<sup>fl/fl</sup> + viral Cre CA1:</b> ↑soma size <b>Tsc2<sup>+/-</sup> CTX:</b> ↑spine density, ↑spine stability	<b>Tsc1 OT KD:</b> ↑mEPSC amp, ↑AMPA/NMDA <b>Tsc1<sup>fl/fl</sup> + viral Cre CA1:</b> ↓mGluR LTD, ↓mEPSC freq, ↑AMPA, ↑NMDA <b>Tsc1<sup>fl/fl</sup> + viral Cre</b> <b>PNC GABAergic:</b> ↓eIPSC amp, ↓mPSC amp <b>Tsc2<sup>+/-</sup> CA1:</b> ↓mGluR LTD
<i>Pten</i>	↑Akt signaling, ↑mTORC1 signaling, ↓mGluR5, ↑FMRP, ↑p-FMRP	<b>DG:</b> ↑cell size, ↑axonal processes, ↑ectopic projections, ↑presynaptic vesicles, ↑spine density, ↑spine size, ↑mature spines <b>CTX:</b> ↑cell size, ↑presynaptic vesicles, ↑PSD size <b>CGC:</b> ↑cell size, ↑presynaptic vesicles, ↑spine density	<b>Pten<sup>+/-</sup> CA1:</b> ↓LTP, ↓NMDA LTD <b>Pten<sup>fl/fl</sup> + CamKIIa-Cre CA1:</b> ↓LTP, ↓NMDA LTD <b>Pten<sup>fl/fl</sup> + GFAP-Cre CA1:</b> ↓NMDA LTD <b>Pten<sup>fl/fl</sup> + Nse-Cre DG:</b> ↓mGluR LTD
<i>Ube3a</i>	<b>m-/p+:</b> ↑Arc, ↓Mecp2 function, ↓BDNF signaling <b>2xTg:</b> ↓Arc	<b>m-/p+ CA1:</b> ↓spine density <b>m-/p+ CTX:</b> ↓apical dendrite length <b>m-/p+ PVC:</b> ↓spine density	<b>m-/p+ CA1:</b> ↓LTP, ↑mGluR LTD, ↓AMPA/NMDA <b>m-/p+ PVC:</b> ↓LTP, ↓NMDA LTD <b>m-/p+ DMS:</b> ↓mEPSC amp, ↓mEPSC freq <b>2xTg BC:</b> ↓eEPSC amp, ↓sEPSC amp, ↓sEPSC freq, ↓sIPSC amp, ↓mEPSC amp, ↓mEPSC freq
<i>Shank1</i>	<b>HS:</b> ↓Homer, ↓SAPAP	<b>CA1:</b> ↓spine density, ↓spine length, ↓PSD thickness	<b>CA1:</b> ↓excitatory synaptic strength, ↓mEPSC freq

Gene	Molecular Changes	Cellular and Spine Morphology	Electrophysiology
<i>Shank2</i>	<p><b>Δe7 HS:</b> ↑NMDA</p> <p><b>Δe7 SS:</b> ↑AMPA, ↑Shank3</p> <p><b>Δe6-7 WB:</b> ↑NMDA, ↓NMDA signaling</p>	<p><b>Δe7 CA1:</b> ↓spine density</p>	<p><b>Δe7 CA1:</b> ↓excitatory synaptic strength, ↓mEPSC frequency, ↓AMPA/NMDA, ↑LTP</p> <p><b>Δe6-7 CA1:</b> ↑AMPA/NMDA, ↓LTP, ↓NMDA LTD</p>
<i>Shank3</i>	<p><b>Δe4-9<sup>J</sup> HPSD:</b> ↓Homer1b/c, ↓GluA1, ↓GluN2A, ↓SAPAP1</p> <p><b>Δe4-9<sup>P</sup> SS:</b> ↓Homer1b/c, ↓PSD-95, ↓GluA2, ↓GluA3</p> <p><b>Δe11 SS:</b> ↑Shank2, ↑GluN2B</p> <p><b>Δe13-16 SPSD:</b> ↓SAPAP3, ↓Homer, ↓PSD-93, ↓GluA2, ↓GluN2A, ↓GluN2B</p> <p><b>Δe21 HS:</b> ↑mGluR5</p> <p><b>Δe21 PFC:</b> ↓Rac1/PAK signaling, ↑active cofilin, ↓F-actin</p>	<p><b>Δe13-16 DLS:</b> ↓spine density, ↑dendritic complexity, ↓PSD thickness</p> <p><b>Δe4-9<sup>J</sup> 4 week CA1:</b> ↓spine density, ↑spine length</p> <p><b>Δe4-9<sup>J</sup> 10 week CA1:</b> ↓spine length</p>	<p><b>Δe9 CA1:</b> ↑mIPSC freq</p> <p><b>Δe9 PFC:</b> ↓mIPSC freq</p> <p><b>Δe4-9<sup>J</sup> CA1:</b> ↓LTP</p> <p><b>Δe4-9<sup>P</sup> CA1:</b> ↓LTP</p> <p><b>Δe4-9<sup>P</sup> DLS:</b> ↑AMPA/NMDA</p> <p><b>Δe4-9<sup>B</sup> CA1:</b> ↓LTP, ↓excitatory synaptic strength, ↓mEPSC amp, ↑mEPSC freq</p> <p><b>Δe13-16 DLS:</b> ↓excitatory synaptic strength, ↓mEPSC freq, ↓mEPSC amp</p> <p><b>Δe21 CA1:</b> ↓LTP, ↓excitatory synaptic strength, ↑AMPA/NMDA, ↓mEPSC freq</p> <p><b>Δe21 PFC:</b> ↑AMPA/NMDA</p> <p><b>21insG CA1:</b> ↓LTD, ↓excitatory synaptic strength, ↑AMPA/NMDA, ↓mEPSC freq</p>
<i>Nrxn</i> family	<p><b>ΔNrxn2a HL:</b> ↓Munc18-1</p>	<p><b>ΔCntnap4 GABAergic synapses:</b> ↓PSD length, ↑cleft width</p>	<p><b>ΔNrxn1α CA1:</b> ↑mEPSC freq, ↓excitatory synaptic strength</p> <p><b>DN-Nrxn1β SCX:</b> ↓mEPSC freq, ↓mIPSC freq</p> <p><b>ΔCntnap4 NAc:</b> ↑DA release</p>

Gene	Molecular Changes	Cellular and Spine Morphology	Electrophysiology
			<b>ΔCntnap4 SCX:</b> ↓sIPSC freq, ↓sIPSC amp, ↓sIPSC kinetics
<i>Nlgn</i> family	<p><b>ΔNlgn2 WB:</b> ↓CSP, ↓Liprin, ↓Munc-18, ↓Nrxn<math>\alpha</math>, ↓Nrxn<math>\beta</math>, ↑Nlgn3, ↑Synapsin1a</p> <p><b>ΔNlgn2 CA1:</b> ↓VGAT</p> <p><b>R451C Nlgn3 WB:</b> ↑VGAT, ↑Gephyrin</p> <p><b>R451C Nlgn3 HL:</b> ↓PSD95, ↓SAP102, ↓NR2A, ↓NR2B</p>	<p><b>sparse Nlgn2 KD CTX:</b> ↓synaptic density</p> <p><b>R451C Nlgn3 KI CA1:</b> ↑dendritic complexity, ↓synaptic terminal size, ↓synaptic vesicles, ↓spine size</p> <p><b>R451C Nlgn3 KI AFC:</b> ↑spine turnover</p>	<p><b>ΔNlgn1 CA1:</b> ↓LTP, ↓AMPA EPSCs, ↓NMDA EPSCs, ↑AMPA/NMDA EPSCs, ↑AMPA/NMDA</p> <p><b>ΔNlgn1 AMG TI:</b> ↓LTP</p> <p><b>ΔNlgn4:</b> ↓excitatory network excitability, ↓inhibitory network excitability, ↓E/I</p> <p><b>R451C Nlgn3 KI SCX:</b> ↑mIPSC freq, ↑eIPSC amp,</p> <p><b>R451C Nlgn3 KI BC:</b> ↓eIPSC amp</p> <p><b>R451C Nlgn3 KI CA3:</b> ↑GDPs freq, ↑mIPSC freq</p> <p><b>R451C Nlgn3 KI CA1:</b> ↑LTP, ↓AMPA/NMDA</p> <p><b>R451C Nlgn3 KI CCK:</b> ↑eIPSC amp, ↓tonic ECB</p> <p><b>ΔNlgn3 CCK:</b> ↑eIPSC amp, ↓tonic ECB</p> <p><b>ΔNlgn3 D1-MSNs NAc:</b> ↓mIPSC freq, ↑E/I</p>

**Legend:**

↓, decreased;

↑, increased;

Δ, deletion;

Δ4-9<sup>B</sup>, Shank3 model created by Bozdagi et al., 2010;

Δ4-9<sup>J</sup>, Shank3 model created by Wang et al., 2011;

Δ4-9<sup>P</sup>, Shank3 model created by Jaramillo et al., 2015;

AAV, adeno-associated virus

AFC, anterior frontal cortex;

AMG TI, thalamic inputs to the amygdala;

amp, amplitude;

AMPA, α-amino-3-hydroxy-5-methyl-4-isoxazolepropionic acid;

AMPA/NMDA, ratio of AMPA-induced to NMDA-induced current

BC, barrel cortex;

BDNF, brain-derived neurotrophic factor;

CA1, region of the hippocampus;

CA3, region of the hippocampus;

CCK, cholecystokinin basket cells

CGC, cerebellar granule cells;

CTX, cortex;

DA, dopamine;

DG, dentate gyrus;

DLS, dorsolateral striatum;

DMS, dorsomedial striatum;

ECB, endocannabinoid

eEPSC, evoked excitatory postsynaptic current;

eIPSC, evoked inhibitory postsynaptic current;

E/I, excitation-inhibition ratio;

GDPs, giant depolarizing potentials

freq, frequency;

HL, hippocampal lysate;

HPSD, hippocampal postsynaptic density fraction;

HS, hippocampal synaptosomal fraction;

IUE, in utero electroporation;

KD, knockdown;

KI, knock-in;

LTD, long-term depression

NMDA LTD, NMDA-dependent LTD

mGluR5 LTD, mGluR5-dependent LTD

LTP, long-term potentiation;

mEPSC, miniature excitatory postsynaptic current;

mGluR5, metabotropic glutamate receptor;

mIPSC, miniature inhibitory postsynaptic current;

NAc, nucleus accumbens;

NMDA, N-methyl-D-aspartate;

OT, organotypic;  
p7, postnatal day 7;  
p14, postnatal day 14;  
PC, Purkinje cells;  
PMC, primary motor cortex;  
PNC, primary neuron culture;  
PVC, primary visual cortex;  
sIPSC, spontaneous inhibitory postsynaptic current  
SCX, somatosensory cortex;  
SPSD, striatal postsynaptic density fraction;  
SS, striatal synaptosomal fraction;  
WB, whole brain

### **1.3.1 Epigenetic and transcriptional regulators**

#### **1.3.1.1 *Mecp2* (Rett syndrome)**

A number of genes classified as transcriptional or epigenetic regulators have been implicated in ASD [20]. These genetic findings support a molecular mechanism involving transcriptional regulation underlying the pathogenesis of ASD. One of the best characterized genes in this category is *MECP2*, a gene encoding a methylated DNA-binding protein [21, 22]. Although the protein was characterized as a transcriptional repressor when it was first identified [23], data from more recent studies indicate that MeCP2 acts as a global transcriptional regulator

involved in both the suppression and activation of targeted genes [24, 25], as well as a regulator of RNA splicing [26, 27].

More than 10 distinct lines of *Mecp2* mutant mice have been produced. Mice with the deletion of exon 3 (*Mecp2*<sup>tm1.1Jae</sup>; [28]), deletion of exons 3 and 4 (*Mecp2*<sup>tm1.1Bird</sup>; [29]), and a 308X point mutation (*Mecp2*<sup>tm1Hzo</sup>; [30]) are among the best characterized. The complete loss of both MeCP2 protein isoforms were revealed in hemizygous males (*Mecp2*<sup>-y</sup>) of *Mecp2*<sup>tm1.1Jae</sup> and *Mecp2*<sup>tm1.1Bird</sup> mutants, whereas the 308X mutation in *Mecp2*<sup>tm1Hzo</sup> mice introduces a premature stop codon that leads to truncation of the MeCP2 protein [30]. It should be noted that female heterozygous mice (*Mecp2*<sup>+/-</sup>) are the model with best construct validity, as Rett syndrome primarily affects females and is lethal in males in most cases. However, most studies use hemizygous male mice because they develop more severe phenotypes. An important question that remains is why humans are more sensitive than rodents to *MECP2* mutations.

Cellular and molecular abnormalities have been identified in *Mecp2* mutant mice that likely contribute to the ASD-like phenotypes. Both *Mecp2*<sup>tm1.1Bird</sup> and *Mecp2*<sup>tm1.1Jae</sup> mice have cortical neurons with decreased spine density [31], and *Mecp2*<sup>tm1.1Bird</sup> mice have decreased dendritic complexity [32]. Similar results have been reported in *Mecp2*<sup>tm1.1Jae</sup> hippocampus [33], but this varies across development: spine density is decreased at postnatal day seven but returns to wild type levels by postnatal day 15 [34]. Moreover, adult *Mecp2*<sup>tm1Hzo</sup> mice have normal spine density and dendritic complexity in both cortex and hippocampus [35]. More recently, it was demonstrated that neurons in somatosensory cortex of *Mecp2*<sup>tm1.1Jae</sup> mice are more stable than controls at postnatal day 25–26 (P25–P26), as assessed by *in vivo* two-photon imaging [36].

The electrophysiological consequences of MeCP2 dysfunction have also been examined. Reduced long-term potentiation (LTP) and long-term depression (LTD) have been reported in hippocampal CA1 synapses in both *Mecp2*<sup>tm1.1Bird</sup> and *Mecp2*<sup>tm1.1Jae</sup> mice [37], as well as *Mecp2*<sup>tm1Hzo</sup> mice [35]. Recordings from sensory and motor cortex from *Mecp2*<sup>tm1Hzo</sup> mice also revealed reduced LTP [35]. Whole-cell patch-clamp recordings from pyramidal neurons in brain slices of somatosensory cortex from *Mecp2*<sup>tm1.1Jae</sup> mice revealed reduced spontaneous activity due to a significant reduction in the amplitude of miniature excitatory postsynaptic currents (mEPSCs) and an insignificant increase in the amplitude of miniature inhibitory postsynaptic currents (mIPSCs; [38]). Similarly, decreased frequency of mEPSCs and amplitude of evoked EPSCs have also been observed in cultured neurons from *Mecp2*<sup>tm1.1Bird</sup> mice and are associated with decreased numbers of glutamatergic synapses on individual neurons [39].

How the deficiency of MeCP2 results in abnormal functioning of neuronal synapses as well as ASD-like phenotypes is still not fully understood. Hundreds of genes are dysregulated in both directions in brains of *Mecp2* mutant mice. These genes are promising candidates to dissect the molecular mechanism underlying the deficiency of *Mecp2* in neurons or synapses. One such candidate is BDNF, a neurotrophic factor that is down-regulated in MeCP2-deficient neurons. Not only do decreases in BDNF expression correlate with symptom severity [40], but treatments that increase BDNF also improve symptoms [41, 42]. Additionally, a non-pharmacological intervention – environmental enrichment, which improves synaptic and behavioral phenotypes in *Mecp2* mutant mice – is associated with increased expression of BDNF [43].

### 1.3.1.2 *Chd8* (non-syndromic ASD)

Another epigenetic regulator implicated in ASD is CHD8, a member of the chromodomain helicase DNA-binding protein family, which functions as an ATP-dependent chromatin remodeling factor and plays important roles in chromatin dynamics, transcription, and cell survival [44]. CHD8 was initially identified as a negative regulator of the Wnt–catenin signaling pathway through promotion of the association between  $\beta$ -catenin and histone H1 and forming a trimeric complex on chromatin [45-47]. Accordingly, Wnt– $\beta$ -catenin signaling is downregulated in *Chd8* mutant mice [47]. Haploinsufficiency of *Chd8* also causes abnormal activation of RE-1 silencing transcription factor (REST), which suppresses the transcription of many neuronal genes.

Homozygous deletion of *Chd8* in mice results in early embryonic lethality as a consequence of massive apoptosis [48, 49], but several different heterozygous mutant mice have been created with various behavioral phenotypes. Haploinsufficient mutant mice have strong construct validity for the human condition, as many patients with ASD have presumed loss-of-function *CHD8* mutations. However, the transcriptional complexity of *CHD8* may be underestimated, which could account for the difference in phenotypes in humans with mutations in different parts of the gene, as well as the differences in behavioral phenotypes presented in different *Chd8* mutant mouse lines.

Cellular and spine morphology have not been reported in *Chd8* mutant mice, but knockdown of *Chd8* via in utero electroporation results in reduced axonal and dendritic growth [50]. More work has been done to show deficits in neuronal function in *Chd8* mutant mice.

Germline haploinsufficient mice generated by a seven-nucleotide deletion in exon 1 by CRISPR/Cas9 show increased frequency and amplitude of spontaneous excitatory postsynaptic currents (sEPSCs) along with reduced amplitude of mIPSCs in medium spiny neurons of the nucleus accumbens [51]. However, mice with a frameshift mutation in exon 36 (*Chd8*<sup>+N2373K</sup>) show sexually dimorphic changes in CA1 pyramidal neurons of the hippocampus [52]. Male mutant mice have decreased mIPSC frequency, whereas female mutant mice have increased mIPSC frequency [52]. There is main effect of genotype (i.e. not sexually dimorphic, and a reduction) on the amplitude of mIPSCs [52].

### **1.3.2 Post-transcriptional protein modifiers and regulators: *Fmr1*, *Tsc1/2*, *Ube3a*, and *Pten***

#### **1.3.2.1 *Fmr1* (fragile X syndrome)**

Fragile X syndrome (FXS), primarily affecting males, also has phenotypic overlap with ASD and is caused by extended CGG trinucleotide repeats in the 5' untranslated region of *FMR1* [53, 54]. Such mutations lead to hypermethylation of the *FMR1* promoter, which transcriptionally silences the fragile X mental retardation protein (FMRP), an RNA binding protein involved in suppressing activity-dependent translation of synaptic proteins, many of which have been independently implicated in ASD [55]. Under normal conditions, FMRP is dephosphorylated after activation of metabotropic glutamate receptors (mGluRs), leading to de-repression of local translation (reviewed in [56]). Extended CGG repeats in *Fmr1* in mice do not recapitulate the hypermethylation and transcriptional silencing of FMRP that is characteristic of human fragile X [57]. However, researchers have mimicked the molecular consequences of the human mutation by

deleting exon 5 [58] or exon 1 [59] of *Fmr1*. Almost all data related to fragile X syndrome mouse models in the literature have been generated from the exon 5 deletion mutant mice, but whereas both models have complete loss of FMRP expression, only the model produced by deleting exon 1 has no detectable *Fmr1* mRNA and is conducive to conditional knockout studies.

Many studies have reported differences in dendritic spines in *Fmr1* knockouts. The first study reported that the cortical neurons have increased numbers of spines in adult mice, most of which morphologically resemble immature spines [60]. Since then, there have been conflicting reports regarding spine density in various brain regions and periods of development, but the immature morphology of spines is a relatively consistent finding (reviewed in [61]). Using *in vivo* two-photon imaging, researchers recently have found increased turnover in dendritic spines from *Fmr1* knockout mice in layer 2/3 neurons in the barrel cortex at P10–P12 [62] and in layer 5 neurons in primary somatosensory cortex at P20–P30 [63]. Together, these findings suggest that FMRP is required for the development of mature, stable dendritic spines.

In addition to dendritic spine morphology and stability, synaptic plasticity has been well characterized in FXS mouse models (reviewed in [64]; [65]). Initial studies reported no change in LTP [66, 67], but a significant enhancement in mGluR-dependent LTD in the hippocampus [68]. More recently, impaired LTP was reported in hippocampal CA1 synapses using threshold-level stimulation parameters, which are thought to more closely mimic *in vivo* conditions [69, 70]. Furthermore, a transient decrease (at postnatal day 14) in the AMPA/NMDA receptor ratio and an increase in NMDA-dependent LTP in hippocampal neurons has been observed [71]. Reduced LTP has also been reported in somatosensory cortical synapses [72], and increased mGluR-

dependent LTD has been reported in cerebellar Purkinje cells [73]. Therefore, like spine morphology, electrophysiological consequences of *Fmr1* knockout vary across brain regions and development, but increased mGluR-dependent LTD seems to be a relatively consistent finding.

The enhanced mGluR-mediated LTD observed in *Fmr1* knockouts [68] paved the way for the mGluR theory for FXS pathogenesis, which posits that FXS symptoms are caused by mGluR5 signaling leading to deregulated mRNA translation in the absence of FMRP [74]. This theory has been supported by the effectiveness of genetic depletion of mGluR5 [75] and mGluR5 negative allosteric modulators (e.g. CTEP) [76] in alleviating behavioral and synaptic abnormalities in *Fmr1* knockout mice. While neither of these studies included analysis of repetitive behaviors or social interactions, negative allosteric modulation of mGluR5 decreased repetitive behaviors and increased sociability of a different mouse model of ASD: the BTBR inbred strain [77]. However, the mGluR5 signaling pathway is not the only molecular cascade that results in FMRP de-repression and subsequent dysregulated translation. For instance, the BDNF/TrkB signaling pathway converges with the mGluR5 pathway to initiate translation (reviewed in [78]). It remains to be determined whether dysregulation of the BDNF/TrkB signaling pathway, the mGluR5 pathway, or another pathway entirely contributes to the ASD-like behaviors in FXS mouse models. There is some evidence which suggests that social deficits in mice lacking FMRP are due to decreased neuroligin1 expression and can be rescued by overexpressing neuroligin1 [79]. Additionally, mice lacking FMRP exhibit elevated postsynaptic Shank1 levels, along with a number of other synaptic proteins [80], but more work needs to be

done to confirm these results and determine whether or how these changes may lead to changes in behavior.

### 1.3.2.2 *Tsc1/Tsc2* (Tuberous sclerosis complex)

Tuberous sclerosis complex (TSC) is a disorder characterized by the formation of benign tumors, intellectual disability, epilepsy, infantile spasm, and ASD [81]. Heterozygous mutations in either *TSC1* or *TSC2* genes that encode the proteins hamartin and tuberin, respectively, are sufficient to cause TSC [82, 83]. Hamartin and tuberin form a heterodimer that negatively regulates the mTORC1 (mammalian target of rapamycin complex 1) signaling cascade by inactivating the small G protein Rheb [84]. The mTORC1 signaling cascade has been implicated in cell growth and proliferation [85] and in synaptic plasticity [86].

Homozygous deletion of *Tsc1* exons 6–8 [87], *Tsc1* exons 17–18 [88], *Tsc1* exons 5–7 [89], *Tsc2* exon 2 [90], or *Tsc2* exons 2–5 [91] in mice all result in embryonic lethality. However, heterozygous mice (*Tsc1*<sup>+/-</sup> or *Tsc2*<sup>+/-</sup>) from these constructs recapitulate many of the phenotypes of TSC observed in humans, including ASD-like behaviors (reviewed in [92]).

Depletion of *Tsc1* or *Tsc2* in cultured post-mitotic hippocampal neurons results in increased soma size, decreased dendritic spine density, and increased spine size [93]. However, loss of *Tsc1* in hippocampal neurons *in vivo* via viral delivery of Cre recombinase, soma size is increased but there is no significant change in spine density [94]. On the other hand, *Tsc2*<sup>+/-</sup> mice have normal spine density in cortical projection neurons at P19–P20, but increased spine density at P29–P30, suggesting a synaptic pruning defect [95]. Thus, whereas the effects of *Tsc1/2* loss

on spine density vary developmentally and across brain regions, soma size is consistently increased.

Decreased expression of *Tsc1* or *Tsc2* has drastic impacts on synaptic function as well, but the findings vary between *in vivo* and *in vitro* experiments, suggesting non-cell-autonomous and network effects. Organotypically cultured hippocampal neurons lacking *Tsc1* have higher amplitudes in mEPSCs and increased AMPA/NMDA current ratios [93]. However, loss of *Tsc1* in hippocampal CA1 neurons *in vivo* impairs mGluR-dependent LTD, decreases the inter-event-interval (a measure of frequency) in mEPSCs without changing mEPSC amplitude, and increases evoked AMPA and NMDA currents proportionally [94]. Mice haploinsufficient for *Tsc2* also have impaired mGluR-dependent LTD [96]. Additionally, knockout of *Tsc1* in primary hippocampal cultures has no effect on mEPSC amplitude in glutamatergic neurons, but whole cell voltage clamp analysis of GABAergic neurons shows a decrease in evoked IPSC (eIPSC) and mIPSC amplitudes [97].

At the cellular level, loss-of-function mutations in *Tsc1* and *Tsc2* lead to hyperactivation of mTORC1, which is one of the major mechanisms for TSC pathogenesis (reviewed in [98]). This mechanism overlaps with other known genetic causes of ASD. For example, long-term potentiation initiated by BDNF is dependent on mTOR signaling [99]. Additionally, as the mTOR pathway is involved in protein translation, it is hyperactivated in FXS [100]. However, *Tsc2*<sup>+/-</sup> mice show reduced protein synthesis, whereas *Fmr1*<sup>-/-</sup> mice have increased protein synthesis [96]. One possible explanation for the different effects on protein synthesis is that Rheb has functions other than to negatively regulate mTORC1 activity, which is evident by the fact that inhibition of

Rheb, but not inhibition of mTORC1, rescues the aberrant spine morphogenesis observed in *Tsc2*<sup>+/-</sup> neurons [101]. More work needs to be done to determine whether ASD-like phenotypes in TSC mouse models are the result from disrupted mTORC1-dependent or mTORC1-independent signaling pathways.

### **1.3.2.3 *Pten* (PTEN hamartoma tumor syndromes and non-syndromic ASD)**

Mutations in phosphatase and tensin homolog (*PTEN*) were first identified in a number of patients with different conditions (reviewed in [102]), together called PTEN hamartoma tumor syndromes (PHTS). Although relatively rare, *PTEN* mutations are consistently identified in non-syndromic ASD comorbid with significant macrocephaly [103, 104], a feature observed in approximately 20% of all ASD cases [105, 106]. The *Pten* protein normally functions as a protein and lipid phosphatase that negatively regulates the Akt signaling pathway, particularly by dephosphorylating phosphatidylinositol (3, 4, 5)-triphosphate (PIP3) [107]. Tuberin, the protein product of *Tsc2*, is one target of the Akt signaling pathway [108], which is inhibited following phosphorylation by Akt [109]. Thus, the PI3K/Akt signaling pathway increases mTORC1 activity and *Pten*, like the *Tsc1* and *Tsc2* products, normally inhibits mTORC1 activity.

The first *Pten* knockout mouse models showed that homozygous deletion of exons 4 and 5 [110] or exons 3, 4, and 5 [111] results in embryonic lethality, whereas heterozygous deletions result in widespread tumorigenesis, resembling PHTS. More recently, conditional *Pten* knockouts have been developed that more closely resemble PTEN-related ASD. Although these models do not have good construct validity because humans with PTEN-related ASD have germline missense mutations in *PTEN*, the various models provide insight into different brain regions and

cell types involved in ASD. Mice with *Pten* deleted selectively in a subset of mature neurons in cortex and hippocampus (*Nse-Cre*) show deficits in social interactions [112] and increased repetitive behaviors [113]. Similar behaviors have been observed in mice with *Pten* deleted in granule cells of the cerebellum and neurons in the dentate gyrus of the hippocampus (*Gfap-Cre*) [114]. Another mouse model of PTEN-related ASD (*Pten<sup>m3m4</sup>*) was created by knocking in missense mutations which decrease the amount of nuclear Pten [115]. Interestingly, only male mice with the missense mutations display increased social behavior, as opposed to the decreased social behavior observed in other mouse models of ASD [115]. While these particular missense mutations have not yet been reported in humans, mutations that similarly affect the subcellular localization of PTEN have been observed in PTHS patients.

Detailed studies of the PTEN-related ASD mouse models have revealed several cellular structural abnormalities. Generally, neuronal cells lacking Pten have increased size, more abundant and ectopic axonal projections, increased numbers of presynaptic vesicles, increased numbers of dendritic spines, and larger postsynaptic densities [112, 116-118]. However, one study suggests that overall numbers of dendritic spines are unchanged in neurons lacking Pten, but the spines are larger and there are a greater proportion of spines with mature morphology [119]. The *Pten<sup>m3m4</sup>* mice, which have decreased nuclear Pten but normal levels of cytoplasmic Pten, have neurons with increased soma size but normal dendritic thickness [115], indicating the importance of Pten in determining cellular morphology locally.

Not only do neurons lacking Pten have drastic morphological aberrations, but they also have significant changes in firing properties and synaptic plasticity. *Pten<sup>+/-</sup>* mice have decreased

LTP and completely abolished NMDA-dependent LTD in hippocampal CA1 synapses [120]. Moreover, *Pten* conditional knockouts (*GFAP-Cre*) also have decreased LTP in CA1 synapses [116], whereas dentate granule cell synapses have impaired mGluR-dependent LTD [121]. Importantly, postnatal deletion of *Pten* with *CamKII $\alpha$ -Cre* reproduced the deficits in LTP and LTD at CA1 synapses but had no effect on neuronal or dendritic morphology, thus indicating these phenotypes are not necessarily associated [122].

*Pten* is involved in suppressing the Akt signaling pathway upstream of mTOR activity, which normally leads to dephosphorylation of FMRP and subsequent protein translation. However, there is some evidence that suggests *Pten* might be acting differently. In particular, deletion of *Pten* leads to decreased expression of mGluR5, increased expression of FMRP, and increased phosphorylation of FMRP [114]. These findings seem to oppose, rather than overlap with, findings from *Fmr1* knockout mice. More work needs to be done to determine the molecular consequences of *Pten* loss-of-function and how this contributes to ASD-like phenotypes.

#### **1.3.2.4 *Ube3a* (Angelman syndrome and non-syndromic ASD)**

Patients diagnosed with Angelman syndrome (AS) frequently meet the diagnostic criteria for ASD [123]. Angelman syndrome is caused by mutations in or lack of expression of the maternal copy of *UBE3A* [124, 125], the paternal copy of which is normally silenced in neurons [126-128]. Maternally derived duplications and triplications of a genomic region which contains *UBE3A* have also been identified in patients with non-syndromic ASD [129-131]. The protein encoded by *UBE3A* is the ubiquitin-protein ligase (UBE3A), also known as E6AP ubiquitin-

protein ligase (E6AP) [132]. The ubiquitin-proteasome degradation system has been implicated in synapse function and plasticity (reviewed in [133]).

Mouse models of AS that recapitulate the major features of the disorder, including some ASD-like phenotypes, have been created and studied extensively. The first *Ube3a* mutant mice were created by making a targeted deletion of coding exon 2 [134] and another model was created by disrupting last two coding exons 15-16 [135], but only the model with exon 2 deletion has been extensively studied subsequently. The brains of the maternally deficient (*Ube3a*<sup>m-/p+</sup>) mice have significantly low or no detectable Ube3a protein, conferring high construct validity. Another group created mice that express either one extra (1xTg) or two extra copies (2xTg) of *Ube3a*, with reasonable construct validity for patients with maternally derived duplications and triplications in the genomic region encompassing *UBE3A* [136].

Maternal deficiency of *Ube3a* affects dendritic and spine morphology. Specifically, *Ube3a*<sup>m-/p+</sup> mice have decreased spine density in hippocampal CA1 and cortical layer 3-5 pyramidal neurons [137]. In contrast, *Ube3a*<sup>m-/p+</sup> mice raised in darkness have similar spine densities in visual cortex, suggesting a deficit specifically in experience-dependent remodeling of synapses [138]. Knockdown of Ube3a isoforms via *in utero* electroporation of shRNA revealed that Ube3a is also required for apical, but not basal, dendrite outgrowth [139]. On the other hand, increased *Ube3a* gene dosage does not affect glutamatergic synapse number in layer 2/3 barrel cortex, as assessed by electron microscopy, immunofluorescence, and golgi staining [136].

Perhaps the best studied aspect of AS and other *Ube3a* mouse models are the electrophysiological properties of affected neurons. Reduced LTP has been observed in

hippocampal CA synapses [134, 140] as well as in visual cortex [138, 141] of AS model mice. Like dendritic spine density, LTP in visual cortex is not significantly different between wild-type and *Ube3a*<sup>m-/p+</sup> mice that were raised in darkness [138]. In addition, reduced NMDA-dependent LTD has been reported in the visual cortex of *Ube3a*<sup>m-/p+</sup> mice raised in normal conditions [138], whereas enhanced mGluR-dependent LTD has been reported in hippocampal CA1 synapses [142]. A decreased AMPA/NMDA current ratio has also been reported in *Ube3a*<sup>m-/p+</sup> CA1 hippocampal neurons [143], but this ratio is unchanged in *Ube3a*<sup>2xTg</sup> barrel cortex [136]. Whole-cell patch clamp recording revealed reduced frequency and amplitude of mEPSCs in the dorsomedial striatum of *Ube3a*<sup>m-/p+</sup> mice, but not in the dorsolateral striatum [144]. Layer 2/3 pyramidal neurons in *Ube3a*<sup>2xTg</sup> barrel cortex display reduced eEPSC amplitude, reduced sEPSC amplitude and frequency, reduced sIPSC amplitude, and reduced mEPSC amplitude and frequency, along with decreased release probability and synaptic glutamate concentration [136]. In general, the mechanisms underlying the different impairments in synapses of different brain regions remains poorly understood.

Numerous targets of Ube3a-dependent ubiquitination have been identified [145-149] in attempts to dissect the molecular mechanisms underlying Angelman syndrome. One target is activity-regulated cytoskeleton protein (Arc), which promotes the internalization of AMPA receptors, and is interesting considering the functional defect of AMPA receptor mediated synaptic transmission [143]. More recent evidence suggests that Ube3a regulates Arc expression through estradiol-induced transcription rather than through ubiquitination [150]. Recent findings also indicate that in *Drosophila* Ube3a acts as a cofactor for some MeCP2 functions [151] and

*Ube3a*<sup>m-/p+</sup> mice demonstrate deficits in BDNF signaling [152]. Additionally, *Ube3a*<sup>m-/p+</sup> mice have presynaptic vesicle cycling defects specifically in inhibitory interneurons [153]. These observations clearly demand further investigation into some very basic questions. For instance, is the dosage of Ube3a in excitatory or inhibitory neurons responsible for the profound neurobehavioral impairment? Moreover, is the dosage of Ube3a primarily affecting pre- or postsynaptic sites?

### **1.3.3 Synaptic organizing and scaffolding**

#### **1.3.3.1 Shanks (Phelan-McDermid syndrome and non-syndromic ASD)**

Mutations in the SHANK/ProSAP family genes (*SHANK1-3*), particularly *SHANK2* and *SHANK3*, have been identified recently as pathogenic for non-syndromic ASD [154-156]. In addition, loss of one copy of *SHANK3* in Phelan-McDermid syndrome is thought to contribute to the neurobehavioral features of the disorder, including ASD [157, 158]. The Shank proteins function as scaffolds that organize postsynaptic densities (PSDs) in glutamatergic synapses and link receptors to cytoskeletal signaling molecules [159]. Shank proteins have also been implicated in spinogenesis and synapse development. In particular, transfection of Shank3 is sufficient to induce dendritic spine formation in otherwise aspiny neurons [160]. Another study provides evidence that Shank2 and Shank3 are involved in spine formation, whereas Shank1 is involved in synapse maturation and stability [161].

Mouse models disrupting expression of each of the three Shank proteins have been created to better understand the role of these proteins *in vivo* and their contributions to ASD. The

first model was created by deleting exons 14-15 of *Shank1* [162] where homozygous deletion (*Shank1*<sup>-/-</sup>) results in some ASD-like features [163-165]. Several lines of *Shank2* mutant mice have been reported, the earliest of which involved deletion of exon 7 [166] or exons 6-7 [167] of the *Shank2a* isoform, corresponding to exon 17 and exons 16-17, respectively, of full length *Shank2* [168]. Both lines are assumed to have disrupted function of all *Shank2* isoforms and display stereotypy, diminished social interactions, and impaired vocalizations [166, 167, 169].

More than ten different lines of *Shank3* mutant mice have been reported, but due to the transcriptional complexity of *Shank3* [170], only two lines disrupt all isoforms [171, 172]. Still, deletion of exons 4-7 [173], exons 4-9 [174-176], exon 9 [177], exon 11 [166], exons 13-16 [173], or exon 21 [178, 179], and an insertion mutation in exon 21 [180] all result in ASD-like behaviors to various degrees. Whereas humans with *SHANK3*-related ASD are either haploinsufficient due to a large chromosomal deletion or have point mutations in one copy of their *SHANK* genes, many of the studies utilizing mouse models only report behavioral abnormalities in homozygous mutants. This, along with the fact that most models do not disrupt all *Shank3* isoforms, limits the construct validity of these models.

Deletion of *Shank1* results in decreased spine density, shorter spines, and thinner PSDs in CA1 pyramidal neurons [162]. However, both normal spine density [167] and decreased spine density [166] have been reported in hippocampal CA1 neurons from *Shank2* mutants. Moreover, PSD length and thickness are not affected in CA1 neurons from either *Shank2* line [166, 167]. Deletion of exons 13-16 of *Shank3* led to decreased spine density, increased dendritic complexity,

and thinner PSDs in medium spiny neurons (MSNs) of the striatum [173]. However, deletion of exon 11 [166] or exon 21 [178] of *Shank3* had no effect on either spine density nor on dendritic complexity in CA1 neurons. This may have been due to the age of the mice tested, as deletion of exons 4-9 of *Shank3* had an age-dependent effect on spine density and morphology: CA1 neurons from 4 week old mice had decreased spine density and increased spine length, whereas CA1 neurons from 10 week old mice had normal spine density, but decreased spine length [175].

Accumulating evidence *in vivo* suggests that Shank proteins are required for proper synaptic function as well, but the findings are somewhat inconsistent. Extracellular recordings in the stratum radiatum of *Shank1*<sup>-/-</sup> mice revealed a significantly decreased excitatory synaptic strength, as assessed by the input-output relationship of field excitatory postsynaptic potentials, and recordings from CA1 hippocampal neurons in these mice revealed decreased mEPSC frequency [162]. The two lines of *Shank2* mutant mice have distinct electrophysiological phenotypes, despite the two mutations having presumably the same effect on Shank2 protein expression. Deletion of *Shank2* exon 7 results in decreased excitatory synaptic strength, decreased mEPSC frequency, a decreased AMPA/NMDA current ratio, and increased LTP in the hippocampus [166]. However, deletion of *Shank2* exons 6-7 results in no significant changes in excitatory synaptic transmission, an increase in the AMPA/NMDA current ratio, and impaired LTP and NMDA-dependent LTD [167].

The findings from *Shank3* mutants are also somewhat inconsistent, but many of the differences can be attributed to different isoforms disrupted due to the transcriptional complexity

of the gene. Deletion of exon 9 leads to increased mIPSC frequency in the hippocampus and decreased mIPSC frequency in the prefrontal cortex [177]. Three models which all have exons 4-9 deleted have reduced LTP in the CA1 region of the hippocampus [174-176]. Whereas the model produced by Bozdagi et al. has reduced excitatory synaptic strength, decreased mEPSC amplitude, increased mEPSC frequency, and a decreased paired-pulse ratio, the other models exhibit none of these phenotypes, but the model produced by Jaramillo et al. did have an increased AMPA/NMDA ratio in the striatum. Deletion of exons 13-16 had similar results to those observed by Wang et al. and Jaramillo et al. in the hippocampus, but resulted in decreased excitatory synaptic strength, reduced mEPSC frequency, and reduced mEPSC amplitude in MSNs of the dorsolateral striatum [173]. On the other hand, deletion of exon 21 results in decreased LTP, an increased AMPA/NMDA current ratio, decreased mEPSC frequency, and reduced excitatory synaptic strength in the CA1 region of the hippocampus [178] as well as an increased AMPA/NMDA current ratio in layer 5 prefrontal cortex pyramidal neurons [179]. The insertion mutation in exon 21 is similar to deletion of exon 21 in terms of hippocampal electrophysiology, but one difference is that LTD, and not LTP, is impaired [180].

The mechanism through which deletion of Shank proteins leads to synaptic dysfunction is likely due to impaired interactions between glutamate receptors and postsynaptic density proteins leading to impaired signaling in dendritic spines. For instance, rescue of NMDA receptor hypofunction with an actin stabilizer after knockdown of Shank3 in cultured rat cortical neurons suggests that some of the synaptic defects are due to disrupted cytoskeleton signaling [181]. Similarly, treating *Shank3* exon 21 deletion mice with an actin stabilizer rescues both behavioral

phenotypes and synaptic deficits [179]. Complete deletion of Shank3 results in disrupted Homer 1b/c and mGluR5 scaffolds [171].

Moreover, changes in the densities of receptors and synaptic proteins have been reported *in vivo*. Mice lacking Shank1 have decreased expression of Homer and GKAP/SAPAP in hippocampal PSD fractions [162]. Deletion of *Shank2* exon 7 results in significantly increased expression of NMDAR subunits in the hippocampus and significantly increased expression of both NMDAR and AMPAR subunits as well as Shank3 in the striatum [166]. Deletion of *Shank2* exons 6-7 also results in increased NMDAR subunit expression, but reduces NMDAR-associated signaling, as assessed by the proportion of phosphorylated CaMKII, ERK1/2, and p38 in whole brain lysates [167].

Mice with different *Shank3* mutations have varying degrees of altered expression of receptors, synaptic proteins, and downstream signaling molecules. Deletion of exon 21 of *Shank3* results in increased mGluR5 expression in hippocampal synaptosome and PSD fractions [178] as well as decreased Rac1/PAK signaling, increased activated cofilin, and decreased expression of F-actin in synapses [179]. Deletion of exons 4-9 of *Shank3* reduces Homer1b/c, GluA1, GluN2A, and SAPAP1 in hippocampal PSD fractions [175] as well as reduces Homer1b/c, PSD-95, GluA2, and GluA3 in striatal synaptosomes [176]. Finally, deletion of exons 13-16 results in reduced expression of SAPAP3, Homer, PSD-93, GluA2, GluN2A, and GluN2B in striatal PSD fractions [173] whereas deletion of exon 11 results in *increased* expression of GluN2B and

Shank2 in striatal synaptosomal fractions [166]. It is currently unclear how these molecular changes lead to synaptic dysfunction and how synaptic dysfunction leads to changes in behavior.

### **1.3.3.2 Neurexins/Neuroligins (non-syndromic ASD)**

Mutations in the genes encoding the presynaptic cell-adhesion molecules, neurexins, and their postsynaptic binding partners, neuroligins, have been implicated in non-syndromic ASD [182-187]. Additionally, mutations in genes coding for other members of the neurexin superfamily, contactin associated protein-2 (*CNTNAP2*) [188, 189] and contactin associated protein-4 (*CNTNAP4*) [190], have been identified in cases of ASD. Each of the three neurexin genes (*NRXN1*, *NRXN2*, *NRXN3*) contains two promoters, which generate a longer  $\alpha$ -NRXN or a shorter  $\beta$ -NRXN, respectively [191]. Moreover, the neurexins undergo extensive alternative splicing, resulting in thousands of different isoforms [192, 193]. On the other hand, the neuroligin genes (*NLGN1*, *NLGN2*, *NLGN3*, *NLGN4X*, *NLGN4Y*) contain one promoter and two alternatively spliced regions, allowing for up to four different isoforms per gene [194]. Together, neurexins and neuroligins form trans-synaptic complexes that facilitate synapse formation and maturation, as well as excitatory and inhibitory transmission (reviewed in [195]).

A multitude of mice with mutations in the neurexins, neuroligins, and related genes have been generated to understand the roles of these cell adhesion molecules in normal development and in ASD. Mice lacking either *Nrxn1 $\alpha$*  [196, 197] or *Nrxn2 $\alpha$*  [198] show some ASD-like features. Additionally, mice with a subset of forebrain neurons overexpressing of a dominant-negative form of *Nrxn1 $\beta$*  missing its cytoplasmic tail display ASD-like behaviors [199]. Mice

lacking *Cntnap2* [200] or *Cntnap4* [190] also have phenotypes which resemble ASD. Likewise, mice lacking *Nlgn1* [201], *Nlgn2* [202, 203], *Nlgn3* [204, 205], or *Nlgn4* [206-208] all have ASD-like behaviors to various degrees. Mice with a knock-in mutation of *NLGN3* (R451C) found in human populations have also been generated and recapitulate some ASD-like features [205, 209, 210].

Unlike the other mouse models of ASD, individual neurexin and neuroligin mutants do not have many reported changes in dendritic spine density, which is somewhat surprising, given that neurexins [211] and neuroligins [212] induce synapse formation in cultured cells *in vitro* and that knockdown of neuroligins in cultured neurons reduces spine density [213]. This suggests that there may be functional redundancy in the different proteins that can compensate for one another during development *in vivo*. However, even mice lacking either all three  $\alpha$ -Nrxn proteins [214] or *Nlgn1*, *Nlgn2*, and *Nlgn3* [215] have normal synapse numbers, suggesting that these molecules may not be required for synapse formation at all. A more recent study showed that knockdown of *Nlgn1* *in vivo* reduces synaptic density when neighboring neurons still express *Nlgn1* [216]. Whereas mice lacking *Nlgn2* have normal numbers of both excitatory and inhibitory synapses, they have decreased expression of VGAT, which represents an impairment in recruiting GABAergic synaptic vesicles to presynaptic terminals [202]. The *Nlgn3*<sup>R451C</sup> mice also have normal numbers of both excitatory and inhibitory synapses, but have increased expression of VGAT [209]. These mice have increased dendritic complexity in the stratum radiatum, decreased synaptic terminal size, fewer vesicles per terminal, and decreased spine size [217]. Additionally, the *Nlgn3*<sup>R451C</sup> mice have increased dendritic spine turnover in pyramidal neurons in the anterior

frontal cortex [218]. Moreover, mice lacking *Cntnap4* have increased width of synaptic clefts and decreased PSD length in GABAergic synapses [190].

Although changes in cellular and spine morphology in neurexin and neuroligin mouse models of ASD are somewhat minor, synaptic function is drastically altered. Deletion of *Nrxn1a* leads to reduced mEPSC frequency and decreased excitatory synaptic strength in the CA1 region of the hippocampus [196]. Mice with the dominant-negative form of *Nrxn1β* have decreased mEPSC frequency and mIPSC frequency in L5/6 pyramidal neurons from the somatosensory cortex [199]. Mice lacking *Cntnap4* have increased dopamine signaling through a presynaptic mechanism in the nucleus accumbens but fewer, smaller, and slower sIPSCs in PV-positive cells of the somatosensory cortex [190]. Deletion of *Nlgn1* results in a decrease in AMPAR EPSCs, NMDA EPSCs, and an increase in the AMPA/NMDA current ratio in the CA1 region of the hippocampus [219] as well as impaired LTP at thalamic inputs to the amygdala [220]. Impaired LTP has also been observed in the hippocampi of *Nlgn1* mutants *in vitro* [201] and *in vivo* [221]. Mice lacking *Nlgn4* have decreased network excitability in both excitatory and inhibitory circuits in layer 2/3 pyramidal cells, but the excitatory circuits are affected more greatly such that the excitation-inhibition ratio is decreased in the mutants [222].

The electrophysiological consequences of the *Nlgn3*<sup>R451C</sup> mutation in particular have been studied extensively. These mice have increased mIPSC frequency and eIPSC amplitude in layer 2/3 somatosensory cortex neurons [209]. However, they have decreased eIPSC amplitude in spiny neurons that receive input from PV-expressing basket cells in layer IV barrel cortex [223]. The

R451C mutation also leads to an increased frequency of giant depolarizing potentials (GDPs) and mIPSCs in the CA3 region of the hippocampus starting during the first two weeks of postnatal life [224]. These mice also exhibit increased excitatory transmission, increased LTP, and a decreased AMPA/NMDA current ratio in the CA1 region of the hippocampus [217]. While most studies failed to find similar deficits in *Nlgn3* knockout mice, one study found that both the *Nlgn3*<sup>R451C</sup> mice and *Nlgn3* knockout mice have increased GABAergic synaptic transmission (eIPSCs) in cholecystinin (CCK) basket cells and impair tonic endocannabinoid (ECB) signaling [225]. Mice lacking Nlgn3 also have decreased frequency of mIPSCs in D1-MSNs of the NAc while having normal frequency of mEPSCs, thereby increasing the excitatory/inhibitory current ratio [205].

Neuroligins interact with multiple postsynaptic proteins, including Shank3 [226]. Moreover, it was shown more recently that Shank3 expression mediates transsynaptic changes in synaptic proteins and that this function depends on the formation of neuroligin/neurexin complexes [227]. Accordingly, neurexin and neuroligin mutants, like Shank mutants, exhibit changes in the expression of synaptic proteins. Specifically, mice lacking *Nrxn2α* have reduced Munc-18 expression in hippocampal lysates [198]. Mice lacking *Nlgn1* have decreased expression of CSP, Liprin, Munc-18, *Nxnα*, and *Nrxnβ*, but increased expression of Nlgn3 and Synapsin1a in whole brain lysates [201]. As mentioned previously, Nlgn2 have decreased VGAT expression in hippocampus [202], whereas *Nlgn3*<sup>R451C</sup> mutants increased VGAT and Gephyrin expression in whole brain lysates [209]. The *Nlgn3*<sup>R451C</sup> mutants also have decreased expression of PSD95, SAP102, NR2A, and NR2B in hippocampal lysates [217]. Analysis of synaptosome

and PSD fractions from neurexin and neuroligin mutant mice could be performed to determine if the changes more similar to changes observed in Shank mutants.

### **1.3.4 Convergent molecular pathways and mechanisms**

Although much remains to be investigated in various directions, it is tempting to generalize these findings on a number of levels. Etiologically, rare and private mutations clustered in select molecular classes appear to be a major driver for a genetic basis in a subset of ASD patients. At the molecular level, several pathways appear to emerge from analyzing the existing ASD mouse models. These include disruption of overlapping signaling pathways mediated by mGluR5, BDNF, and mTOR, although the degree of evidence varies depending on the model.

Moreover, the available evidence strongly supports dysfunctional synapses as a component of autism pathophysiology. However, although there are widespread disruptions in synaptic function across the mouse models of ASD, the direction of change and magnitude of effect are inconsistent between different models, as well as between different types of synapses within any given model. Although there are many apparent differences between models, it is difficult to compare results that were reported in different brain regions or at different times during development. For instance, *Fmr1* knockout mice have decreased spine stability in somatosensory cortex [62], whereas *Mecp2*<sup>tm1.1Jae</sup> mice have increased spine stability in the same region [36], but the former study used mice that were postnatal day 10–12, whereas the latter study used mice that were postnatal day 25–26. Therefore, more side-by-side comparisons of

different mouse models of ASD would be valuable. One interesting discovery from genetics studies of ASD is the frequent mutations in genes encoding epigenetic machinery. However, it is not immediately clear how deficiency of these proteins contributes to autism pathophysiology. As has been demonstrated in Rett syndrome mouse models, the dysfunction of synapses could still be the major mechanism. However, a mechanism that is independent from synaptic dysfunction may also be possible.

There are some glaring missing links in our understanding of the pathophysiology of ASD. Specifically, how the mutation of an individual gene, a disrupted molecular pathway, and dysfunctional synapses affect the circuitry and produce ASD-like behavioral manifestations is unclear. Understanding the circuitry underlying autism, both anatomically and functionally, is critical to the development of effective clinical intervention. Several competing hypotheses regarding the circuit-level mechanisms have been proposed in the human literature. One widely tested hypothesis is altered structural and functional brain connectivity [228-230]. Structural connectivity is the physical connections between different brain regions, while functional connectivity refers to the integrated relationship between spatially separated brain regions. It is believed that structural connections within the brain give rise to functional network activity as measured by coherence or information flow. Neuroimaging investigations indicate that ASD are associated with perturbed connectivity at both structural and functional levels [231, 232]; however, the exact nature and pattern of this aberrant neural connectivity remains uncertain due to inconsistent findings from neuroimaging studies in patients [230, 233, 234]. While early studies reported reduced functional connectivity [235], recent investigations implicate hyper-

connectivity in multiple brain regions and across neural circuits [236, 237]. In addition to methodological and conceptual controversy, this uncertainty reflects the substantial molecular heterogeneity of human patients. Notably, these studies were conducted primarily in high-functioning ASD patients for whom the etiologies are mostly unknown. For these reasons, autism animal models offer a unique opportunity to test the functional connectivity hypothesis because of homogenous genetic defects. Using optogenetic tools, Gunaydin et al. have shown that the activity of ventral tegmental area to nucleus accumbens projections could encode and predict key features of social interaction in wild type mice [238]. Similarly, Felix-Ortiz and Tye revealed the role of projections from the basolateral complex of the amygdala to the ventral hippocampus in two different social interaction tests [239]. Few reports have investigated the circuit-level mechanisms underlying autism-like behaviors in genetically modified autism models with strong construct validity. Therefore, the combination of optogenetics and CRISPR/Cas9 genome editing tools in ASD models is expected to produce significant insight into whether there are common circuits disrupted in ASD models with different genetic defects.

#### ***1.4 Temporospatial manipulation of ASD-causing mutations and behavior***

The neurobiological basis of autism spectrum disorder (ASD) has been a growing area of research during the past few decades. While substantial progress has been made to uncover the molecular underpinnings of the disorders, the cell types and circuits underlying autistic behaviors remain largely unknown [240]. This knowledge, however, is critical to developing targeted therapy. Neuroimaging in human patients has provided correlates between the function of certain brain regions and behavior [233, 241]. Such studies are limited by the phenotypic heterogeneity

that is characteristic of ASD, the individuals available for study, the low resolution of imaging techniques, and the inability to manipulate molecules and circuits in the human brain. For these reasons, it is technically challenging to establish causality between circuits and behavior in studies involving humans. However, animal models allow researchers to determine causation because the genetic background and environmental factors can be controlled. Furthermore, the use of laboratory rodents allows for more invasive studies that would not be feasible or ethical in humans.

Transgenic mice with ASD-causing mutations that are present in the germline have provided clues to the molecular underpinnings of the disorders, and some degree of overlap is seen across multiple mouse models [242]. However, germline, or conventional, mutant mice do not provide enough evidence to causally link a particular brain region or circuit to ASD-like behaviors. More recently, several groups have taken advantage of tools that allow for the manipulation of genes across space and time in animal models to begin dissecting the cell types, brain regions, and associated circuits contributing to ASD phenotypes. Here, I have focused on studies that utilize conditional gene-expression technology combined with mouse models of ASD that have high construct validity (i.e. the molecular consequences of the mutations mimic those observed in humans) and report phenotypes that have strong face validity (i.e. appear to mimic the behavioral features of the disorders) for the core symptoms of ASD, impaired social communication and repetitive behaviors.

#### **1.4.1 Assays for ASD-related behaviors**

Currently, ASD is diagnosed purely on the assessment of behavioral features [1].

Therefore, behavioral analysis is an important part of the strategy to model human mutations and understand the cellular and circuitry bases of the disorders. To help achieve this goal, a number of assays that test behaviors resembling the core symptoms of ASD have been developed for laboratory mice [19, 92]. Commonly tested behaviors are briefly described here and are summarized in Table 3.

**Table 3: Summary of behavioral assays**

Assay	Resemblance to core feature of ASD	Quantitative measurements
Three chamber test	Social communication deficits	Phase 1: “Sociability” - preference for social stimulus (stranger mouse) over an inanimate object  Phase 2: “Social novelty” - preference for an unfamiliar mouse over the stranger mouse used in the sociability phase
Habituation/dishabituation	Social communication deficits	Time spent interacting with a the same mouse during the trial period over several days and time spent with a novel mouse on the last trial
Partition test	Social communication deficits	Time spent near a barrier that separates the test mouse from a stranger mouse
Direct social interaction tests	Social communication deficits	Duration, type (e.g. aggressive), and amount of social interactions
Ultrasonic vocalizations	Social communication deficits	Number, duration, and complexity of vocalizations
Nest building	Social communication deficits	Amount of nesting material used, size of nest, or numerical scoring system

Assay	Resemblance to core feature of ASD	Quantitative measurements
Self-grooming	Repetitive behavior	Time spent grooming or number of grooming bouts
Jumping	Repetitive behavior	Time spent jumping or number of jumping bouts
Digging	Repetitive behavior	Time spent digging or number of digging bouts
Hole board test	Repetitive behavior	Number of total hole pokes or number of consecutive (2+) pokes in the same hole
Marble burying test	Repetitive behavior	Number of marbles buried

#### 1.4.1.1 Tests to assess social communication

The three chamber test consists of two phases. The first phase has a caged stranger mouse in one of the chambers, a novel object in the opposing chamber, and a neutral central chamber [243]. The second phase has the caged mouse from the first phase in one chamber, a neutral central chamber, and a novel caged mouse in the opposing chamber. The first phase is considered a test for “sociability” where wild-type mice tend to spend more time in the chamber with the caged stranger mouse than in either other chamber. The second phase is a test for “preference for social novelty” or “social preference,” where most wild-type mice spend more time with the novel stranger mouse than with the familiar stranger mouse or in the neutral chamber.

The habituation/dishabituation test involves introducing the test mouse to the same

contained stimulus mouse over several days and then introducing a novel contained stimulus mouse [244]. Wild-type mice tend to spend less time engaging with the familiar mouse over time, but have increased interactions with the novel mouse. This is a measure of social recognition.

In the partition test, the test mouse and a stimulus mouse are in an arena on opposite sides of a clear acrylic barrier with holes [245, 246]. The amount of time the test mouse spends near the partition is a measure of social behavior.

In direct social interaction tests, the test mouse and stimulus mouse are allowed to freely interact. The type, duration, and amount of contacts are scored [247]. One variant of this test is resident-intruder, where the stranger mouse is introduced into the test mouse's home cage [248].

Ultrasonic vocalizations (USVs) can be recorded in pups (~postnatal days 3–12) and in adults [249]. For pups, this simply involves briefly separating the pups from their mother. For adults, the most common test involves exposing male mice to females in estrous or their urine. The number, duration, and complexity of USVs can be compared.

Nest-building is considered to be another measure of social behavior. The test mouse is given a small amount of cotton or other material to build a nest in its home cage. The amount of material used, the size of the nest, or a scoring system can be used to compare experimental groups [250].

#### **1.4.1.2 Tests to assess repetitive behavior**

Spontaneous repetitive behaviors include excessive self-grooming, jumping, or digging

[251]. The time spent engaging in each behavior or number of bouts can be compared.

The hole board test also measures repetitive behavior. Mice are placed on an apparatus with circular holes arranged in a grid [252]. Mice that display repetitive behavior have more nose-pokes into the holes, or explore the same hole repeatedly.

Finally, in the marble burying test, the test mouse is placed in a clean cage with marbles positioned on top of bedding [253]. Mice with repetitive behavior bury more marbles in the bedding than their wild-type littermates.

### **1.4.2 Tools to manipulate gene expression**

The Cre-*loxP* system is the approach taken most often to manipulate gene expression in a cell-type-specific or time-dependent manner [254]. For cell-type-specific manipulations, this method typically involves breeding mice that contain the Cre recombinase transgene under the control of a specific promoter with mice that have the target gene flanked by *loxP* sequences (floxed) [255]. Deletions, and rarely duplications, of the target DNA occur when the *loxP* sequences are oriented in the same direction in either the *cis* or *trans* configuration, whereas inversions occur if the *loxP* sequences are oriented in opposite directions. For more precisely-timed manipulations, the Cre recombinase protein is fused to a mutated estrogen receptor, so that tamoxifen treatment causes translocation into the nucleus and subsequent site-specific recombination [256]. Other, but less common, methods for inducible gene expression include the Tet-Off (tTA) and Tet-On (rtTA) systems, where doxycycline treatment represses and activates transcription, respectively [257].

While extraordinarily useful for temporospatial manipulation of genes in mice, the Cre-*loxP* system is not without its limitations. The major limiting factor is the availability of Cre lines that meet the needs of an experiment, in terms of timing and spatial distribution of Cre expression. The specificity and efficiency of recombination relies on the promoter, which may be expressed at various levels in off-target tissues or cell-types. One way to circumvent this problem is to deliver a lentivirus or adeno-associated virus construct containing Cre to mice with the target gene floxed [258]. While this method may limit the expression of Cre to a particular brain region, it is more difficult to control the expression of Cre in different cell types within a particular region. Another potential problem is that Cre expression itself can induce a phenotype by causing recombination at cryptic *loxP* sites in the mouse genome [259], or by affecting the expression of surrounding genes, depending on the insertion site of the transgene. Therefore, it is important that proper controls are implemented to compare the phenotypes.

New advances in gene-editing technologies may eventually overcome the limitations of the Cre-*loxP* and similar systems. For example, it has been demonstrated that CRISPR/Cas9 can be used to edit the genome of adult mice and rescue disease phenotypes [260]. Moreover, methods are being developed to increase the cell-type specificity of CRISPR/Cas9-mediated mutations [261]. However, off-target mutations using this system remain a concern and must be assessed individually [262]. Thus, some refinement of this newer technology is necessary before using it to answer questions about the neuroanatomical bases of ASD.

### **1.4.3 The roles of excitatory and inhibitory neurons in ASD**

The two major classes of neurons in the brain are excitatory neurons, those which depolarize the neurons they project onto and thus make them more likely to produce action potentials, and inhibitory neurons, those which hyperpolarize their outputs and make them less likely to produce action potentials. It has been proposed that a common mechanism underlying ASD is an imbalance between inhibitory and excitatory synaptic transmission in particular circuits. This may reflect a relative increase of function in excitatory neurons compared to that of inhibitory neurons [263], or *vice versa*. Although support for this hypothesis is currently somewhat limited, studies have begun to address it.

One important question is whether disrupting the function of either major class of neurons is sufficient to produce phenotypes related to ASD and, if so, which types of neurons within these major classes contribute to the phenotypes. Another important question is whether different ASD-causing mutations affect the same neuronal types and circuits, or have shared circuit-level mechanisms. This may translate into whether patients with different mutations require individualized therapy in the clinic. Fortunately, the advent of conditional gene expression technologies and the production of multiple mouse models of ASD with high construct validity have made it possible to start exploring these questions.

#### **1.4.3.1 Excitatory (glutamatergic) neurons**

Most of the published work on conditional gene expression for ASD involves manipulation of the mouse version of the genes that are mutated in syndromic autism, such as

Rett syndrome (*MECP2*), tuberous sclerosis complex (*TSC1* or *TSC2*), *PTEN*-related disorders, and Angelman syndrome (*UBE3A*). One group found that restricting the deletion of *Mecp2* (*loxP/y*) to excitatory neurons in the forebrain postnatally, starting around postnatal day 21 (P21), with Tg(Camk2a-cre)<sup>93</sup>Kln (CamKII-cre<sup>93</sup>; EMMA 01137) results in mice that display reduced sociability in a test similar to the first phase of the three chamber test and reduced preference for the novel mouse in the habituation-dishabituation test [264]. However, another group used Emx1<sup>tm1</sup>(cre)Krlj (Emx1-cre; JAX 005628) to delete *Mecp2* (*loxP/y*) in forebrain excitatory neurons and glia embryonically, starting around embryonic day 9.5 (E9.5), and found no significant changes in either sociability or preference for social novelty in the three chamber test [265]. Neither study reported any repetitive behaviors. Deletion of *Mecp2* (*loxP/y*) selectively in glutamatergic neurons, the most abundant neurotransmitter class of excitatory neurons, in embryos with Slc17a6<sup>tm2</sup>(cre)Lowl (Vglut2-cre; JAX 028863) does not impact social behavior in the partition test or nose-pokes on the hole board [266]. However, selectively expressing *Mecp2* (*loxP-stop/y*) in glutamatergic neurons with the same Cre line rescues a hypersocial phenotype on the partition test and repetitive nose-pokes on the hole board that occur in the global knockout, which suggests that restoring function to glutamatergic neurons may have network effects that subsequently increase the function of other excitatory neurotransmitters or inhibitory neurons as well [266].

On the other hand, mice that carry a deletion of another ASD candidate gene, *Mef2c* (*loxP/loxP*) with Emx1-cre spend less time interacting with the social stimulus in the first phase of the three chamber test, emit fewer USVs as pups and adults, have lower nest-building scores,

and display increased repetitive jumping and fine motor movements [267]. Similarly, deletion of *Cc2d1a* (*loxP/loxP*) with Tg(CamK2a-cre)T29-1Stl (CamKII $\alpha$ -cre T29-1; JAX 005359) results in mice that display reduced sociability in the first phase of the three chamber test, reduced social approach in a direct social interaction test, reduced numbers of adult USVs, and increased repetitive self-grooming (but no changes in marble-burying) [268]. Mice with *Tsc1* (*loxP/loxP*) deleted with CamKII $\alpha$ -cre T29-1 also display reduced sociability in the three chamber test and increased marble-burying behavior [269]. However, deletion of exons 4-22 of *Shank3* with Neurod6tm1(cre)Kan (NEX-cre), which similarly restricts the mutation to forebrain excitatory neurons, results in increased grooming behavior, but no changes in adult USVs [270].

Together, these findings indicate that disrupting the function of excitatory neurons can be sufficient to produce ASD-like behaviors, but conflicting findings between models indicate that manipulating one gene may not be generalizable to all ASD. Therefore, studies using conditional gene expression of other ASD candidate genes are necessary to obtain a more complete understanding.

#### **1.4.3.2 Inhibitory (GABA-ergic) neurons**

Although there is some evidence that the dysfunction of excitatory neurons contributes to ASD-like phenotypes, there is accumulating evidence for a role of inhibitory neurons as well. Using the line Tg(Slc32a1-cre)2.1Hzo (Vaat-cre; JAX 017535) to delete *Mecp2* (*loxP/y*) specifically in GABAergic cells in embryos results in mice that show nearly the full spectrum of phenotypes observed in the conventional knockout, including repetitive forelimb stereotypies,

increased grooming, sequential head-pokes on the hole board task, decreased nest-building, and increased sociability in the partition test and the three chamber test [271]. Accordingly, selectively restoring *Mecp2* (*loxP-stop/y* and *loxP-stop/+*) to GABAergic cells with *Viaat-cre* rescues the hypersocial phenotype in the partition test and nest-building deficits in both male and female mice (but repetitive behaviors were not reported) [272]. Using the same *Viaat-cre* line, deletion of exons 14-16 of *Shank3* (*loxP/loxP*) recapitulates many of the behavioral phenotypes observed in germline deletion of the same exons, including hypersociability in a direct social interaction test, decreased number of USVs, and increased self-grooming [273].

More specifically, deleting *Mecp2* (*loxP/y*) in a subset of GABAergic cells in the forebrain, embryonically, with *Tg(Dlx6a-cre)1Mekk* (*Dlx5/6-cre*; JAX 008199) recapitulates the nest-building, hole board, and hypersocial phenotypes, but not grooming, indicating that some features of ASD may involve other brain regions or cell types [271]. Similarly, deleting exons 4-22 of *Shank3* (*loxP/loxP*) with *Dlx5/6-cre* recapitulates the hole board phenotype observed in the germline exons 4-22 knockout, but does not increase grooming or impair USVs [270].

Two of the major subclasses of GABAergic neurons are parvalbumin-positive (PV+) and somatostatin-positive (SOM+) neurons [274]. Thus, one important question is whether either or both of these cell types contribute to ASD phenotypes. Mice that lack *Mecp2* (*loxP/y*) in PV+ neurons, embryonically, created by crossing the floxed mice with *Pvalbtm1(cre)Arbr* (*PV-cre*; JAX 008069), display a hypersocial phenotype on the partition test, but show no differences on the hole board [275]. In contrast, mice that lack *Mecp2* (*loxP/y*) in SOM+ neurons, embryonically, created by crossing floxed mice with *Ssttm2.1(cre)Zjh* (*SOM-cre*; JAX 013044),

display repetitive nose-pokes on the hole board, but have no social phenotype [275]. A different study found no differences in sociability in mice lacking *Mecp2* in PV+ neurons, using the same PV-cre [276]. However, another study confirmed that dysfunctional PV+ neurons contribute to social phenotypes whereas SOM+ neurons do not by heterozygous deletion of the mouse version of the gene underlying Dravet syndrome, *Scn1a* (*loxP/+*), in either type of neuron using PV-cre and SOM-cre, respectively [277]. In this case, the mice lacking *Scn1a* in PV+ neurons show decreased sociability in the three chamber test [277].

It is likely, given that the conditional knockouts restricting *Mecp2* deletion to GABAergic neurons almost completely recapitulate all of the phenotypes observed in the conventional knockout, that the pathogenesis of Rett syndrome primarily involves dysfunctional inhibitory neural networks. Some behavioral deficits have also been reported in conditional *Mecp2* knockouts where the deletion is limited to excitatory neurons, but the decrease in social behavior is distinct from the global knockout, which shows increased social interest in the partition test. It is less clear at this time whether this is generalizable to other ASD, as restricting other ASD-causing mutations to subsets of either neuron class can recapitulate some but not all of the behaviors observed in the germline mutants for these lines. Therefore, more research is needed that uses conditional gene expression technology and highly penetrant ASD-causing mutations.

#### **1.4.4 Other neurotransmitter systems**

Other neurotransmitters can either be excitatory or inhibitory, depending on the action of the postsynaptic receptors that are expressed. Since the majority of neurons in the brain are either glutamatergic or GABAergic, less is known about the roles of other neurotransmitters in ASD

models. However, some groups have started dissecting the roles of dopamine, serotonin, acetylcholine, and oxytocin.

Restricting the deletion of *Mecp2* (*loxP/y*) to serotonergic neurons, embryonically, with *Tg(Fev-cre)1Esd* (PET-1 cre; JAX 012712) results in mice that display a hypersocial phenotype on the partition test as well as increased aggression during the resident-intruder test [278]. On the other hand, selectively deleting *Mecp2* (*loxP/y*) in dopaminergic neurons, embryonically, with *Thtm1(cre)Te* (TH-cre; EMMA 00254) does not influence social behavior in these assays [278]. The PET-1 cre knockout does not have repetitive grooming or marble-burying, but these behaviors were not assessed in the TH-cre knockout [278]. This study, along with others, suggests that dysfunctional serotonergic neurons may contribute to the core symptoms of ASD, whereas dopaminergic neurons are implicated in comorbid motor functions [279-281]. More support for the role of serotonergic neurons in ASD behaviors comes from deleting *Tsc1* (*loxP/loxP*) selectively in serotonergic neurons, embryonically, with *Tg(Slc6a4-cre)ET33Gsat* (*Slc6a4-cre*; MMRRC 031028-UCD), which results in mice with decreased sociability in the first phase of the three chamber test and increased repetitive marble-burying behaviors [269].

Recently, the cholinergic system has also been implicated in the pathogenesis of ASD with conditional gene expression in mice. Selectively deleting *Mecp2* (*loxP/y*) in cholinergic neurons, embryonically, with *Chattm2(cre)Lowl* (*Chat-cre*; JAX 006410) produces mice that fail to show a preference for social novelty in the three chamber test, show decreased social investigation in a direct interaction test, and have impaired nest-building [282]. Interestingly, re-expression of *Mecp2* (*via* microinjection of an AAV) in the basal forebrain, but not in the

caudate-putamen, of adult mice rescues the social deficit in the three chamber test [282]. Again, this phenotype is distinct from that in the global *Mecp2* knockout, but nonetheless provides insight into circuits underlying ASD.

So far, the role of oxytocinergic neurons is less clear. Neither heterozygous (*loxP/+*) nor homozygous (*loxP/loxP*) deletion of *Pten* in oxytocinergic neurons, embryonically, with *Oxttm1.1(cre)Dolsn* (*Oxt-cre*; JAX 024234) results in deficits in the three chamber, habituation/dishabituation, or marble-burying tests [283]. This is somewhat puzzling, given that *Pten* haploinsufficient, oxytocin knockout, and oxytocin receptor knockout mice show some overlapping impairments on these assays [284-287]. Perhaps mutations in *PTEN* and other ASD-causing mutations have more of an effect on neurons expressing the oxytocin receptor, rather than on oxytocinergic neurons. More work needs to be done to clarify the role of oxytocin and other neurotransmitters in ASD.

#### **1.4.5 The role of the cerebellum in ASD**

In recent years, the cerebellum has emerged as a brain region that may be implicated not only in motor impairments, but also in the core behaviors of ASD, particularly because cerebellar Purkinje cells project to the thalamus and, for example, affect dopamine efflux in the prefrontal cortex [288]. Mice with heterozygous (*loxP/+*) or homozygous (*loxP/loxP*) deletion of *Tsc1* mostly restricted to Purkinje cells, postnatally, by means of *Tg(Pcp2-cre)2Mpin* (*L7-cre*; JAX 004146) fail to demonstrate preference for a social stimulus over a non-social stimulus or for novel social interactions over familiar ones in the three chamber test [289]. These mice also engage in elevated rates of self-grooming [289]. Similarly, mice with *Tsc2* homozygously deleted

in Purkinje cells with L7-cre and heterozygously deleted in all other cell types (*loxP*<sup>-/-</sup>) have impaired social interactions and increased rates of marble-burying [290]. Mice with *Pten* deleted (*loxP/loxP*) in Purkinje cells by L7-Cre display reduced sociability and engage in repetitive upright scrabbling, but have reduced self-grooming [291]. Interestingly, deleting *Pten* (*loxP/loxP*) primarily in cerebellar granule cells with Tg(*Gfap-cre*)1Sbk (*Gfap-cre*) results in mice that are hyposocial in the partition test and show reduced sociability in the three chamber test, but show reduced repetitive behaviors in the marble-burying and hole board tests, and have no changes in USVs as pups [114].

Most recently, two similar studies produced opposite conclusions regarding the cerebellum's role in social behavior. Purkinje cell deletion of exon 7 of *Shank2* (*loxP/loxP*) with L7-Cre resulted in mice that failed to demonstrate a preference for sociability or for social novelty [292]. However, mice with a deletion of exons 6-7 of *Shank2* (*loxP/loxP*) with Tg(*Pcp2-cre*)3555Jdhu (*Pcp2-cre*; JAX 010536) were similar to controls on the three chamber task and had similar USVs, but had increased nose-pokes on the hole board [293]. Both groups of mice showed normal levels of self-grooming and marble-burying.

The divergent findings regarding social behavior between the two studies using *Shank2* conditional mutants have several possible explanations. One is that minor differences in the exonic deletions could disrupt the expression of different sets of *Shank2* isoforms, but current knowledge regarding the structure of *Shank2* suggests this unlikely to be the case [168]. Another possibility is that the use of different Cre lines (JAX 004146 vs. JAX 010536) in the two studies may have some effect on behavior; although both Cre lines involve the same promoter, there may

be differences in the spatial pattern and timing of Cre expression. The most likely explanation is that the two labs used different methods for determining behavioral phenotypes (for example, strains chosen for the stranger mice and habituation times). This last explanation is especially convincing because the wild-types in one study showed a preference for social novelty [292], whereas those in the other study did not [293], most likely indicating differences in behavioral methods.

Further investigation into the cerebellum's contributions to ASD phenotypes is clearly warranted. Moreover, the contradictory findings from similar studies underscore the need for stricter standards for behavioral methods or more side-by-side comparisons between lines of mice within investigating laboratories to make the strongest conclusions. It is unclear at this time whether, for instance, *Tsc1*, *Tsc2*, *Pten*, and *Shank2* deletions in the cerebellum have different effects on self-grooming, or whether the discrepancies between the studies are due to varying methods. It is even less clear which cerebellum-related circuitry is responsible for the ASD-like behaviors and whether there is any translational value of these findings for human patients.

#### **1.4.6 Developmental time points implicated through inducible mutations and rescues**

Clinically, ASD is classified as a neurodevelopmental disorder. However, the developmental origin of ASD has not been clearly defined. This knowledge is likely critical for effective clinical intervention. Conditional gene expression, through inducible mutations and rescues, allows researchers to determine whether ASD is the result of disrupted development and/or ongoing neuronal dysfunction. Conditional-rescue mice also provide proof of principle for

the potential of gene therapy. One attractive hypothesis for the origin of ASD is that perturbations to synaptic development prevent patients from developing skills during a limited window of opportunity, or a critical period [294]. This would suggest that reversing the symptoms of ASD may be difficult, if not impossible. Some studies suggest that early intervention is necessary for preventing the onset of ASD-like phenotypes. However, multiple studies have also challenged the notion that ASD represents an irreversible disruption of brain development.

Deleting *Mecp2* in adulthood (*loxP/y*) using the ubiquitously-expressed, inducible Cre line, Tg(CAG-cre/Esr1\*)5Amc (CAGGS-CreER; JAX 004453) and tamoxifen administration, causes the impaired nest-building phenotype that is observed in germline knockouts [295]. Reactivating *Mecp2* in male (*loxP-stop/y*) and female (*loxP-stop/+*) model mice with the same Cre line and tamoxifen administration partially and completely rescue this nest-building impairment, respectively [296]. Neither of these studies reported any other ASD-related behaviors, nor did two other studies that reactivated *Mecp2* expression [297, 298]. However, reinstating *Ube3a* (*loxP-stop/p+*) using the same inducible Cre line fails to rescue impaired nest-building in these mice, even when tamoxifen is administered to newborn mice; only embryonic reinstatement of *Ube3a* successfully rescues this phenotype [299].

On the other hand, several ASD-related behaviors are rescued by repressing the expression of a dominant-negative form of *Nrxn1β* in excitatory neurons in adulthood using Tg(Camk2a-tTA)1Mmay (CaMKII-tTA; JAX 003010) with the administration of doxycycline, which reverses increased self-grooming and impaired sociability and preference for social novelty in the three chamber test [300]. Similarly, re-expressing normal *Shank3* isoforms by reverting an

inverted portion of the gene after administering tamoxifen to adult mice (*loxP/loxP*; CAGGS-CreER) rescues increased grooming, impaired sociability in the first phase of the three chamber test, and reduced preference for social novelty in the second phase of this test [301].

While in general these studies provide some promising evidence for the reversibility of the core symptoms of ASD, research using other models and additional ASD-relevant behaviors is necessary to make more definitive conclusions. An interesting and important question is whether the findings from mouse models can be translated to humans and if the reversibility of symptoms holds true.

#### **1.4.7 Conclusions from temporospatial manipulation of ASD-causing mutations**

The findings reviewed in this section (summarized in Table 4) support the value of conditional gene-expression technology to delineate the cells and circuits underlying ASD. However, because these studies are mostly conducted in syndromic ASD models, it remains to be seen whether these findings and conclusions are unique to these specific ASD-causing mutations. Since there are inconsistencies between studies that manipulate the same gene, it may be premature to generalize the limited available evidence. Human genetics studies have supported the role of several hundreds of genes in ASD, so one challenge is to find out whether there are shared circuit-level mechanisms among ASDs caused by different mutations or etiologies. Caution must be taken when interpreting the results from studies that utilize conditional gene expression. Too often the efficiency and specificity of the Cre lines are overestimated. Moreover, disruption of one set of cells may have downstream or compensatory effects on other cell types in

the same brain region, or even in different brain regions due to axonal projections. Hopefully, the development of more precise technology for manipulating cell types and circuits will facilitate a more complete understanding of the neural underpinnings of ASD.

**Table 4: Summary of transgenic mouse lines used for the temporospatial manipulation of ASD genes in the mouse brain.**

Cre line (or “Tet-Off” line)	Commercial availability	Cells targeted	Timing of gene expression manipulation	Social communication phenotypes	Repetitive behavior phenotypes	References
CamKII-cre93	EMMA 01137	Excitatory forebrain neurons	Postnatal (~P21)	<i>Mecp2 (loxP/y)</i> ↓ sociability* ↓ social novelty*** NR USVs NR nest building	<i>Mecp2 (loxP/y)</i> NR grooming NR hole board NR marble burying	Cre line primary: [302]  <i>Mecp2</i> study: [264]
CamKIIa-cre T29-1	JAX 005359	Excitatory forebrain neurons	Postnatal (~P21)	<i>Cc2d1a (loxP/loxP)</i> ↓ sociability*, **** NR social novelty ↓ adult USVs NR nest building  <i>Tsc1 (loxP/loxP)</i> ↓ sociability* NR social novelty NR USVs NR nest building	<i>Cc2d1a (loxP/loxP)</i> ↑ grooming NR hole board ↔ marble burying  <i>Tsc1 (loxP/loxP)</i> NR grooming NR hole board ↑ marble burying	Cre line primary: [255]  <i>Cc2d1a</i> study: [268]  <i>Tsc1</i> study: [269]

Cre line (or "Tet-Off" line)	Commercial availability	Cells targeted	Timing of gene expression manipulation	Social communication phenotypes	Repetitive behavior phenotypes	References
Emx1-cre	JAX 005628	Excitatory forebrain neurons and glia	Embryonic	<p><u>Mecp2 (loxP/y)</u>  ↔ sociability*  ↔ social novelty*  NR USVs  NR nest building</p> <p><u>Mef2c (loxP/loxP)</u>  ↓ sociability*  NR social novelty  ↓ pup, adult USVs  ↓ nest building</p>	<p><u>Mecp2 (loxP/y)</u>  NR grooming  NR hole board  NR marble burying</p> <p><u>Mef2c (loxP/loxP)</u>  NR grooming  NR hole board  NR marble burying</p>	<p>Cre line primary: [303]</p> <p><i>Mecp2</i> study: [265]</p> <p><i>Mef2c</i> study: [267]</p>
NEX-cre	N/A	Excitatory neocortex and hippocampus neurons	Embryonic	<p><u>Shank3e4-22 (loxP/loxP)</u>  ↔ sociability*  NR social novelty  ↔ adult USVs  NR nest building</p>	<p><u>Shank3e4-22 (loxP/loxP)</u>  ↑ grooming  ↔ hole board  NR marble burying</p>	<p>Cre line primary: [304]</p> <p>Shank3 e4-22 study: [270]</p>

Cre line (or "Tet-Off" line)	Commercial availability	Cells targeted	Timing of gene expression manipulation	Social communication phenotypes	Repetitive behavior phenotypes	References
Vglut2-cre	JAX 028863	All glutamatergic neurons	Embryonic	<p><i>Mecp2 (loxP/y)</i> ↔ sociability** NR social novelty NR USVs NR nest building</p> <p><i>Mecp2 (loxP-stop/y)</i> ↑ sociability** resc. NR social novelty NR USVs NR nest building</p>	<p><i>Mecp2 (loxP/y)</i> NR grooming ↔ hole board NR marble burying</p> <p><i>Mecp2 (loxP-stop/y)</i> NR grooming ↑ hole board resc. NR marble burying</p>	<p>Cre line primary: [305]</p> <p><i>Mecp2</i> study: [266]</p>
Viaat-cre	JAX 017535	All GABAergic neurons	Embryonic	<p><i>Mecp2 (loxP/y)</i> ↑ sociability*, ** NR social novelty NR USVs ↓ nest building</p> <p><i>Mecp2 (loxP-stop/y)</i> ↑ sociability** resc. NR social novelty NR USVs ↓ nest building resc.</p> <p><i>Shank3e14-16 (loxP/loxP)</i> ↑ sociability**** ↔ sociability* ↔ social novelty* ↓ adult USVs NR nest building</p>	<p><i>Mecp2 (loxP/y)</i> ↑ grooming ↑ hole board NR marble burying</p> <p><i>Mecp2 (loxP-stop/y)</i> NR grooming NR hole board NR marble burying</p> <p><i>Shank3e14-16 (loxP/loxP)</i> ↑ grooming NR hole board NR marble burying</p>	<p>Cre line primary: [271]</p> <p><i>Mecp2</i> deletion study: [271]</p> <p><i>Mecp2</i> rescue study: [272]</p> <p>Shank3 e14-16 study: [273]</p>

Cre line (or "Tet-Off" line)	Commercial availability	Cells targeted	Timing of gene expression manipulation	Social communication phenotypes	Repetitive behavior phenotypes	References
Dlx5/6-cre	JAX 008199	Subset of GABAergic neurons in forebrain	Embryonic	<p><u>Mecp2 (loxP/y)</u>  ↑ sociability*, **  NR social novelty  NR USVs  ↓ nest building</p> <p><u>Shank3e4-22 (loxP/loxP)</u>  ↔ sociability*  NR social novelty  ↔ adult USVs  NR nest building</p>	<p><u>Mecp2 (loxP/y)</u>  ↔ grooming  ↑ hole board  NR marble burying</p> <p><u>Shank3e4-22 (loxP/loxP)</u>  ↔ grooming  ↑ hole board  NR marble burying</p>	<p>Cre line primary: [306]</p> <p><i>Mecp2</i> study: [271]</p> <p>Shank3 e4-22 study: [270]</p>
PV-cre	JAX 008069	PV+ GABAergic neurons	Embryonic	<p><u>Mecp2 (loxP/y)</u>  ↑ sociability**  ↔ sociability*  NR social novelty  NR USVs  NR nest building</p> <p><u>Scn1a (loxP/+)</u>  ↓ sociability*  NR social novelty  NR USVs  NR nest building</p>	<p><u>Mecp2 (loxP/y)</u>  NR grooming  ↔ hole board  NR marble burying</p> <p><u>Scn1a (loxP/+)</u>  NR grooming  NR hole board  NR marble burying</p>	<p>Cre line primary: [307]</p> <p><i>Mecp2</i> studies: [275, 276]</p> <p><i>Scn1a</i> study: [277]</p>

Cre line (or "Tet-Off" line)	Commercial availability	Cells targeted	Timing of gene expression manipulation	Social communication phenotypes	Repetitive behavior phenotypes	References
SOM-cre	JAX 013044	SOM+ GABAergic neurons	Embryonic	<p><i>Mecp2 (loxP/y)</i> ↔ sociability** NR social novelty NR USVs NR nest building</p> <p><i>Scn1a (loxP/+)</i> ↔ sociability* NR social novelty NR USVs NR nest building</p>	<p><i>Mecp2 (loxP/y)</i> NR grooming ↑ hole board NR marble burying</p> <p><i>Scn1a (loxP/+)</i> NR grooming NR hole board NR marble burying</p>	<p>Cre line primary: [308]</p> <p><i>Mecp2</i> study: [275]</p> <p><i>Scn1a</i> study: [277]</p>
PET-1 cre	JAX 012712	All serotonergic neurons	Embryonic	<p><i>Mecp2 (loxP/y)</i> ↑ sociability** ↑ aggression**** NR social novelty NR USVs NR nest building</p>	<p><i>Mecp2 (loxP/y)</i> ↔ grooming NR hole board ↔ marble burying</p>	<p>Cre line primary: [309]</p> <p><i>Mecp2</i> study: [278]</p>
Slc6a4-cre	MMRRC 031028-UCD	All serotonergic neurons	Embryonic	<p><i>Tsc1 (loxP/loxP)</i> ↓ sociability* NR social novelty NR USVs NR nest building</p>	<p><i>Tsc1 (loxP/loxP)</i> NR grooming NR hole board ↑ marble burying</p>	<p>Cre line primary: [309]</p> <p><i>Tsc1</i> study: [269]</p>

Cre line (or "Tet-Off" line)	Commercial availability	Cells targeted	Timing of gene expression manipulation	Social communication phenotypes	Repetitive behavior phenotypes	References
TH-cre	EMMA 00254	All dopaminergic neurons	Embryonic	<i>Mecp2 (loxP/y)</i> ↔ sociability** ↔ aggression**** NR social novelty NR USVs NR nest building	<i>Mecp2 (loxP/y)</i> NR grooming NR hole board NR marble burying	Cre line primary: [310]  <i>Mecp2</i> study: [278]
Chat-cre	JAX 006410	All cholinergic neurons	Embryonic	<i>Mecp2 (loxP/y)</i> ↓ sociability**** ↓ social novelty* NR USVs ↓ nest building	<i>Mecp2 (loxP/y)</i> NR grooming NR hole board NR marble burying	Cre line primary: [311]  <i>Mecp2</i> study: [282]
Oxt-cre	JAX 024234	All oxytocinergic neurons	Embryonic	<i>Pten (loxP/+)</i> and <i>Pten (loxP/loxP)</i> ↔ sociability*, *** ↔ social novelty*, *** NR USVs NR nest building	<i>Pten (loxP/+)</i> and <i>Pten (loxP/loxP)</i> NR grooming NR hole board ↔ marble burying	Cre line primary: [312]  <i>Pten</i> study: [283]

Cre line (or “Tet-Off” line)	Commercial availability	Cells targeted	Timing of gene expression manipulation	Social communication phenotypes	Repetitive behavior phenotypes	References
L7-cre	JAX 004146	Cerebellar Purkinje cells	Early postnatal	<p><u>Tsc1 (loxP/+)</u> and <u>Tsc1 (loxP/loxP)</u>  ↓ sociability*  ↓ social novelty*  NR USVs  NR nest building</p> <p><u>Tsc2 (loxP/-)</u>  ↓ sociability*  ↓ social novelty*  NR USVs  NR nest building</p> <p><u>Pten (loxP/loxP)</u>  ↓ sociability*  NR social novelty  NR USVs  NR nest building</p> <p><u>Shank2e6-7 (loxP/loxP)</u>  ↓ sociability*  ↓ social novelty*  NR USVs  NR nest building</p>	<p><u>Tsc1 (loxP/+)</u> and <u>Tsc1 (loxP/loxP)</u>  ↑ grooming  NR hole board  NR marble burying</p> <p><u>Tsc2 (loxP/-)</u>  NR grooming  NR hole board  ↑ marble burying</p> <p><u>Pten (loxP/loxP)</u>  ↓ grooming  NR hole board  NR marble burying</p> <p><u>Shank2e7 (loxP/loxP)</u>  ↔ grooming  NR hole board  ↔ marble burying</p>	<p>Cre line primary: [313]</p> <p><i>Tsc1</i> study: [289]</p> <p><i>Tsc2</i> study: [290]</p> <p><i>Pten</i> study: [291]</p> <p><i>Shank2</i> study: [292]</p>
Pcp2-cre	JAX 010536	Cerebellar Purkinje cells	Early postnatal	<p><u>Shank2e7 (loxP/loxP)</u>  ↔ sociability*  ↔ social novelty*  ↔ adult USVs  NR nest building</p>	<p><u>Shank2e6-7 (loxP/loxP)</u>  ↔ grooming  ↑ hole board  ↔ marble burying</p>	<p>Cre line primary: [314]</p> <p><i>Shank2</i> study: [293]</p>

Cre line (or "Tet-Off" line)	Commercial availability	Cells targeted	Timing of gene expression manipulation	Social communication phenotypes	Repetitive behavior phenotypes	References
Gfap-cre	N/A	Mostly cerebellar granule cells, few hippocampal neurons	Unclear	<u><i>Pten (loxP/loxP)</i></u> ↓ sociability*, ** NR social novelty ↔ pup USVs NR nest building	<u><i>Pten (loxP/loxP)</i></u> NR grooming ↓ hole board ↓ marble burying	Cre line primary: [315]  <i>Pten</i> study: [114]

Cre line (or "Tet-Off" line)	Commercial availability	Cells targeted	Timing of gene expression manipulation	Social communication phenotypes	Repetitive behavior phenotypes	References
CAGGS-CreER	JAX 004453	Ubiquitous	Concurrent with tamoxifen administration (P60+ for all examples)	<p><u>Mecp2 (loxP/y)</u> NR sociability NR social novelty NR USVs ↓ nest building</p> <p><u>Mecp2 (loxP-stop/y)</u> and <u>Mecp2 (loxP-stop/+)</u> NR sociability NR social novelty NR USVs ↓ nest building resc.</p> <p><u>Ube3a (loxP-stop/p+)</u> NR sociability NR social novelty NR USVs ↓ nest building no resc.</p> <p><u>Shank3 (loxP/loxP) inverted</u> ↓ sociability* resc. ↓ social novelty* resc. NR USVs NR nest building</p>	<p><u>Mecp2 (loxP/y)</u> NR grooming NR hole board NR marble burying</p> <p><u>Mecp2 (loxP-stop/y)</u> and <u>Mecp2 (loxP-stop/+)</u> NR grooming NR hole board NR marble burying</p> <p><u>Ube3a (loxP-stop/p+)</u> NR grooming NR hole board NR marble burying</p> <p><u>Ube3a (loxP-stop/p+)</u> NR grooming NR hole board ↓ marble burying no resc.</p> <p><u>Shank3 (loxP/loxP) inverted</u> ↑ grooming resc. NR hole board NR marble burying</p>	<p>Cre line primary: [316]</p> <p><i>Mecp2</i> deletion study: [295]</p> <p><i>Mecp2</i> rescue study: [296]</p> <p><i>Ube3a</i> study: [299]</p> <p><i>Shank3</i> study: [301]</p>

Cre line (or “Tet-Off” line)	Commercial availability	Cells targeted	Timing of gene expression manipulation	Social communication phenotypes	Repetitive behavior phenotypes	References
CaMKII-tTA	JAX 003010	Excitatory forebrain neurons	Concurrent with doxycycline administration (P60+ for this example)	<i>TRE-HAβnrxLAC</i> ↓ sociability* resc. ↓ social novelty* resc. NR USVs NR nest building	<i>TRE-HAβnrxLAC</i> ↑ grooming resc. NR hole board NR marble burying	Tet-Off line primary: [317]  <i>Nrxn1β</i> study: [300]

**Table Key:**

\* In the three chamber test

\*\* In the partition test

\*\*\* In the habituation/dishabituation test

\*\*\*\* In a direct social interaction test

NR: behavioral test not reported

↑: mutant mice have significantly elevated amounts of this behavior when compared to controls

↓: mutant mice have significantly decreased amounts of this behavior when compared to controls

↔: there were no significant differences between mutants and their controls on this behavioral test

resc.: abnormal phenotype was rescued with genetic manipulation

no resc.: genetic manipulation failed to rescue abnormal phenotype

JAX: The Jackson Laboratory

EMMA: The European Mouse Mutant Archive

MMRRC: Mutant Mouse Resource & Research Centers

### ***1.5 Attribution of work within this dissertation***

Portions of this dissertation were published previously [50, 171, 240, 318, 319] or will be used for future publications. A few experiments were conducted by others and are individually attributed as appropriate.

## **2. Behavioral characterization of *Shank3* and *Chd8* conventional mutant mice**

### ***2.1 Introduction***

Mutations in *SHANK3* and *CHD8* are among the most common and most well-replicated findings in genetic studies of ASD [154, 320-325]. Although these two genes are believed to have very different functions, as a postsynaptic density protein and a transcriptional regulator, the clinical diagnosis is similar. Modeling the mutations in mice is an important step to determine whether there is some overlapping molecular pathway that is disrupted, or whether there are multiple unrelated etiologies of ASD.

The most common *SHANK3* mutations involve deletion of the entire gene, which causes Phelan-McDermid syndrome, and these patients have high rates of ASD [326, 327]. The transcriptional complexity of the *SHANK3* gene, due to multiple intragenic promoters and alternative splice sites, makes small exonic deletions lack construct validity for the human condition [170]. Therefore, our lab created a mouse model that lacks all protein isoforms to best replicate the mutations observed in Phelan-McDermid syndrome [171]. Another lab took a similar approach and replicated our results [172]. The transcriptional regulation of *CHD8* is much less characterized, but mutations in patients are found throughout the gene, with various clinical phenotypes [324]. We therefore created a novel *Chd8* mutant mouse, which has unique behavioral phenotypes compared to previously published lines.

## **2.2 Methods**

### **2.2.1 Generation of mutant lines**

Generation of the *Shank3*  $\Delta e4-22^{-/-}$  mice is described in Wang et al. 2016 and was performed by Xiaoming Wang. The *Chd8* mutant line characterized in this dissertation is currently unpublished and was created by inserting a gene trap vector around exon 31. Embryonic stem cells (SIGTR ES cell line AY0061) were ordered from the Mutant Mouse Resource & Research Center. The gene trap vector used to generate these ES cells is shown in Figure 1. ES cells were injected into C57BL/6J blastocysts for germline transmission as described [134]. The offspring with the mutation were identified by genotyping with PCR and were subsequently backcrossed onto a C57BL/6J background for more than 5 generations. Homozygous mutants are embryonic lethal, but heterozygous mutants, which are haploinsufficient for the full-length protein (Figure 2) were used for subsequent behavioral phenotyping.

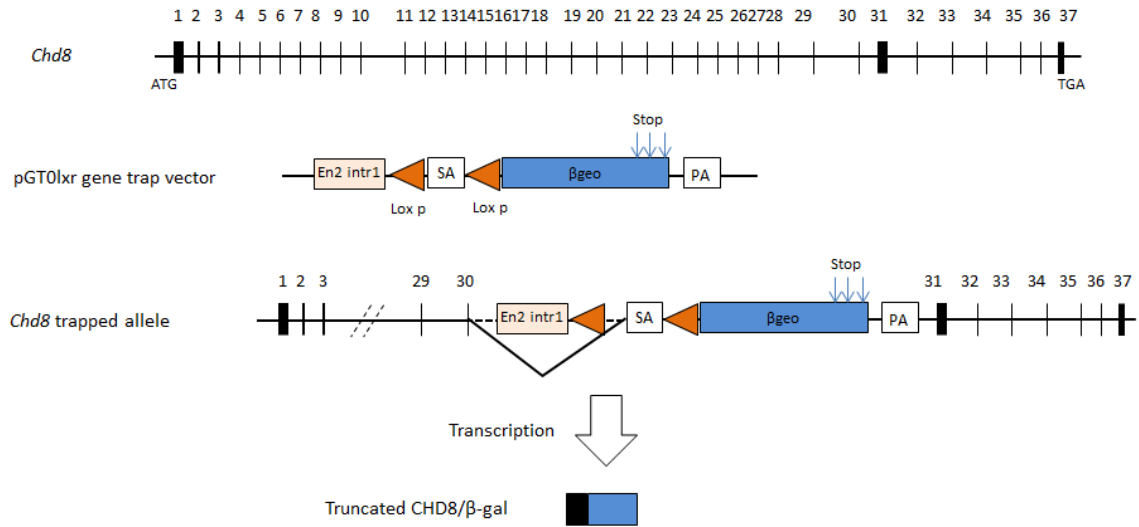


**Figure 1: Generation of *Chd8* mutant mice.**

The pGT01xr gene trap vector was inserted around exon 31 of *Chd8*. Intron 1 of *Engrailed2* (*En2 intr1*) and the following splice acceptor (SA) site are recognized by transcriptional machinery and as a result, *LacZ* ( $\beta$ geo) is incorporated into the immature mRNA. At the end of the  $\beta$ geo cassette are three stop codons which terminate translation of the mRNA, which forms a CHD8/ $\beta$ -gal fusion protein. This figure was made by Xiaoming Wang.

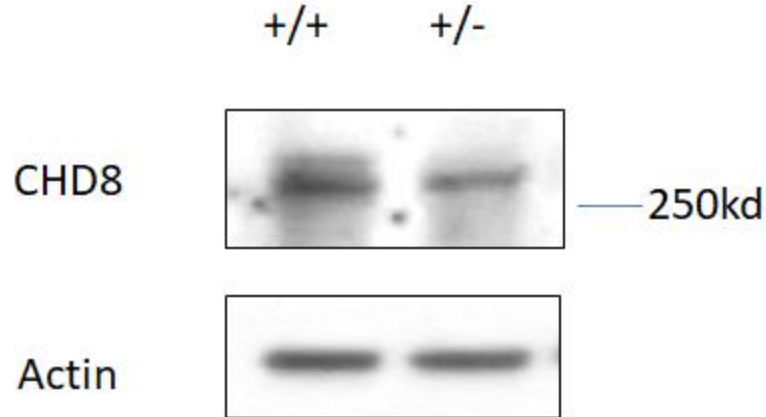


**Figure 2: *Chd8* mutant mice are haploinsufficient for CHD8**

**Western blot shows a reduction in expression of the full-length CHD8 protein (~290 kDa) in *Chd8* mutant (+/-) mice compared to wildtype (+/+) controls. This experiment was conducted by Xiaoming Wang.**

## 2.2.2 Behavioral phenotyping

### 2.2.2.1 Cohorts for behavioral assays

Data I collected from one of my *Shank3*  $\Delta e4-22^{-/-}$  cohorts was used for the Wang et al. 2016 manuscript, which was published as “Cohort 6.” This data was combined with data from the same assays on other cohorts, tested by Alexandra Bey. For this cohort, heterozygous crosses were used to produce male  $\Delta e4-22^{+/+}$ ,  $\Delta e4-22^{+/-}$ , and  $\Delta e4-22^{-/-}$  littermates. I produced another cohort of *Shank3* heterozygous mice and wildtype littermates by crossing  $\Delta e4-22^{+/-}$  with C57BL/6J mice to test for an effect of parental origin on heterozygous mice of both sexes. In addition, I generated two cohorts of mixed sex *Chd8* mutant mice for behavioral testing by

crossing *Chd8*<sup>+/-</sup> mice with C57BL/6J mice. For the first cohort, I crossed male *Chd8*<sup>+/-</sup> mice with female C57BL/6J mice and for the second I crossed female *Chd8*<sup>+/-</sup> mice with male C57BL/6J mice, again to test for a potential parental origin effect. There were no differences between cohorts, so I pooled the data together. I also intercrossed the first cohort together and used their offspring for pup USVs. In all cases, mice were tested beginning at two months of age, except for the pup USVs, which were done at postnatal day 4 (P4). The number of mice and behavior assays, in order of testing, are presented in Table 5. All handling of mice and scoring of behavior was done blind to genotype. Mice were housed 4-5 per cage on a 14 hour light and 10 hour dark cycle, with all testing except for social dyadic done during the light cycle.

**Table 5: Cohorts and order of behavior testing for *Shank3* and *Chd8* mutant mice**

Wang et al. 2016 <i>Shank3</i> Δe4-22 <sup>-/-</sup> “Cohort 6”	<i>Shank3</i> Δe4-22 <sup>m-/p+</sup> and Δe4-22 <sup>m+/p-</sup> Cohort	<i>Chd8</i> <sup>m+/p-</sup> Cohort	<i>Chd8</i> pup USVs Cohort	<i>Chd8</i> <sup>m-/p+</sup> Cohort
+/+ n = 5 +/- n = 5 -/- n = 6	+/, n = 28 m-/p+, n = 19 m+/p-, n = 16	+/, n = 19 +/-, n = 15	+/, n = 15 +/-, n = 16	+/, n = 10 +/-, n = 5
Adult USVs	Neonatal Nest Preference	Open Field	Pup USVs	Light-Dark Emergence
Social Dyadic	Elevated Zero Maze	Grooming		Elevated Zero Maze
	Open Field	Elevated Zero Maze		Accel. Rota-rod
	Accel. Rota-rod	Light-Dark Emergence		Steady Speed Rota-rod
		Accel. Rota-rod		Open Field
		Steady Speed Rota-rod		Grooming
		Operant Conditioning		3-chamber
		3-chamber		Operant Conditioning
		Adult USVs (males only)		Adult USVs (males only)

### **2.2.2.2 Three chamber test for sociability and social novelty**

Mice were tested in the 3-chamber assay as described with a few modifications [328]. Testing was conducted in a white acrylic apparatus with no walls dividing the chambers and two stainless-steel wire-mesh cages (10 cm diameter x 11 cm high; Rolodex, Oak Brook, IL) each stabilized with a 28 g steel sinker (Cabella, Oshkosh, NE) to prevent the cage from being repositioned. Age- and sex-matched C3H/HeJ mice (Charles River) were used as friendly conspecific social stimuli. The chambers and cages were all cleaned between each test mouse with LabSan 256CPQ solution (Sanitation Strategies LLC, Williamston, MI). Testing was divided into three phases. During each test phase, the cages were placed in the center of the two outer thirds of the chamber. The first phase began when a test mouse was placed into the center of the chamber and given free exploration of the apparatus, and the two cages contained non social stimuli. After 10 minutes, the test mouse was removed and a C3H stimulus mouse was placed into one of the wire-mesh cages, replacing one of the non-social stimuli. The second phase (sociability) began with reintroduction of the test mouse into the center of the chamber. After 10 minutes, the test mouse was removed and a novel C3H mouse replaced the remaining non-social stimulus. The test mouse was reintroduced into the chamber for the third phase (social novelty), which also lasted 10 minutes. All tests were filmed and the digital videos were analyzed subsequently using EthoVision software (Noldus) that included the frequency and duration of contacts with each cage. Preference scores were calculated, where time spent with one stimulus (non-social stimulus 1, social stimulus 1, or novel social stimulus 2) was subtracted from the time spent with the other stimulus (non-social stimulus 2, non-social stimulus, and familiar social

stimulus 1, respectively) and divided by the total time spent exploring both stimuli. Positive scores indicate a preference for the novel social stimulus relative to the non-social or familiar social stimulus, negative scores reflect preference for the non-social or familiar stimulus, and scores approximating “0” indicate no preference.

### **2.2.2.3 Social dyadic**

Male mice were individually housed for at least 14 days prior to testing, which was performed under red-light illumination (< 5 lux) 2-6 hours after onset of the dark cycle. Plexiglass chambers (48 x 26 x 20 cm) were filled with 1/8” cob bedding. The test mouse and a sex- and age-matched C3H mouse were placed on opposite sides of the test chamber separated by a solid partition. After habituating for five minutes, the partition was removed so the two mice could interact freely. Interactions were filmed for 10 minutes and the plexiglass test chambers were cleaned between each test with LabSan 256CPQ solution (Sanitation Strategies LLC, Williamston, MI) and were refilled with the cob bedding. The videos were scored using Observer XT 9 software for time spent engaging in bidirectional social interaction and non-reciprocated interaction, where the test mouse attempted to interact with the C3H mouse.

### **2.2.2.4 Adult ultrasonic vocalizations**

Male mice were given breeding experience with an age-matched female mouse for at least four days (the duration of the estrous cycle) and then were individually housed for at least 24 hours. For testing, the male mice were placed in a sound-attenuating styrofoam chamber equipped with an externally polarized condenser CM16/CMPA microphone with a frequency range of 10-200 kHz (Avisoft Bioacoustics Inc.) suspended 20 cm above the floor of the

chamber. After the test mouse acclimated for 10 minutes, an 8-10 week old virgin female C57BL/6J mouse (Jackson Labs) was added to the chamber and vocalizations were recorded for five minutes as waveform audio files using Avisoft-RECORDER. The files were analyzed later using Avisoft SASLab Pro software. Mice that did not call were excluded from analysis.

#### **2.2.2.5 Pup ultrasonic vocalizations**

Postnatal day four (P4) pups were briefly separated their mothers and placed in the chambers described in the previous section. Vocalizations were recorded and analyzed as before, but the neonatal mice did not require any acclimatization time and vocalizations were recorded for one minute instead of five.

#### **2.2.2.6 Neonatal nest preference**

Postnatal day 15 (P15) pups were given a choice between their mother's nest and the nest of a stranger with pups at the same developmental age. Two cubic centimeters of each nest were placed at opposite ends of a clean cage. A single pup was placed in the center of the cage and given one minute to find its home nest. If the pup failed to find the home nest after 60 seconds or chose the stranger nest instead, the latency to enter the home nest was recorded as 60 seconds. If the pup chose the home nest within 60 seconds, the time it took to enter the nest was recorded.

#### **2.2.2.7 Self-grooming**

Individual animals were placed into clean home cages without bedding and acclimated for five minutes. Mice were filmed for 10 minutes and then videos were later manually scored for time spent grooming.

#### **2.2.2.8 Hole-board**

Mice were placed individually into a 42 x 42 x 30 cm plexiglass container containing a 42 x 42 x 3 cm hole-board apparatus made of white plexiglass with 16 equidistant holes 3 cm in diameter. Animals were hand-scored live for sequence and location of nose-pokes into the holes.

#### **2.2.2.9 Elevated zero maze**

Mice were placed in a closed portion of the elevated zero maze and were allowed five minutes of exploration under dim (40-60 lux) illumination. Activity was measured by Ethovision XT 7 (Noldus) using a high-resolution camera suspended two meters above the maze. Tracking profiles generated by Ethovision were used to calculate time spent in open and closed portions of the maze.

#### **2.2.2.10 Dark-light emergence**

Mice were placed into a dark side of a 2-chamber apparatus (Med-Associates, St. Albans, VT) consisting of a dark chamber and a light chamber and were allowed 5 minutes to freely explore the dark (< 2 lux) and heavily lit (> 750 lux) chambers. Infrared diodes within the test chamber tracked the location and activity of the mouse throughout testing. The behaviors tracked by the Med-Associates software included the latency to enter the well-lit chamber and the time spent in each of the dark and light chambers.

#### **2.2.2.11 Rotarod**

Performance on the rotarod (Med-Associates) was assessed over four trials lasting five minutes each. The intertrial interval was 30 minutes. In the accelerating condition, the rod started at four rotations per minute (RPM) and slowly increased to 40 RPM over the five minute trial. In

the steady state condition, the rod maintained either 20 RPM or 32 RPM, depending on how well the mice performed during the accelerating condition. Graphs showing the steady speed data are labeled accordingly with which speed was chosen.

#### **2.2.2.12 Open field locomotion**

Activity in the open field was measured for 1 hour in an automated Omnitech Digiscan apparatus (AccuScan Instruments, Columbus, OH). AccuScan software calculated the total distance traveled and time spent in the center of the arena.

#### **2.2.2.13 Operant conditioning**

Mice were food restricted until they reached approximately 85% of their original body weight. Individual operant conditioning chambers (Med-Associates) were equipped with a retractable lever and a liquid dipper that delivered a drop of sweetened condensed milk as a food reward. The Med-PC-IV program was used to create the reinforcement schedule and record the data. The paradigm consisted of seven days of continuous reinforcement (one lever press earned one drop of sweetened condensed milk every time). Each session began with illumination of the chamber and presentation of the lever and ended with extinguishing the light and retracting the lever. Trials ended after either one of two conditions had been satisfied: 60 minutes had passed or the mouse had pressed the lever 100 times.

## ***2.3 Results***

### **2.3.1 *Shank3* $\Delta e4-22^{-/-}$ mice have impaired social communication**

Social communication deficits are a core feature of ASD. Thus, a mouse model with strong face validity will show impairments on assays meant to assess social interaction and communication. In the social dyadic test, *Shank3*  $\Delta e4-22^{-/-}$  mice spent more time trying to engage with the social stimulus when these interactions were non-reciprocated compared to both wildtype and heterozygous mice (Figure 3).

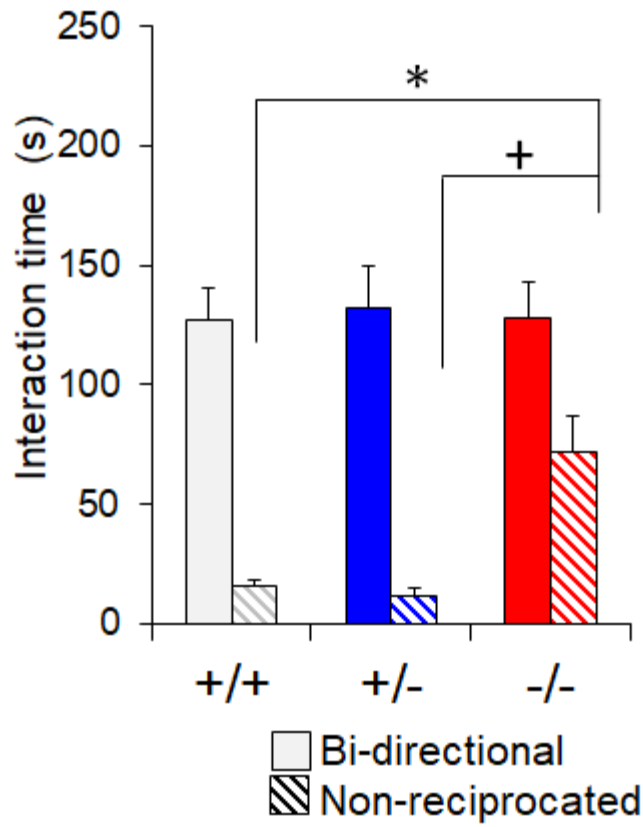


**Figure 3: *Shank3*  $\Delta e4-22^{-/-}$  mice show abnormal social interaction in the social dyadic test.**

No genotype differences were observed in the duration of bidirectional contact between the test mouse and the social stimulus, but *Shank3*  $\Delta e4-22^{-/-}$  mice spent more time attempting to engage in contact that was not reciprocated compared to wildtype and heterozygous mice [F(2,37)=11.30, p<0.001]; n=10-15/genotype. Data represent means  $\pm$  SEM. \* signifies a significant difference between  $\Delta e4-22^{-/-}$  and +/+ mice and + signifies a significant difference between  $\Delta e4-22^{-/-}$  and  $\Delta e4-22^{+/-}$  mice. This figure was made by Alexandra Bey.

For USVs, *Shank3*  $\Delta e4-22^{-/-}$  mice showed a reduction in the number of calls (Figure 4a) as well as a reduction in the average duration of these calls (Figure 4b) compared to both wildtype and heterozygous littermates.

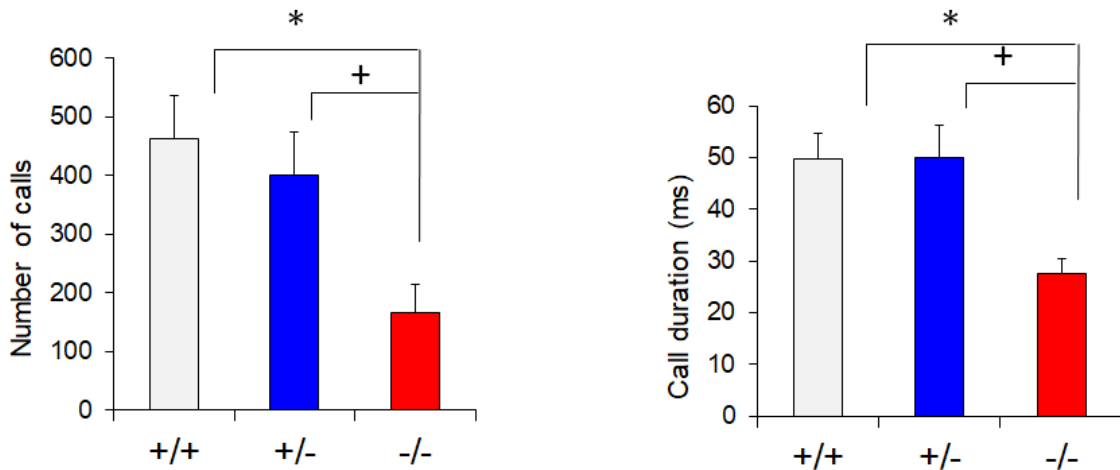


**Figure 4: *Shank3*  $\Delta e4-22^{-/-}$  mice show impairments in ultrasonic vocalizations.**

Adult -/- males emitted fewer USVs (a) [ $F(2,38)=6.15$ ,  $p<0.01$ ] that were of significantly shorter duration (b) [ $F(2,34)=7.12$ ,  $p<0.01$ ] than the other genotypes ( $ps<0.02$ ). Data represent means  $\pm$  SEM. \* signifies a significant difference between  $\Delta e4-22^{-/-}$  and +/+ mice and + signifies a significant difference between  $\Delta e4-22^{-/-}$  and  $\Delta e4-22^{+/-}$  mice. This figure was made by Alexandra Bey.

### 2.3.2 The *Shank3* $\Delta e4-22^{+/-}$ phenotype is independent of parental origin

A puzzling finding from our initial characterization of the  $\Delta e4-22$  mice was that heterozygous mice showed a very mild, if any, phenotype, even though Phelan-McDermid syndrome results from one missing copy of the *SHANK3* gene. One possible explanation for this

is a parental origin effect. It is known that some genes show unequal expression of the maternal and paternal alleles (sometimes in a tissue-specific manner such as in Angelman syndrome; see section 1.3.2.4), thus causing different phenotypes depending on whether the mutation is inherited from the mother or the father [329]. Since Prader-Willi syndrome and Angelman syndrome are dependent on parental origin and since patients with these syndromes often meet the diagnostic criteria for ASD, it is reasonable to suspect that other forms of ASD may also be susceptible to parent-of-origin effects. Therefore, we tested whether the *Shank3*  $\Delta e4-22^{+/-}$  mice had a phenotype that was dependent on the inheritance pattern of the mutation.

*Shank3*  $\Delta e4-22^{+/-}$  mice showed significantly reduced spontaneous motor activity in the open field compared to wildtype mice, regardless of whether the null allele was inherited from the mother or the father (Figure 5). The two groups of heterozygous mice were not significantly different than one another. Homozygous deletion of *Shank3* exons 4-22 results in profound hypoactivity in the open field to a greater extent than heterozygous deletion [171, 172, 318].

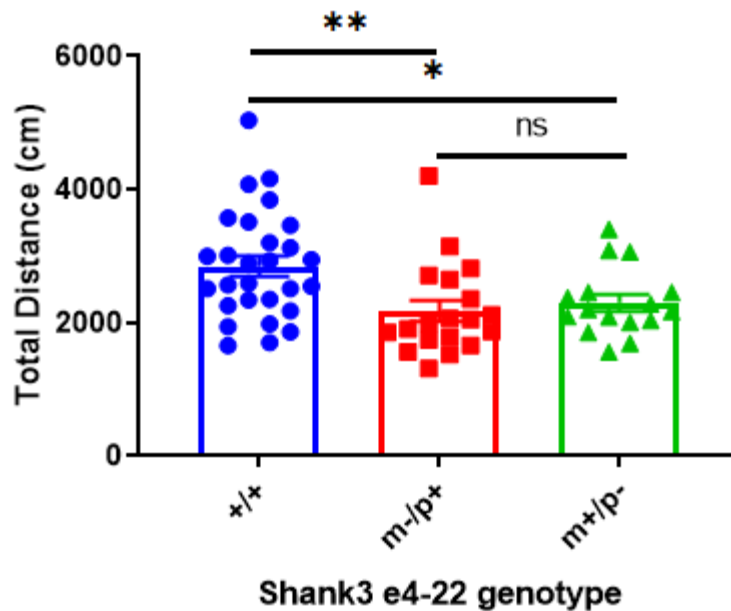


**Figure 5: Heterozygous *Shank3*  $\Delta$ e4-22 mice show mild hypoactivity in the open field, regardless of the parental origin of the mutation.**

**Both m-/p+ and m+/p- mice were significantly hypoactive compared to +/+ mice, but were not significantly different than one another (one-way ANOVA,  $p < 0.01$ ; Tukey's posthoc comparisons +/+ vs. m-/p+,  $p < 0.01$ ; +/+ vs. m+/p-,  $p < 0.05$ ; m-/p+ vs. m+/p-,  $p > 0.05$ ).**

**Individual data points are superimposed onto bar graphs with error bars representing means  $\pm$  SEM. \* represents  $p < 0.05$ . \*\* represents  $p < 0.01$ . "ns" stands for not significant.**

*Shank3*  $\Delta$ e4-22<sup>+/-</sup> and wildtype mice spent a similar amount of time in the center of the arena and this was independent of the parental origin of the null allele (Figure 6). However, homozygous deletion of *Shank3* exons 4-22 results in thigmotaxis, or decreased time spent in the center of the open field arena [171, 318].

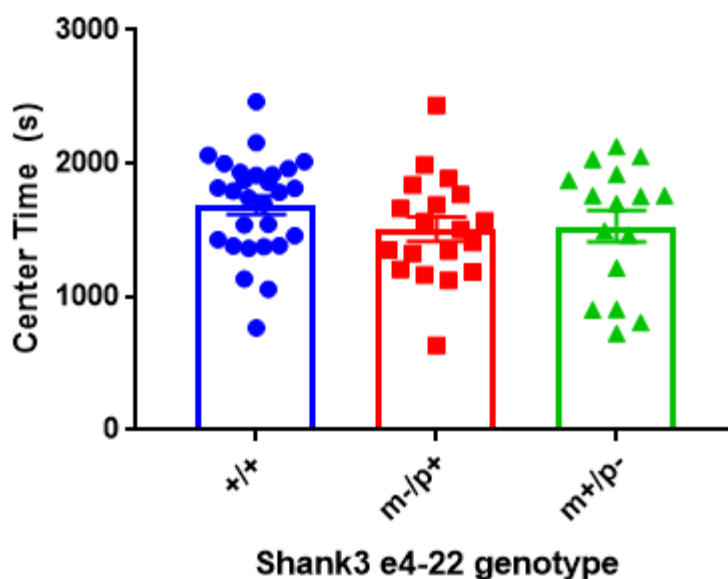


**Figure 6: Parental origin of *Shank3*  $\Delta$ e4-22 mutation does not affect the lack of thigmotaxis phenotype in heterozygous mice.**

**There was no effect of genotype on time spent in the center of the open field (one-way ANOVA,  $p > 0.05$ ). Individual data points are superimposed onto bar graphs with error bars representing means  $\pm$  SEM.**

*Shank3*  $\Delta$ e4-22<sup>+/-</sup> mice tend to spend more time in the open areas of the elevated zero maze, but these differences were not significant and were not dependent on parental origin of the mutation (Figure 7). We previously reported that heterozygous and homozygous mutations have similar effects on performance in the zero maze [318].

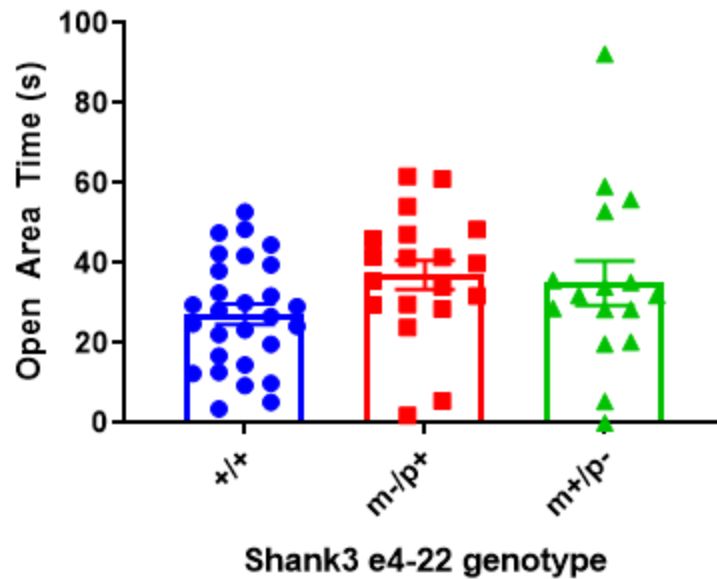


**Figure 7: Parental origin of *Shank3*  $\Delta e4-22$  mutation does not influence the tendency to spend more time in the open areas of the elevated zero maze**

**Both groups of heterozygous mice trended towards spending more time in the open areas of the elevated zero maze, but these differences were not significant (one-way ANOVA,  $p > 0.05$ ). Individual data points are superimposed onto bar graphs with error bars representing means  $\pm$  SEM.**

*Shank3*  $\Delta e4-22^{-/}$  mice showed impaired ability to distinguish between their home nest and a stranger's nest in the neonatal nest preference test, but heterozygous mice were not significantly different than wildtype mice [171]. The lack of phenotype in heterozygous mice holds true whether the null allele is inherited from the pup's father or the pup's mother (Figure 8).

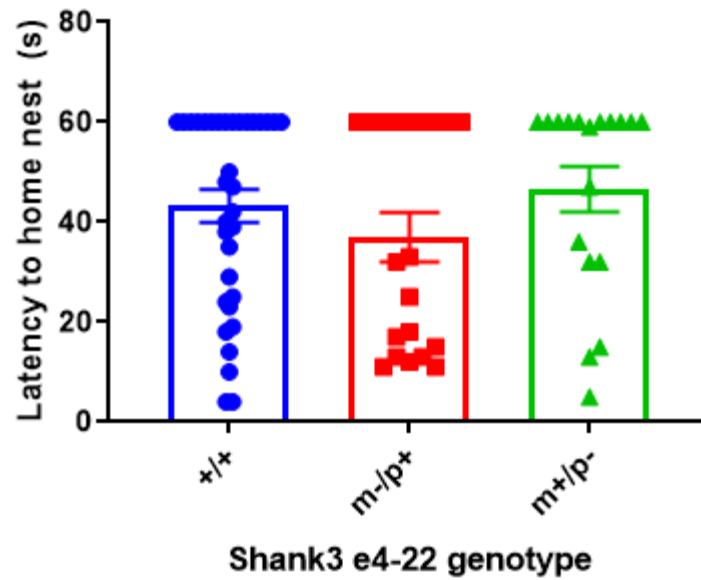


**Figure 8: Parental origin of *Shank3*  $\Delta$ e4-22 mutation does not influence the neonatal nest preference test**

**There were no significant differences on performance in the nest preference test between wildtype mice or either group of heterozygous mice (one-way ANOVA,  $p > 0.05$ ). Individual data points are superimposed onto bar graphs with error bars representing means  $\pm$  SEM.**

*Shank3*  $\Delta$ e4-22<sup>-/-</sup> have impaired performance on the accelerating rotarod, but heterozygous mice perform statistically the same as wildtype mice [171]. The lack of phenotype in heterozygous mice holds true regardless of parental origin of the mutation (Figure 9).

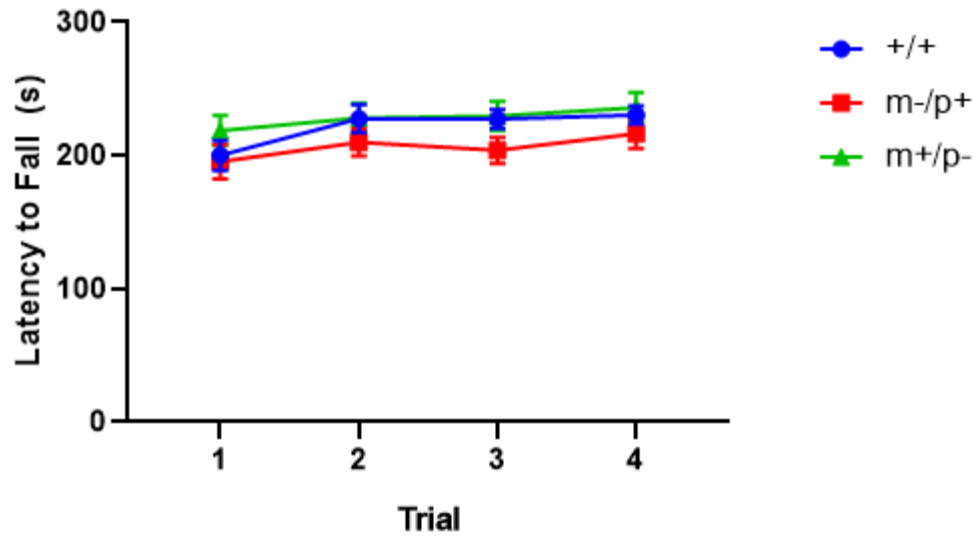


**Figure 9: Parental origin of *Shank3*  $\Delta e4-22$  mutation does not influence performance on the accelerating rotarod.**

**There was no significant effect of genotype on the accelerating rotarod (4-40 RPM; RMANOVA, effect of genotype  $p > 0.05$ ). Data represents means  $\pm$  SEM.**

### **2.3.3 *Chd8* mutant mice present with alterations in USVs and motor function**

Our homozygous *Chd8* mutant mice are embryonic lethal, consistent with previously published *Chd8* mutant lines [51, 52, 330-332]. However, behavioral phenotyping of the heterozygous mutants, which have strong construct validity for the human disorder, from these different lines has produced inconsistent results, as summarized in Table 6 and graphically represented in Table 7.

**Table 6: Summary of behavioral phenotyping of *Chd8* mutant lines.**

**Red text represents significant differences, whereas black text represents no change in a given phenotype.**

Reference	Mutation	Sex, Age, and Genetic Background of Mice Tested	Repetitive Behavior	Social Behavior	Ultrasonic Vocalizations	Anxiety-like Behavior	Motor Function	Learning and Memory	Other
Our mice	Gene trap around exon 31	Male + female, except only males for adult USVs  8-12 weeks, except for pup USVs at P4  C57Bl/6J	↔Self-grooming (n = 20-29)	↔ 3-chamber sociability (n = 20-29)  ↔ 3-chamber social novelty (n = 20-29)	↔ Call number in adults (n = 7-12)  ↑ Call length in adult (male) USVs (n = 7-12)  ↑ Call number in P4 USVs (n = 15-16)  ↔ Call length in P4 USVs (n = 15-16)	↔ Center time in open field (n = 20-29)  ↔ Latency to enter light in LDE (n = 20-29)  ↔ Time in light chamber in LDE (n = 20-29)  ↔ Time in open arms of EZM (n = 20-29)	↑ Accelerating rota-rod (n = 20-29)  ↑ Steady speed rota-rod (n = 20-29)  ↔ Activity in open field (n = 20-29)	↔ Operant conditioning (n = 20-27)	↔ Body weight (n = 23-26)

[52]	Frameshift knock-in at exon 36	<p>Male + female for pup and juvenile behaviors, males only for adult behaviors</p> <p>P5, P7, P9, and P11 for pup USVs</p> <p>P19 for maternal attachment</p> <p>P21-26 for open field, juvenile play, repetitive behaviors</p> <p>8-9 weeks for isolation-induced grooming,</p> <p>Age for other tests in adulthood not specified.</p> <p>C57Bl/6J</p>	<p>↑ Self-grooming after social isolation in males only (n = 24-26)</p> <p>↔ Self-grooming under standard conditions in juveniles (n = 17-22)</p> <p>↔ Digging or jumping behavior in juveniles (n = 17-22)</p>	<p>↑ Maternal attachment at P19 in males only (n = 14-22)</p> <p>↔ Juvenile play duration (n = 6-11 pairs)</p> <p>↔ 3-chamber sociability (n = 15)</p> <p>↔ 3-chamber social novelty (n = 15)</p> <p>↔ Duration of contacts in direct social interaction (n = 6 pairs)</p> <p>↔ Nest building (n = 6 cages)</p>	<p>↑ Call number in P5 USVs in males only (n = 31-38)</p> <p>↔ Call number in P7, P9, or P11 USVs (n = 31-38)</p> <p>↓ Latency to first call in P7, P9, and P11 USVs in males only (n = 31-38)</p> <p>↔ Latency to first call in P5 USVs (n = 31-38)</p> <p>↔ Call number in adults (n = 13-14)</p> <p>↔ Call duration in adults (n = 13-14)</p>	<p>↔ Center time in open field for juveniles (n = 34-40)</p> <p>↔ Time spent in open arms of EPM (n = 12)</p> <p>↔ Time in light chamber in LDE (n = 12)</p>	<p>↓ Activity in open field for juveniles (n = 34-40)</p> <p>↔ Accelerating rota-rod (n = 12)</p>	<p>↔ Novel object recognition (n = 12)</p> <p>↔ Morris Water Maze acquisition (n = 12)</p> <p>↔ Morris Water Maze reversal (n = 12)</p> <p>↔ Contextual fear conditioning (n = 9)</p>	<p>↑ Brain volume (n = 30)</p> <p>↔ Body weight (n = 7-19)</p> <p>↔ Tail suspension test (n = 12)</p>
------	--------------------------------	----------------------------------------------------------------------------------------------------------------------------------------------------------------------------------------------------------------------------------------------------------------------------------------------------------------------------------------------------------	-----------------------------------------------------------------------------------------------------------------------------------------------------------------------------------------------------------------	-----------------------------------------------------------------------------------------------------------------------------------------------------------------------------------------------------------------------------------------------------------------------------------------------------------------	--------------------------------------------------------------------------------------------------------------------------------------------------------------------------------------------------------------------------------------------------------------------------------------------------------------------------------------------------	--------------------------------------------------------------------------------------------------------------------------------------------------------------	---------------------------------------------------------------------------------------------------	---------------------------------------------------------------------------------------------------------------------------------------------------------------------------------------	-------------------------------------------------------------------------------------------------------

[330]	Deletion of exon 3 via Cre-loxP gene targeting	Male + female  9-22 weeks, except for motor development and USVs assessed in pups at P2, P4, P6, P8, and P12  C57Bl/6J	↔ Self-grooming (n = 29-30)  ↔ Marble burying (n = 29-30)	↔ 3-chamber sociability (n = 29-30)  ↑ Duration of contacts during direct social interaction (n = 29-30)	↔ Call number at P2, P4, P6, P8, and P12 (n = 31-42)	↔ Center time in open field (n = 29-30)  ↔ Time in light chamber in LDE (n = 29-30)	↓ Righting reflex P2-P12 (n = 31-42)  ↑ Locomotion at P12 (n = 31-42)  ↓ Activity in open field (n = 29-30)  ↓ Running wheel activity (n = 29-30)  ↓ Forelimb grip strength (n = 14-16)  ↔ Accelerating rota-rod (n = 29-30)	↔ Morris Water Maze acquisition (n = 29-30)  ↔ Morris Water Maze reversal (n = 29-30)	↑ Brain volume (n = 11-12)  ↓ Body weight (n = 27-46)  ↑ Brain weight at P35 (n = 27-46)  ↑ Brain weight at P0 and P7 (n = 14-18)
-------	------------------------------------------------	------------------------------------------------------------------------------------------------------------------------------------	-----------------------------------------------------------------	----------------------------------------------------------------------------------------------------------------	------------------------------------------------------	-------------------------------------------------------------------------------------------	------------------------------------------------------------------------------------------------------------------------------------------------------------------------------------------------------------------------------------------------------------	---------------------------------------------------------------------------------------------	-----------------------------------------------------------------------------------------------------------------------------------------------------

[331]	CRISPR/Cas9-mediated frameshift deletion in exon 5	Male + female, except only males for direct social interaction and USVs  6-16 weeks  C57Bl/6N	↔ Self-grooming (n = 20)  ↔ Marble burying (n = 20)	↔ 3-chamber sociability (n = 19-20)  ↔ 3-chamber social novelty (n = 19-20)  ↔ Duration of contacts during direct social interaction (n = 9-10)	↔ Call number (n = 9-10)	NR	↔ Activity in open field (n = 20)	↓ Contextual fear conditioning (n = 19-20)  ↓ Tone fear conditioning (n = 19-20)  ↓ Novel object recognition (n = 19-20)	↑ Brain volume (n = 18-19)
[51]	CRISPR/Cas9-mediated frameshift deletion in exon 1	Male only  10-14 weeks, except for juvenile play at P23-25  C57Bl/6J	↔ Self-grooming (n = 17)  ↔ Marble burying (n = 23-25)	↔ Number of contacts during juvenile play (n = 15-17)  ↑ Duration of contacts during juvenile play (n = 15-17)  ↔ 3-chamber sociability (n = 20-24)  ↓ 3-chamber social novelty (n = 20-24)	NR	↓ Center time in open field (n = 55-64)  ↑ Latency to enter light chamber in LDE (n = 19-25)  ↓ Time in light chamber in LDE (n = 19-25)	↑ Accelerating rota-rod (n = 10)  ↓ Activity in open field (n = 55-64)	↔ Contextual fear conditioning (n = 16-21)  ↔ Tone fear conditioning (n = 16-21)	↓ Body weight (n = 58-64)  ↑ Intraocular distance (n = 8)  ↑ Brain volume (n = 8)

<p>[332]</p>	<p>Deletion of exons 13-16 (“ΔL”)  AND  Deletion of 9 exons (“ΔSL”)</p>	<p>Male only  12-50 weeks  C57Bl/6J</p>	<p>↔ Self-grooming (n = 40)</p>	<p>↔ Nest building (n = 40)  ↔ 3-chamber sociability (n = 40)  ↓ 3-chamber social novelty (n = 40)  ↓ Number of contacts in direct social interaction (n = 40)  ↑ Duration of contacts in direct social interaction (n = 40)  ↓ Duration of “active” contacts in direct social interaction (n = 40)</p>	<p>NR</p>	<p>↓ Center time in open field (n = 40)  ↓ Time in light chamber in LDE (n = 40)  ↓ Time in open arms of EPM (n = 40)</p>	<p>↔ Accelerating rota-rod (n = 40)  ↔ Wire hang (n = 40)  ↔ Activity in open field (n = 40)</p>	<p>↔ T-maze discrimination (n = 19-20)  ↓ T-maze reversal (n = 19-20)  ↔ Barnes maze test (n = 40)</p>	<p>↑ Brain weight (n = 15)  ↔ Body weight (n = 15)  ↔ Forced swim test (n = 40)  ↔ Hot plate reaction (n = 40)  ↓ Intestine length (n = 30)  ↓ Startle response, ↑ PPI (n = 40)</p>
--------------	-----------------------------------------------------------------------------------------	---------------------------------------------------------	---------------------------------	-------------------------------------------------------------------------------------------------------------------------------------------------------------------------------------------------------------------------------------------------------------------------------------------------------------------------------------------------	-----------	-------------------------------------------------------------------------------------------------------------------------------------------	------------------------------------------------------------------------------------------------------------------	------------------------------------------------------------------------------------------------------------------------	-----------------------------------------------------------------------------------------------------------------------------------------------------------------------------------------------------------------------------

**Table 7: Representation of significant findings from *Chd8* behavioral phenotyping.**

**Cyan represents a significant decrease in a given behavior, whereas magenta represents a significant increase. Grey boxes represent no change or a nonsignificant difference in the reported behavior. White boxes represent a behavior that was not reported in the manuscript.**

Reference	Self-grooming	3-chamber sociability	3-chamber social novelty	Adult USVs	Pup USVs	Latency to Enter Light Chamber in LDE	Time Spent in Light Chamber in LDE	Elevated Zero or Elevated Plus Maze	Rotarod	Open Field Activity	Open Field Center Time	Body weight
[332]	Grey	Grey	Cyan	NR	NR	NR	Cyan	Cyan	Grey	Grey	Cyan	Grey
[51]	Grey	Grey	Cyan	NR	NR	Magenta	Cyan	NR	Magenta	Cyan	Cyan	Cyan
[331]	Grey	Grey	Grey	Grey	NR	NR	NR	NR	NR	Grey	NR	NR
[330]	Grey	Grey	NR	NR	Grey	NR	Grey	NR	Grey	Cyan	Grey	Cyan
[52]	Magenta	Grey	Grey	Grey	Magenta	NR	Grey	Grey	Grey	Cyan	Grey	Grey
Our mice	Grey	Grey	Grey	Magenta	Magenta	Grey	Grey	Grey	Magenta	Grey	Grey	Grey

Reduced body weight has been reported in two previous lines of *Chd8* mutant mice [51, 330]. However, two other previously reported lines have no difference in body weight compared to wildtype littermates [52, 332]. Our new line of mice falls into the latter group, with no genotype effect on body weight (Figure 10).

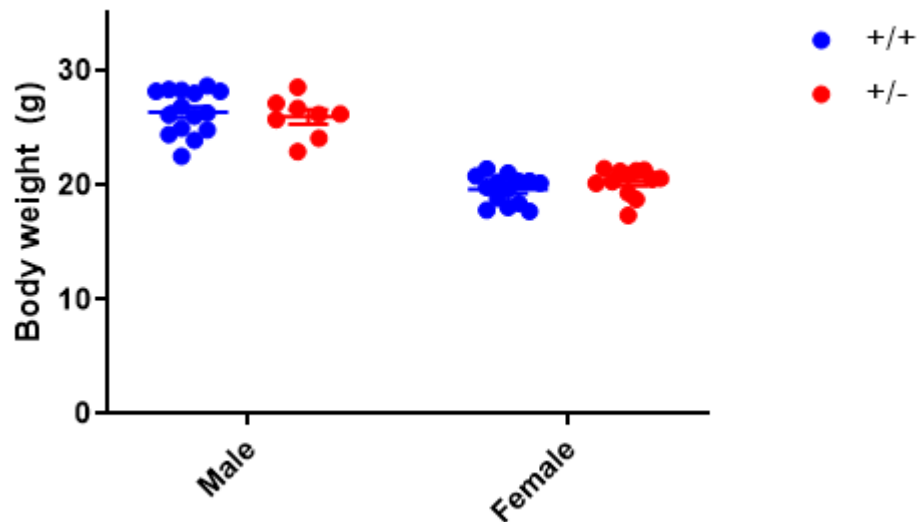


**Figure 10: *Chd8* mutant mice are similar in body weights to their sex-matched wildtype littermates**

**There is no effect of genotype on body weight (two-way ANOVA, effect of genotype  $p > 0.05$ ). Individual data points are superimposed onto means  $\pm$  SEM.**

Similarly, there have been conflicting reports of previous lines of *Chd8* mice in their activities in the open field. Some groups have reported hypoactivity in their lines [51, 52, 330], whereas others have reported no changes in activity [331, 332]. Our mice did not display hypoactivity and instead trended towards hyperactivity in the open field, although this difference was not significant (Figure 11).

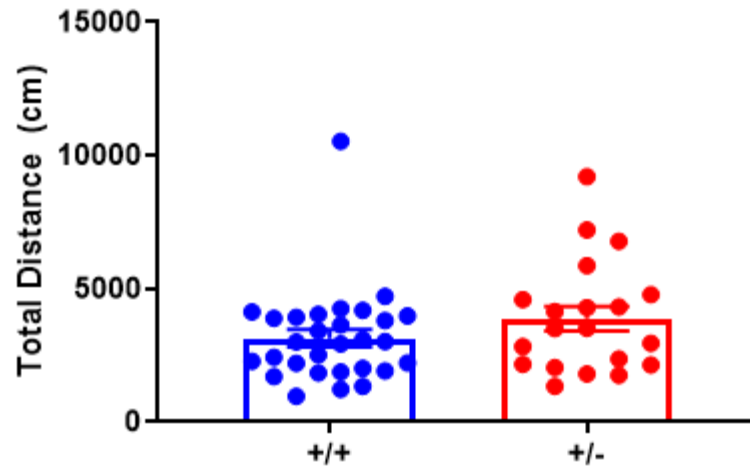


**Figure 11: *Chd8* mutant mice show normal levels of activity in the open field**

**Although mutant mice tended to travel farther in the open field, the difference between genotypes was not significant (unpaired t-test,  $p > 0.05$ ). Individual data points are superimposed onto bar graphs with error bars representing means  $\pm$  SEM.**

Likewise, some previous lines spend less time in the center of the open field compared to their wildtype littermates [51, 332], whereas others show no thigmotaxis [52, 330]. Our line of *Chd8* mutant mice shows no difference in time spent in the center of the open field compared to their wildtype littermates (Figure 12).

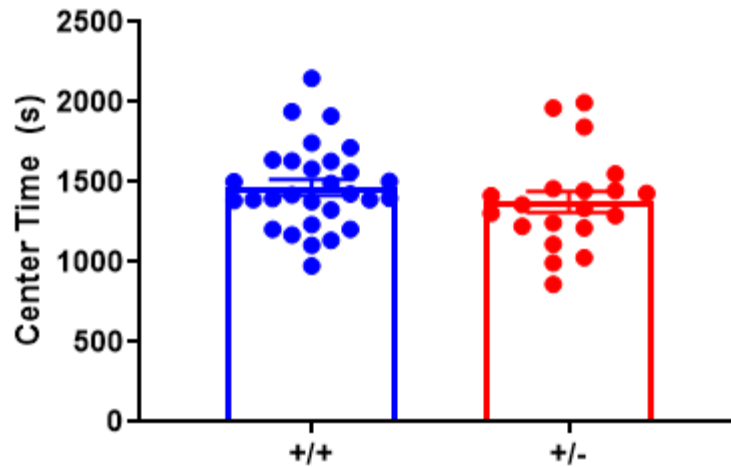


**Figure 12: *Chd8* mutant mice and their wildtype littermates spend similar amounts of time in the center of the open field**

**There was no significant difference between genotypes in time spent in the center of the open field (unpaired t-test,  $p > 0.05$ ). Individual data points are superimposed onto bar graphs with error bars representing means  $\pm$  SEM.**

The frequency to enter the light chamber in the light-dark emergence task, an assay for anxiety-like behavior, was only reported in one previous study, which showed an increase for the *Chd8* mutant mice [51]. We observed a similar phenotype in our line of *Chd8* mutant mice, but the difference between the groups was not significant (Figure 13a). Additionally, two previous lines displayed decreased time spent in the light chamber during this task [51, 332], but our mice showed no significant difference between genotypes for this measurement (Figure 13b).

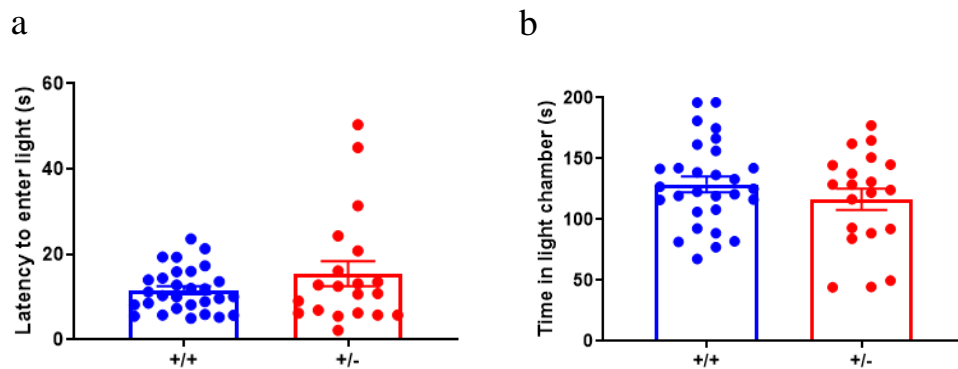


**Figure 13: *Chd8* mutant mice do not show significant differences in the light-dark emergence task**

**Although there was a trend for the *Chd8* mutant mice to exhibit increased latency to enter the light chamber, the difference between groups was not significant (unpaired t-test,  $p > 0.05$ ). (b) There was no significant difference between *Chd8* mutant mice and their wildtype littermates in time spent in the light chamber during the light-dark emergence task. Individual data points are superimposed onto bar graphs with error bars representing means  $\pm$  SEM.**

The elevated zero maze and its alternate form, the elevated plus maze, have also been used to test for anxiety-like behavior in *Chd8* mutant mice. One previously reported line of *Chd8* mutant mice spends less time in the open arms of the elevated plus maze compared to wildtype littermates [332]. However, another previously reported line of *Chd8* mutant mice is not significantly different than wildtype mice on this test [52]. Our line of *Chd8* mutant mice also does not show deficits in the amount of time spent in the open areas of the elevated zero maze (Figure 14).

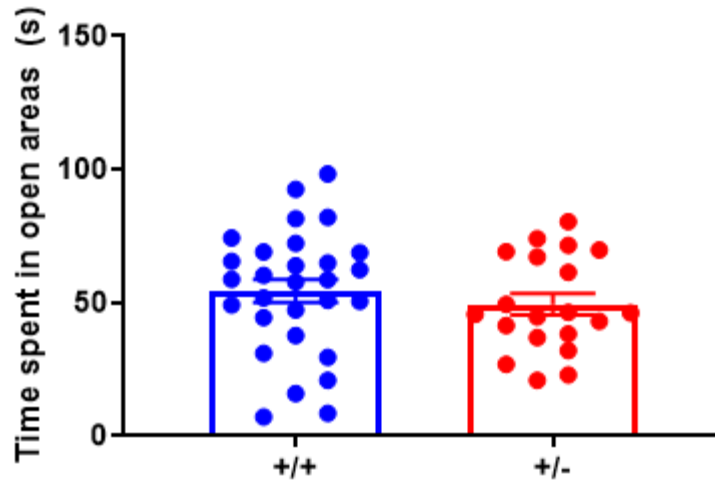


**Figure 14: *Chd8* mutant mice and their wildtype littermates spend similar amounts of time in the open areas of the elevated zero maze**

**There was no significant difference between genotypes in time spent in the open areas of the elevated zero maze (unpaired t-test,  $p > 0.05$ ). Individual data points are superimposed onto bar graphs with error bars representing means  $\pm$  SEM.**

Ultrasonic vocalizations in adult *Chd8* mutant mice have been reported by two previous groups and in both cases, there were no significant differences between mutants and wildtype littermates [52, 331]. We observed no difference between groups in the number of calls made (Figure 15a). However, we report a novel finding of increased call duration in *Chd8* mutant mice (Figure 15b).

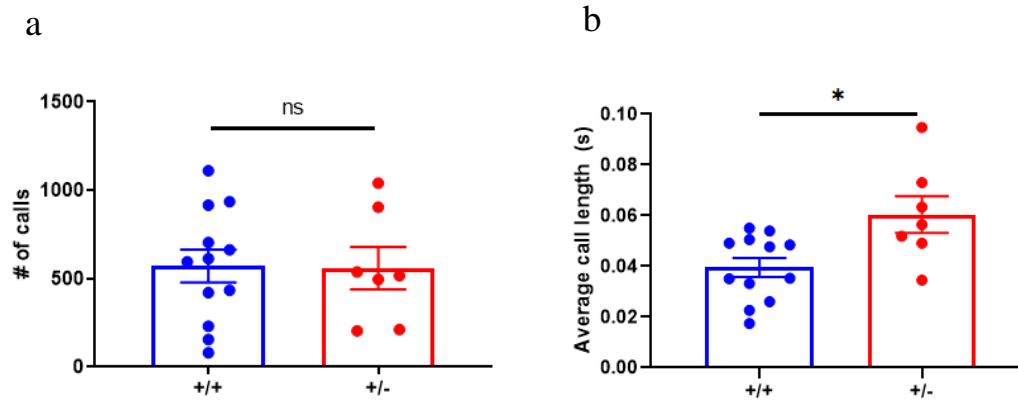


**Figure 15: *Chd8* mutant mice show altered ultrasonic vocalizations in adulthood.**

**(a) There was no difference between *Chd8* mutant mice and their wildtype littermates in the number of USVs (unpaired t-test,  $p > 0.05$ ). (b) The average duration of the calls made by the *Chd8* mutant mice were significantly longer than their wildtype littermates (unpaired t-test,  $p < 0.05$ ). Individual data points are superimposed onto bar graphs with error bars representing means  $\pm$  SEM. \* represents  $p < 0.05$ .**

In pups, we observed a similar phenotype. *Chd8* mutant pups had an increased number of calls compared to wildtype littermates (Figure 16a), but no significant difference in the average call length (Figure 16b). There was, however, a strong trend towards increased call length, with a borderline significant p value of 0.08. Two previous studies of *Chd8* mutant mice reported pup USVs. One study reported a similar finding of increased number of USVs, but only under certain conditions: only pups at a certain developmental stage and only male pups showed this phenotype [52]. The other study reported no changes in pup USVs at any developmental stage [331].

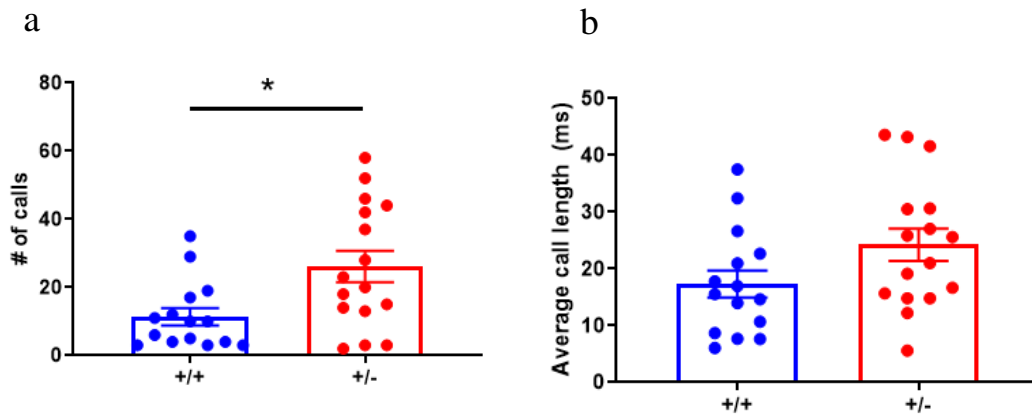


**Figure 16: *Chd8* mutant mice show altered ultrasonic vocalizations as pups.**

- (a) *Chd8* mutant mice have increased numbers of USVs as pups (unpaired t-test,  $p < 0.05$ ).**  
**(b) The average duration of the calls made by the *Chd8* mutant pups tended to be higher than the calls of the wildtype littermates, but this difference was not quite significant (unpaired t-test,  $p = 0.08$ ). Individual data points are superimposed onto bar graphs with error bars representing means  $\pm$  SEM. \* represents  $p < 0.05$ .**

Self-grooming is often elevated in mouse models of ASD and is thought to represent a repetitive behavior. However, most lines of *Chd8* mutant mice have normal rates of self-grooming [51, 330-332]. One line of *Chd8* mutant mice has elevated rates of self-grooming, but only under certain conditions: it only occurs after prolonged social isolation and it only occurs in male mice [52]. Like previously published *Chd8* mutant mice, our line did not show elevated rates of self-grooming under our standard protocol (Figure 17).

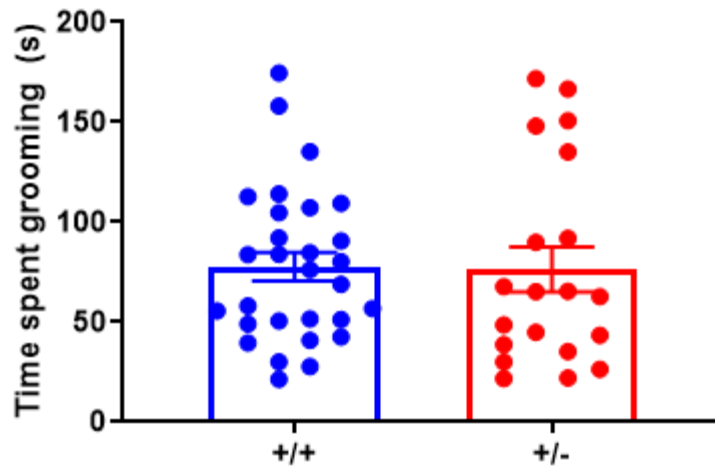


**Figure 17: *Chd8* mutant mice show normal rates of self-grooming behavior.**

**There was no significant difference in time spent grooming between *Chd8* mutant mice and their wildtype littermates (unpaired t-test,  $p > 0.05$ ). Individual data points are superimposed onto bar graphs with error bars representing means  $\pm$  SEM.**

Most of the previous studies characterizing behavior in *Chd8* mutant mice also used the rotarod to assess motor function and reported no genotype effect on this behavior [52, 330, 332]. One study reported an increase in motor performance in the *Chd8* mutant mice on the rotarod [51]. We found our line of *Chd8* mice to perform significantly better than wildtype mice on this task, to an even greater extent than what was previously reported in the other line. *Chd8* mutant mice outperformed wildtype mice on both the accelerating rotarod (Figure 18a) and on a steady speed of 32 RPM condition (Figure 18b).

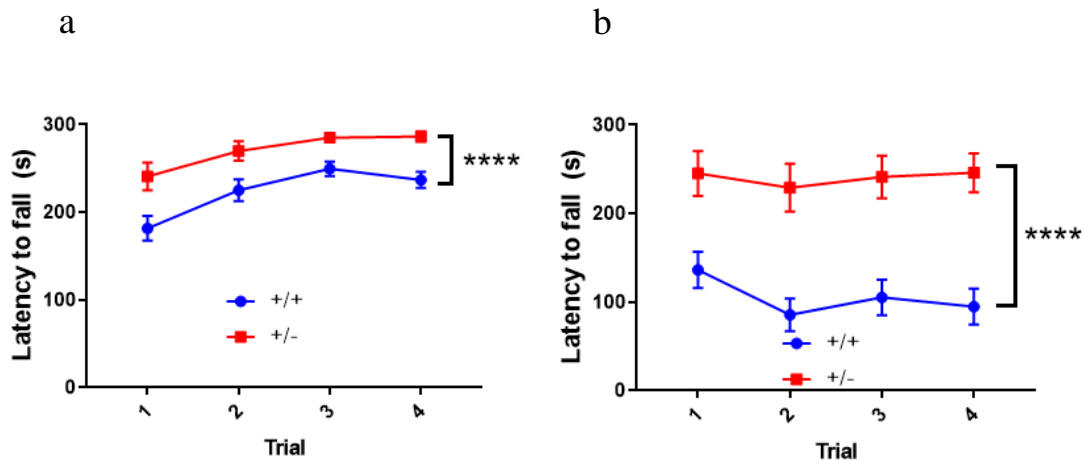


**Figure 18: *Chd8* mutant mice have improved performance on the rotarod.**

**(a) *Chd8* mutant mice take significantly longer to fall off the rotarod in the accelerating (4-40 RPM) condition (RMANOVA, effect of genotype  $p < 0.0001$ ). (b) *Chd8* mutant mice take significantly longer to fall of the rotarod in the steady speed (32 RPM) condition (RMANOVA, effect of genotype  $p < 0.0001$ ). Data represents means  $\pm$  SEM. \*\*\*\* represents  $p < 0.0001$ .**

A commonly used assay to test for social deficits in mice is the 3-chamber test for sociability and social novelty. Previous characterizations of *Chd8* mutant mice revealed no deficits in sociability on this assay [51, 52, 330-332]. Some groups reported a deficit in recognizing social novelty [51, 332], whereas other groups reported no changes in the second phase of the 3-chamber test [52, 331]. Our *Chd8* mutant mice perform statistically the same as wildtype in both the sociability and social novelty phases of the 3-chamber test (Figure 19).

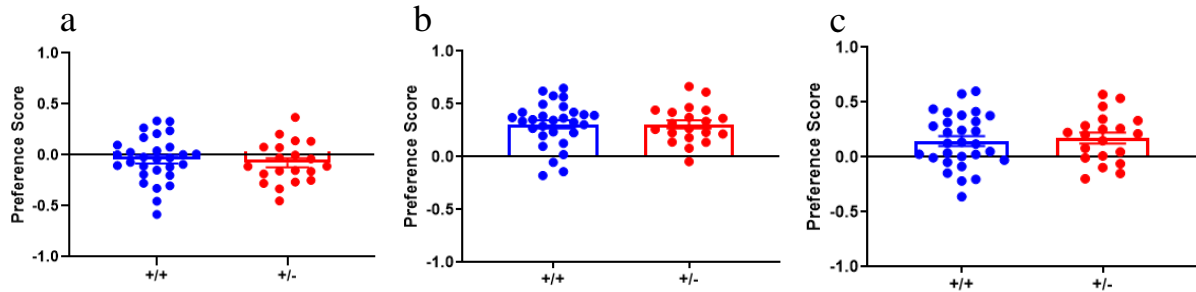


**Figure 19: *Chd8* mutant mice show no deficits in the 3-chamber test.**

(a) Neither *Chd8* mutants nor wildtype mice form a preference for one of two identical nonsocial stimuli (unpaired t-test,  $p > 0.05$ ). (b) Both *Chd8* mutants and wildtype mice display a strong preference for a social stimulus over a nonsocial stimulus (unpaired t-test,  $p > 0.05$ ). (c) Both *Chd8* mutant mice and wildtype mice form a mild preference for a novel social stimulus over a familiar social stimulus (unpaired t-test,  $p > 0.05$ ). Individual data points are superimposed onto bar graphs with error bars representing means  $\pm$  SEM.

## 2.4 Conclusions

Our mouse model was the first to disrupt all isoforms of Shank3, best replicating the most common *SHANK3* mutations found in humans [171]. The *Shank3* gene is known to have multiple intragenic promoters and alternative splice sites [170]. Thus, mutations that disrupt only a small portion of exons only disrupt a subset of possible protein isoforms. The *Shank3*  $\Delta e4-22^{-/-}$  mice present with a number of behaviors that have face validity for the human condition, including altered interactions in the social dyadic test and impaired USVs.

One question that remains is why the heterozygous mice do not present with a strong phenotype. Parental origin of the mutation was one possible explanation, but our data suggests that this does not contribute to the lack of phenotype observed in the heterozygotes. It remains to be determined whether humans are more sensitive to smaller changes in dosage of the SHANK3 protein, whether the highly controlled environment of the laboratory prevents the expression of ASD-like phenotypes in heterozygotes, or whether the current methods used for assessing behavior in rodents prevent us from detecting more subtle changes most relevant to ASD.

*CHD8* mutations are also often observed in human patients with ASD, but the nature of the mutations is less homogenous than with *SHANK3*. Frameshift mutations have been reported throughout the gene, rather than deletions of the entire gene. Several different *Chd8* models have been reported with highly variable behavioral phenotypes. Unlike for *Shank3*, the transcriptional regulation of *Chd8* is not well-characterized. So, one plausible explanation for the variable phenotypes observed in different lines of *Chd8* mutant mice is that the mutations disrupt different sets of CHD8 isoforms. This is a hypothesis that clearly needs further testing.

Generating and characterizing mouse models is a necessary first step that must be accomplished before testing potential therapeutic interventions, one of which is discussed in Chapter 3. Characterizing mouse models is also important to get a baseline for generating hypotheses that can further be tested with tools to manipulate gene expression over space and time, which is done in Chapter 4.

### **3. Environmental enrichment has minimal effects on behavior in *Shank3* $\Delta e4-22^{-/-}$ mice**

#### ***3.1 Introduction***

Currently no pharmaceutical compound is approved to alleviate the core symptoms of Autism Spectrum Disorder (ASD): restricted, repetitive behaviors and impaired social communication. Early behavioral intervention has led to long-lasting improvements in human patients with ASD (e.g. [333, 334]). Attempts to use sensorimotor enrichment on human patients based on findings in rodents have also reported some initial success [335, 336]. However, these studies often exclude participants with known genetic conditions, warranting further investigation into interventions that can improve outcomes for individuals with genetic syndromes, who often have the most severe symptom presentation.

Numerous animal models have been created to tease apart the complex pathophysiology of ASD [92, 240, 319]. One interesting finding from across various models is that housing rodents in an enriched environment, including more space and objects in which to interact and in some cases more rodents, prevents the expression of ASD-like behavioral phenotypes [43, 337-347]. Although the type of enrichment and the developmental stages during exposure varied considerably, all these previous studies reported improvements on at least one behavioral outcome and seldom reported any adverse effects of enrichment. Moreover, some of the models utilized previously lack construct validity in terms of a known, highly penetrant cause of ASD, such as a genetic mutation that has been consistently linked to the disorder in humans.

Among the most prevalent genetic contributors to ASD are mutations in and deletions of *SHANK3* [154, 321, 348]. More than fourteen different lines of *Shank3* germline mutant mice have been reported [166, 171, 173-180, 301, 349, 350]. The expression of ASD-like behaviors in each of these lines of mice confirms an important role for *Shank3* in shaping behavior, but the majority

of ASD patients with *SHANK3* mutations are missing the entire gene, so the  $\Delta e4-22$  mice, which lack all protein isoforms, have the greatest construct validity for the human condition [171]. One group demonstrated that behaviors observed in *Shank3* exons 4-9 deletion ( $\Delta e4-9$ ) mice are highly penetrant across different genetic backgrounds [351], which contrasts findings in mice lacking the gene underlying fragile X syndrome, *Fmr1* [352-356].

We tested the effect of early environmental enrichment on some of the most robust behavioral phenotypes that we previously reported in our complete *Shank3* knockout model ( $\Delta e4-22$ ) of ASD. We found that, contrary to previous findings using other mouse models of ASDs, early environmental enrichment did not prevent the manifestation of behaviors that resemble repetitive behaviors in *Shank3*  $\Delta e4-22$  mice: self-grooming and restricted head poking on the hole-board task. We also found that enrichment decreased motor performance on the rotarod task specifically in wildtype mice and increased anxiety-like behavior in all mice, regardless of genotype.

## **3.2 Methods**

### **3.2.1 Animals**

*Shank3*  $\Delta e4-22$  mice were previously generated and characterized by our lab and were maintained on a C57BL/6J background after backcrossing for at least 8 generations [171]. All experiments were conducted with protocols approved by the Institutional Animal Care and Use Committee at Duke University.

### **3.2.2 Rearing conditions**

Similar to a previous study utilizing a mouse model of Rett syndrome, mice were placed in enriched environment early in development (starting at postnatal day 10, P10) in an attempt to maximize effectiveness of the enrichment paradigm [43]. In the enrichment condition, starting at P10, mice were housed with two lactating dams and two litters per cage, whereas in the standard

condition mice were housed with one lactating dam and one litter per cage. The enriched cages were modeled after those depicted in [357]. They were larger than the standard mouse cage (approximately  $30 \times 15 \times 15$  cm) with approximate dimensions of  $75 \times 45 \times 25$  cm. Moreover, mice in the enriched environments had running wheel access as well as various shelters and objects in which to interact. The positions of the objects, shelters, and running wheels were rotated daily to maintain novelty and the items were completely changed out weekly. Once the mice reached weaning age (P21), they were housed with same-sex cage mates of seven per enriched cage or five per standard cage. Immediately prior to behavioral testing (starting once all mice in each cohort reached P60), all mice were transferred to standard cages so that the experimenter was blind to both genotype and rearing conditions.

### **3.2.3 Behavioral testing**

Three cohorts of approximately 45 *Shank3*  $\Delta e4-22$  (+/+, +/-, and -/-) mice were tested in a battery of assays in order to assess the effects of environment on anxiety-like behavior, motor function, and stereotypy at 8-10 weeks of age. The experimenter was blind to both genotype and rearing conditions until data analysis. The assays were performed in order they are described, but not every cohort was put through every test. See Table 8 for details of each cohort, including the numbers of mice in each experimental group and the tests performed. Both male and female mice were used for all experiments presented in this study.

**Table 8: Order of behavioral tests for environmental enrichment cohorts and number of mice per group**

Cohort 1	Cohort 2	Cohort 3	TOTALS
+/+ Standard: n = 11 +/+ Enriched: n = 6 +/- Standard: n = 8 +/- Enriched: n = 7 -/- Standard: n = 7 -/- Enriched: n = 7	+/+ Standard: n = 4 +/+ Enriched: n = 14 +/- Standard: n = 5 +/- Enriched: n = 2 -/- Standard: n = 14 -/- Enriched: n = 6	+/+ Standard: n = 4 +/+ Enriched: n = 8 +/- Standard: n = 15 +/- Enriched: n = 10 -/- Standard: n = 4 -/- Enriched: n = 3	+/+ Standard: n = 19 +/+ Enriched: n = 28 +/- Standard: n = 28 +/- Enriched: n = 19 -/- Standard: n = 25 -/- Enriched: n = 16
Elevated Zero Maze (EZM)	Open Field	Rotarod	EZM: n = 13-25 per group
Open Field	EZM		Open Field: n = 13-25 per group
Rota-rod	Hole-board		Rotarod: n = 10-25 per group
Grooming			Grooming: n = 7-11 per group
Hole-board			Hole-board: n = 9-21 per group

**Zero Maze:** Mice were introduced into a closed portion of the maze and were given 5 minutes of free exploration under dim (40-60 lux) illumination. Activity was scored by Ethovision XT 7 (Noldus Information Technologies) using a high-resolution camera suspended 180 cm above the center of the maze. Tracking profiles were generated by Ethovision XT software and were used to measure the time each mouse spent in the open portions of the maze.

**Open Field:** Activity in the open field was measured over 1 hour in an automated Omnitech Digiscan apparatus (AccuScan Instruments, Columbus, OH). Accuscan software scored the total distance traveled and the time spent in the center of the apparatus.

**Rota-rod:** Motor performance was assessed on a steady-speed rota-rod (Med-Associates) set to 20 rotations per minute. Each mouse attempted four trials with an inter-trial interval of 30 minutes. The latency to fall off the apparatus was recorded. If a mouse displayed three successive passive rotations this was also counted as a fall. Each trial ended after 5 minutes and any mouse that successfully remained on the rod at the end of the trial was recorded as a latency of 300 seconds.

**Grooming:** Individual animals were acclimated to clean home cages for 5 minutes prior to filming (MediaRecorder2; Noldus Information Technologies). Mice were filmed for 10 minutes and grooming behavior was hand-scored using Observer 9 XT (Noldus Information Technologies).

**Hole-board:** Mice were allowed 5 minutes of exploration on a 16-hole-board apparatus. Animals were filmed with a digital video camera and hand-scored for the numbers of nose-pokes and the location of each nose poke. Back-to-back nose pokes were defined as when the animal made two or more consecutive visits to the same hole.

### **3.2.4 Statistical analysis**

Graphs were produced and statistical analysis was performed in GraphPad Prism 7. For the rotarod data, a repeated measures ANOVA was performed and each of the six groups (three genotypes x two rearing conditions) was independently compared to each other group with Tukey's multiple comparison post-hoc test. For all other tests, a two-way ANOVA for genotype and rearing condition was performed. Significant differences in genotype were followed up with Tukey's multiple comparison post-hoc test. Statistical significance was defined as  $p < 0.05$ .

## **3.3 Results**

### **3.3.1 *Shank3* $\Delta e4-22^{-/-}$ display repetitive behaviors which are not ameliorated by early environmental enrichment**

Consistent with our previous reports, the *Shank3*  $\Delta e4-22^{-/-}$  mice engaged in increased amounts of repetitive self-grooming, compared to both *Shank3*  $\Delta e4-22^{+/-}$  and  $+/+$  mice (Figure 20). There was no effect of environment on the expression of this behavior. Similarly, the *Shank3*  $\Delta e4-22^{-/-}$  mice engaged in repetitive behavior, in terms of increased back-to-back pokes compared to  $+/+$  mice, on the hole-board task and this phenotype was not affected by the rearing conditions of the mice (Figure 21).

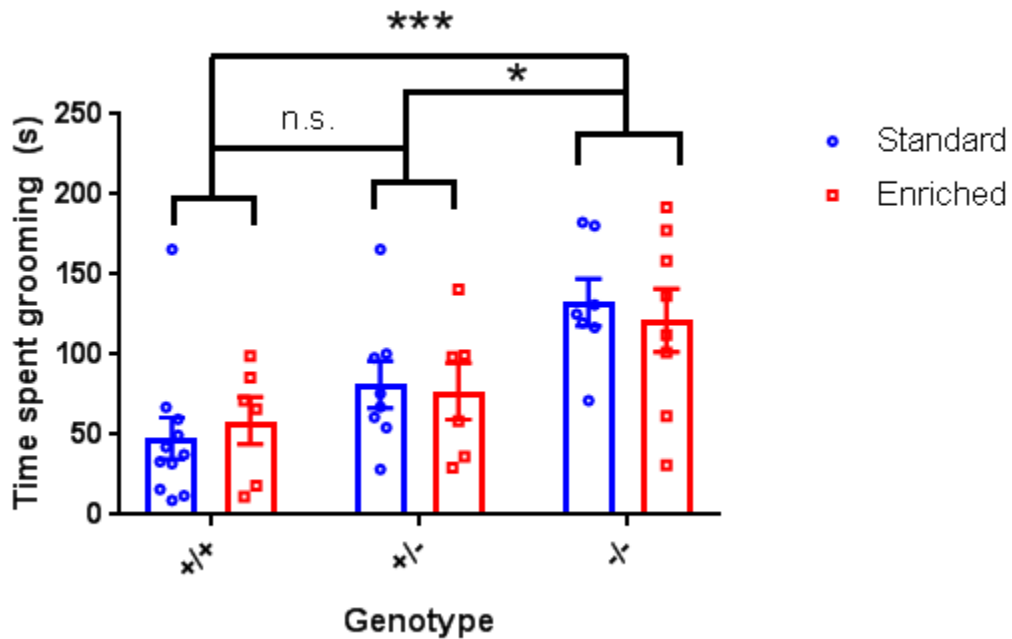


**Figure 20: Grooming in *Shank3*  $\Delta e4-22^{-/-}$  mice is elevated whether they are reared in standard or enriched environments**

*Shank3*  $\Delta e4-22^{-/-}$  mice show elevated rates of grooming compared to both  $+/+$  and *Shank3*  $\Delta e4-22^{+/-}$  mice (two-way ANOVA main effect of genotype,  $p < 0.001$ ; Tukey's multiple comparisons  $-/-$  vs.  $+/+$ ,  $p < 0.001$ ;  $-/-$  vs.  $+/-$ ,  $p < 0.05$ ). There was no effect of rearing condition.  $n = 6-11$  per group. Individual data points are superimposed over bar graphs and error bars representing means  $\pm$  SEM. \* represents  $p < 0.05$  and \*\*\* represents  $p < 0.001$ .

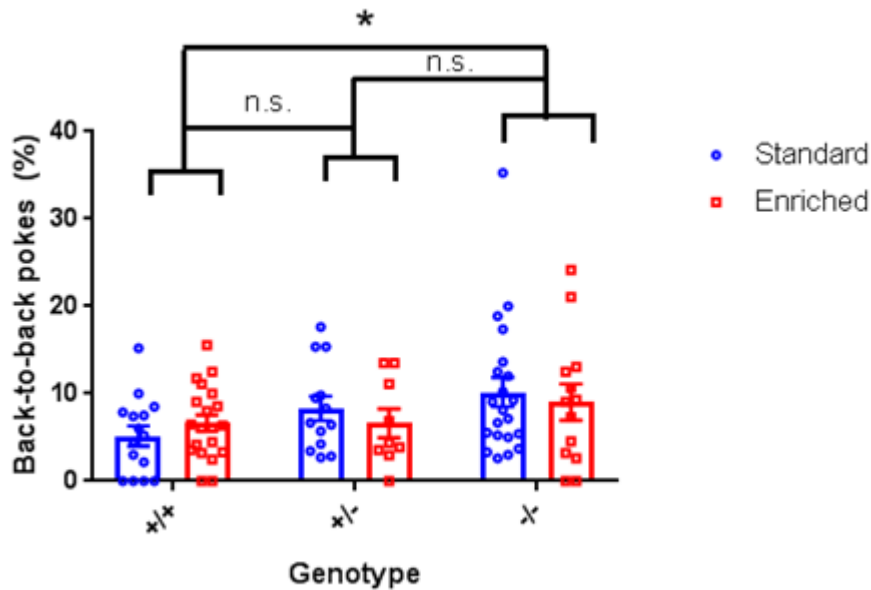


**Figure 21: Back-to-back pokes on the hole-board test are increased in *Shank3*  $\Delta e4-22^{-/-}$  mice, but there is no effect of environment**

*Shank3*  $\Delta e4-22^{-/-}$  mice perform a higher percentage of back-to-back pokes compared to +/+ mice (two-way ANOVA main effect of genotype,  $p < 0.05$ , Tukey's multiple comparisons -/- vs. +/+,  $p < 0.05$ ).  $n = 13-21$  per group. There was no effect of rearing condition.  $n = 6-11$  per group. Individual data points are superimposed over bar graphs and error bars representing means  $\pm$  SEM. \* represents  $p < 0.05$ .

### **3.3.2 Early environmental enrichment does not affect spontaneous motor activity, but increases anxiety-like behavior irrespective of genotype**

*Shank3*  $\Delta e4-22^{-/-}$  mice are hypoactive in the open field exploration task, compared to both +/+ and *Shank3*  $\Delta e4-22^{+/-}$  mice, and there is no effect of rearing condition on this phenotype (Figure 22). However, contrary to our previous findings, we did not see an effect of genotype on time spent in the center of the open field (Figure 23). Rather, we observed a main effect of rearing condition, where mice raised in enriched environments spent significantly less time in the center of the arena, regardless of genotype (Figure 23). We further tested anxiety-like behavior on the elevated zero maze and found that both *Shank3*  $\Delta e4-22^{-/-}$  and *Shank3*  $\Delta e4-22^{+/-}$  mice spend more

time in the open areas than  $+/+$  mice, but that this phenotype was not influenced by environmental enrichment (Figure 24).

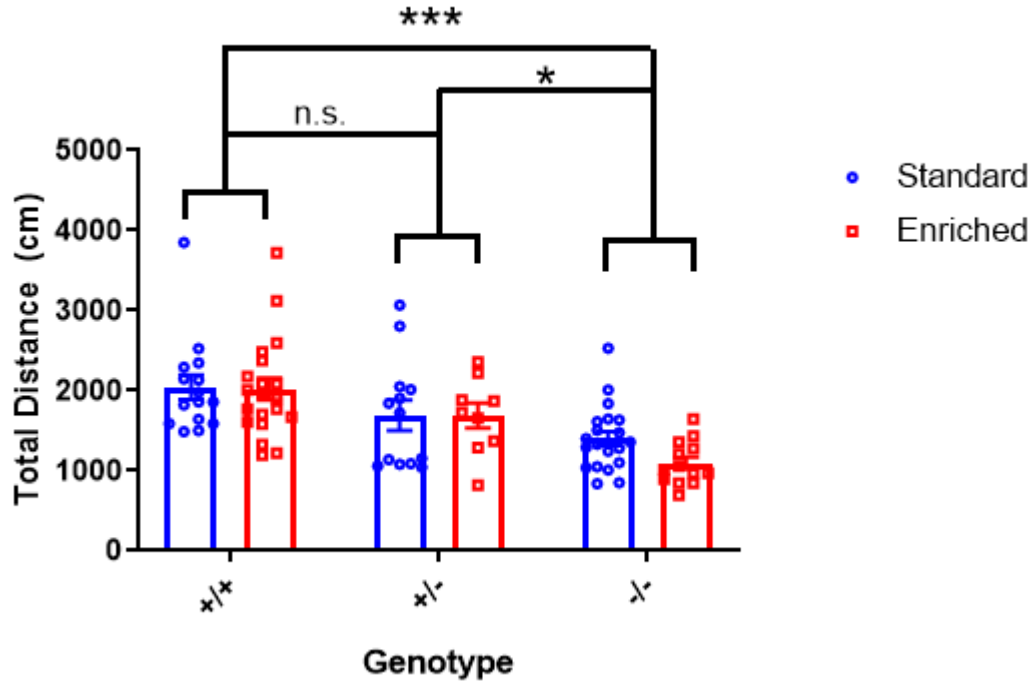


**Figure 22: *Shank3*  $\Delta e4-22^{-/-}$  mice display reduced spontaneous motor activity which is unaffected by rearing condition**

*Shank3*  $\Delta e4-22^{-/-}$  mice are hypoactive in the open field, as total distance travelled is significantly reduced compared to both  $+/+$  and *Shank3*  $\Delta e4-22^{+/+}$  mice (two-way ANOVA main effect of genotype,  $p < 0.001$ ; Tukey's multiple comparisons  $-/-$  vs.  $+/+$ ,  $p < 0.001$ ,  $-/-$  vs.  $+/-$ ,  $p < 0.05$ ). There is no effect of rearing condition on this phenotype.  $n = 9-21$  per group.

Individual data points are superimposed over bar graphs and error bars representing means  $\pm$  SEM. \* represents  $p < 0.05$  and \*\*\* represents  $p < 0.001$ .

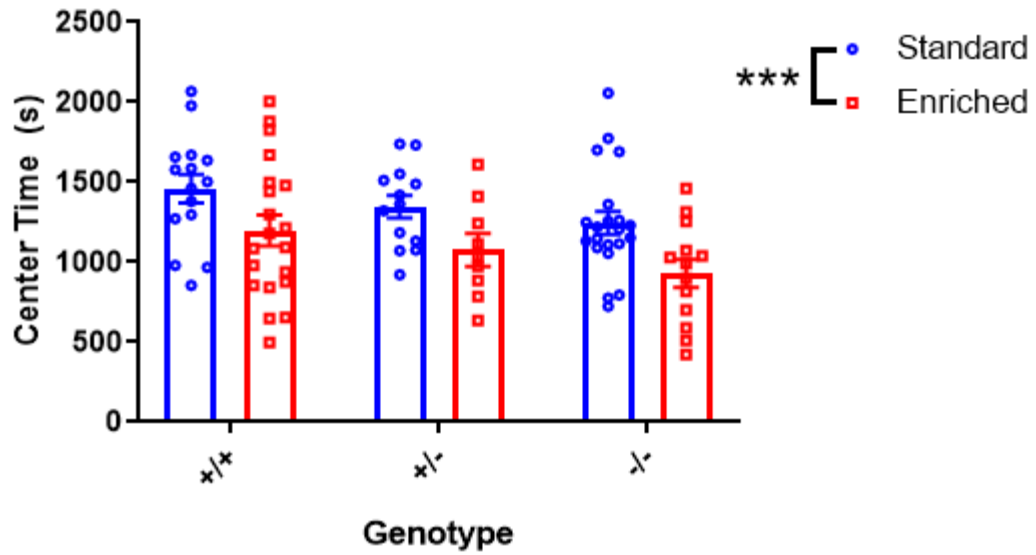


**Figure 23: Environmental enrichment decreases time spent in the center of the open field regardless of genotype**

There is no significant effect of genotype on time spent in the center of the open field apparatus, but there is a main effect of environment where enriched mice spend significantly less time in the center of the arena (two-way ANOVA main effect of genotype,  $p < 0.05$ , but no significant post-hoc comparisons; two-way ANOVA main effect of environment,  $p < 0.001$ ).  $n = 9-21$  per group. Individual data points are superimposed over bar graphs and error bars representing means  $\pm$  SEM. \*\*\* represents  $p < 0.001$ .

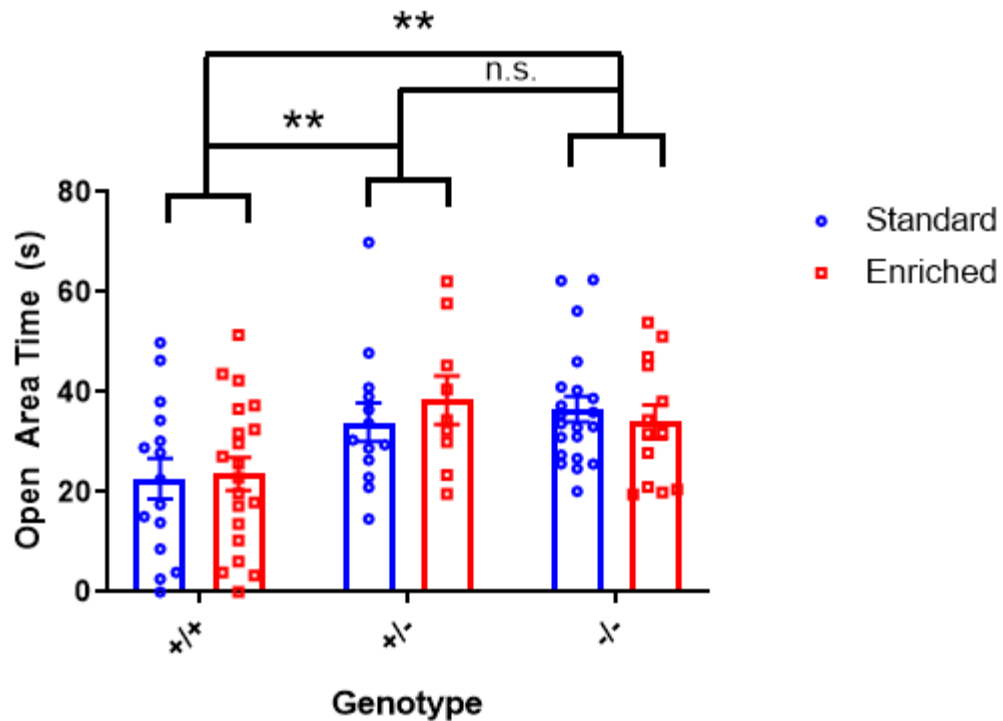


**Figure 24: Environmental enrichment does not affect time spent in the open areas of the elevated zero maze**

*Shank3*  $\Delta e4-22^{-/-}$  and  $\Delta e4-22^{+/-}$  mice spend more time in the open areas of the elevated zero maze compared to  $+/+$  mice (two-way ANOVA main effect of genotype,  $p < 0.001$ ; Tukey's multiple comparisons  $-/-$  vs.  $+/+$ ,  $p = 0.001$ ,  $+/-$  vs.  $+/+$ ,  $p < 0.01$ ).  $n = 13-25$  per group.

Individual data points are superimposed over bar graphs and error bars representing means  $\pm$  SEM. \*\*\* represents  $p < 0.001$ .

### 3.3.3 Early environmental enrichment has a negative impact on motor performance which is specific to wildtype mice

In our previous characterization of the *Shank3* complete knockouts, we found the most severe motor performance deficits on the steady-speed variation of the rotarod. All fifteen of the  $+/+$  mice that were raised in standard conditions performed perfectly throughout all four trials and this was not true for mice in any other experimental condition (Figure 25a-c). By repeated measures ANOVA, there was a significant effect of experimental group on motor performance; however,

the only significant differences in post-hoc analysis were between +/+ mice raised under standard conditions and +/+ mice raised in enriched environments (Figure 25a).

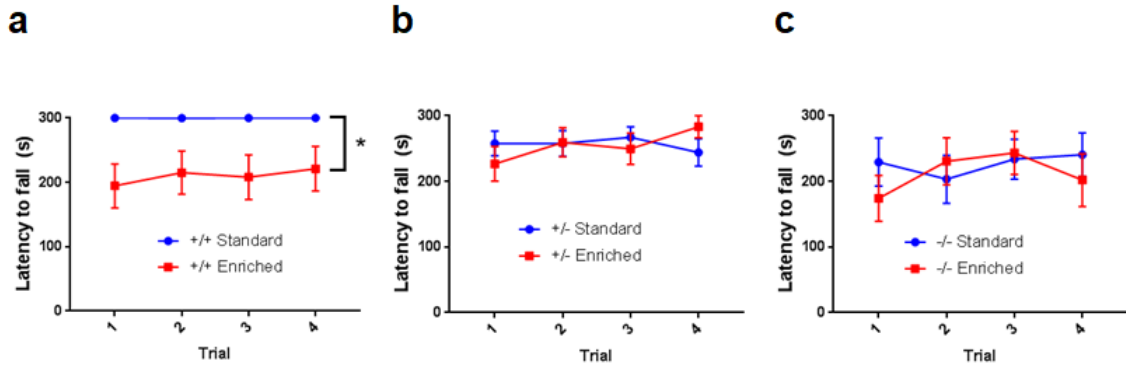


**Figure 25: Environmental enrichment impairs performance on the accelerating rotarod specifically in wildtype mice.**

(a) All +/+ mice raised under standard conditions performed perfectly on the 20 r.p.m. steady-speed rotarod. However, +/+ mice raised in enriched environments performed significantly worse than +/+ raised in standard cages (RMANOVA, main effect of genotype/environment group,  $p < 0.05$ ; Tukey's multiple comparisons +/+ Standard vs. +/+ Enriched,  $p < 0.05$ ).  $n = 14-15$  per group. (b) There was no statistically significant effect of environment for the +/- mice.  $n = 17-23$  per group. (c) There was no statistically significant effect of environment for the -/- mice.  $n = 10-11$  per group. Data represents means  $\pm$  SEM. \* represents  $p < 0.05$ .

### 3.4 Conclusions

Our results indicate that raising *Shank3* mutant mice in enriched environments has little effect on their behavior, which is somewhat surprising, given that environmental enrichment has been shown to alleviate behavioral phenotypes in a number of other rodent models of ASDs [43, 337-347]. A summary of previous findings along with findings from the current study is provided in Table 9.

**Table 9: Summary of key findings from previous studies utilizing environmental enrichment and rodent models of ASD.**

Reference	Type of ASD Model	Enrichment Paradigm	Effect on Behavior
Current study	Male and female <i>Shank3</i> Δe4-22 <sup>-/-</sup> mice	Mice were transferred to enriched environments starting at PND 10 and were returned to normal environments on PND 60, when behavioral studies began. Enriched environments consisted of larger (75 x 45 x 25 cm) cages with an assortment of toys that were repositioned daily and completely changed out weekly. Prior to weaning, mice were housed with two dams and two litters per enriched cage.	<p>Positive effects:</p> <ul style="list-style-type: none"> <li>• None observed</li> </ul> <p>Phenotypes that failed to improve:</p> <ul style="list-style-type: none"> <li>• <i>Shank3</i> Δe4-22<sup>-/-</sup> mice show elevated rates of self-grooming that were not affected by housing condition.</li> <li>• <i>Shank3</i> Δe4-22<sup>-/-</sup> mice perform more repetitive nose pokes on the hole-board test and this phenotype was not influenced by housing condition.</li> <li>• <i>Shank3</i> Δe4-22<sup>-/-</sup> mice are hypoactive in the open field and this phenotype was not influenced by housing condition.</li> <li>• <i>Shank3</i> Δe4-22<sup>-/-</sup> and <i>Shank3</i> Δe4-22<sup>+/-</sup> mice spend more time in the open areas of the elevated zero maze compared to +/+ mice, and this phenotype did not depend on rearing condition.</li> </ul> <p>Exacerbations</p> <ul style="list-style-type: none"> <li>• Enrichment reduced the amount of time mice spent in the center of the open field, regardless of genotype.</li> <li>• Enrichment produced deficits on the rotarod test specifically in wildtype mice.</li> </ul>

Reference	Type of ASD Model	Enrichment Paradigm	Effect on Behavior
[337]	Male FMR1-KO mice on a C57BL/6 background	Starting at PND 21 and lasting for 60 days, enriched mice were housed in groups of 3 in 35 x 20 x 25 cm cages with an assortment of toys that were changed every 3 days	<p>Positive effects:</p> <ul style="list-style-type: none"> <li>● Thigmotaxis in open field was prevented in enriched FMR1-KO mice</li> <li>● Impaired habituation to objects was prevented in enriched FMR1-KO mice</li> </ul> <p>Phenotypes that failed to improve:</p> <ul style="list-style-type: none"> <li>● Hyperactive locomotion in the open field was not affected by housing condition of the FMR1-KO mice</li> </ul> <p>Exacerbations:</p> <ul style="list-style-type: none"> <li>● Not reported</li> </ul>
[339]	Hemizygous male and heterozygous female <i>Mecp2</i> knockout mice on a mixed C57BL/6 and 129 background	Starting at PND 28 and continuing throughout behavioral testing (at 6-29 weeks), enriched mice were housed in groups of 5-6 and were in larger (size not specified) cages with access to toys that were changed every 2 days.	<p>Positive effects:</p> <ul style="list-style-type: none"> <li>● Deficits in rota-rod performance were prevented in heterozygous females</li> <li>● Enrichment improved motor performance on rota-rod in wildtype males</li> </ul> <p>Phenotypes that failed to improve:</p> <ul style="list-style-type: none"> <li>● Hemizygous males displayed similarly impaired performances on the rota-rod regardless of housing condition</li> <li>● Decreased vertical activity of heterozygous females and hemizygous males were not affected by housing condition</li> </ul> <p>Exacerbations:</p> <ul style="list-style-type: none"> <li>● Enriched housing induced a hypolocomotive phenotype in female heterozygous mice</li> </ul>

Reference	Type of ASD Model	Enrichment Paradigm	Effect on Behavior
[340]	<i>Mecp2</i> hemizygous hypomorphic male mice ( <i>Mecp2<sup>1lox</sup></i> ) on a C57BL/6 background	At PND 21, enriched mice were housed in larger (47 x 25 x 21 cm) cages in groups of 4-6. Enriched mice had access to various toys which were exchanged weekly.	<p>Positive effects:</p> <ul style="list-style-type: none"> <li>● Enrichment prevented a hypolocomotive phenotype observed in standard-housed mutant mice</li> </ul> <p>Phenotypes that failed to improve:</p> <ul style="list-style-type: none"> <li>● Mutant mice had decreased performance on the accelerating rota-rod and this phenotype was not affected by housing condition</li> <li>● Enrichment did not significantly improve contextual or cued fear conditioning, which is impaired in mutant mice</li> </ul> <p>Exacerbations</p> <ul style="list-style-type: none"> <li>● Not reported</li> </ul>
[341]	Hemizygous male <i>Mecp2</i> knockout mice on a mixed C57BL/6 and 129 background and hemizygous male <i>Mecp2</i> knockout mice on a pure 129 background	PND 21 mice were transferred to enriched environments for two weeks and then were returned to normal conditions. Enriched cages consisted of two connected 30 x 30 cm cages with toys that were changed daily.	<p>Positive effects:</p> <ul style="list-style-type: none"> <li>● Impaired gait in mutants was prevented by enrichment</li> <li>● Mutants showed impaired performance on the elevated beam task and this phenotype was rescued in enriched mutants</li> <li>● Mutant mice spent significantly more time in the open areas of the elevated plus maze and enriched housing prevented this phenotype</li> </ul> <p>Phenotypes that failed to improve:</p> <ul style="list-style-type: none"> <li>● Mutant mice have impaired survival and this is not improved by enrichment</li> </ul> <p>Exacerbations</p> <ul style="list-style-type: none"> <li>● Not reported</li> </ul>

Reference	Type of ASD Model	Enrichment Paradigm	Effect on Behavior
[43]	Hemizygous male and heterozygous female <i>Mecp2</i> knockout mice on a mixed C57BL/6 and 129 background	Mice were transferred to enriched environments starting at PND 10 and were returned to normal environments on PND 60. Hemizygous males were used for tests of motor functions and were testing during the enrichment period (PND 30-60), whereas heterozygous females were used for the other tests, which were performed after PND 60. Enriched environments consisted of larger (44 x 62 x 28 cm) cages with an assortment of toys that were repositioned daily and completely changed out weekly. Prior to weaning, mice were housed with two dams and two litters per enriched cage.	<p>Positive effects:</p> <ul style="list-style-type: none"> <li>● Enrichment prolonged survival of hemizygous male mutants, although this was not statistically significant</li> <li>● Enrichment prevented impairment on the rotarod that was present for mutants raised in standard conditions</li> <li>● Heterozygous female mutants raised in standard conditions displayed spatial learning deficits on the Morris Water Maze, but this was prevented in the mice that were reared in enriched environments</li> <li>● Female heterozygous mutants raised in standard conditions displayed thigmotaxis in the open field, but mutants raised in enriched conditions did not</li> </ul> <p>Phenotypes that failed to improve:</p> <ul style="list-style-type: none"> <li>● Not reported</li> </ul> <p>Exacerbations:</p> <ul style="list-style-type: none"> <li>● Not reported</li> </ul>

[342]	Male Dp(11)17/+ mice on a C57BL/6J background	Enriched housing began at PND 21, which consisted of groups of 7-8 mice in larger (27.3 x 22.6 x 48.9 cm) cages with toys that were replaced weekly. Mice were transferred back to standard cages prior to behavior testing.	<p>Positive effects:</p> <ul style="list-style-type: none"> <li>● Mutants raised in standard conditions showed impaired (not statistically significant) social recognition in the partition test, but enriched mutants did not show this phenotype.</li> <li>● Mutants raised in standard conditions showed increased aggression in a direct social interaction test and enrichment reduced the amount of contact aggression in these mice.</li> <li>● Enrichment increased the amount of nose pokes on the hole-board test in both wildtypes and mutants.</li> <li>● Mutants in standard housing showed impaired contextual fear conditioning, but this phenotype was prevented by environmental enrichment.</li> <li>● Standard-housed, but not enriched, mutants showed thigmotaxis in the open field.</li> <li>● Standard-housed, but not enriched mutants had decreased entries into the open arms of the elevated plus maze.</li> <li>● Enrichment improved motor coordination on the wire-hang test for both wildtypes and mutants.</li> </ul> <p>Phenotypes that failed to improve:</p> <ul style="list-style-type: none"> <li>● Mutant mice showed increased social dominance in the tube test and this was not influenced by housing condition.</li> <li>● Mutant mice spent less time sniffing social odors and this was not impacted by housing condition.</li> <li>● Mutant mice showed increased repetitive nose pokes on the hole-board test and this was not influenced by housing condition.</li> </ul> <p>Exacerbations:</p> <ul style="list-style-type: none"> <li>● Enriched housing increased non-contact aggression in the direct social interaction test in both wildtypes and mutants.</li> <li>● Enrichment introduced a hyperactive phenotype in wildtype mice in the open field.</li> </ul>
-------	-----------------------------------------------	------------------------------------------------------------------------------------------------------------------------------------------------------------------------------------------------------------------------------	------------------------------------------------------------------------------------------------------------------------------------------------------------------------------------------------------------------------------------------------------------------------------------------------------------------------------------------------------------------------------------------------------------------------------------------------------------------------------------------------------------------------------------------------------------------------------------------------------------------------------------------------------------------------------------------------------------------------------------------------------------------------------------------------------------------------------------------------------------------------------------------------------------------------------------------------------------------------------------------------------------------------------------------------------------------------------------------------------------------------------------------------------------------------------------------------------------------------------------------------------------------------------------------------------------------------------------------------------------------------------------------------------------------------------------------------------------------------------------------------------------------------------------------------------------------------------------------------------------------------------------------------------------------------------------------------------------------------------------------------------------------------------------------------------------------------

Reference	Type of ASD Model	Enrichment Paradigm	Effect on Behavior
[345]	Male FMR1-KO mice on a FVB background	Enriched mice were housed with an additional non-lactating dam 1 week prior to birth until weaning. After weaning, they were housed under standard conditions.	<p>Positive effects:</p> <ul style="list-style-type: none"> <li>● Enrichment reduced the number and duration of PND8 USVs and increased PND8 body weight in both wildtypes and mutants.</li> <li>● Mutants reared in standard conditions were hyperactive in the open field, but enriched mutants were similar to wildtype.</li> <li>● Mutants reared in standard conditions spent less time interacting with a social stimulus, but enriched mutants were similar to wildtype.</li> <li>● Mutants reared in standard conditions showed deficits in spontaneous alteration in the T-maze and in context fear conditioning, but enriched mutants did not</li> </ul> <p>Phenotypes that failed to improve:</p> <ul style="list-style-type: none"> <li>● Not reported</li> </ul> <p>Exacerbations:</p> <ul style="list-style-type: none"> <li>● Not reported</li> </ul>

Reference	Type of ASD Model	Enrichment Paradigm	Effect on Behavior
[346]	Male and female mice lacking the $\mu$ -opioid receptor gene ( <i>Oprm1</i> $-/-$ )	Enriched mice were housed with an additional lactating female from approximately 1 week before birth to weaning.	<p>Positive effects:</p> <ul style="list-style-type: none"> <li>• Enrichment increased body weight of all mice at PND8, but this normalized by weaning.</li> <li>• There was a significant effect of environment such that enriched mice (of both genotypes) spent more time interacting with the social stimulus in the juvenile Social Approach-Avoidance Test compared to standard-housed mice.</li> <li>• For male mice specifically, there was also an effect of enrichment on adult social behavior. While mutant mice spent less time investigating an intruder mouse regardless, enrichment increased the investigation time in both wildtypes and mutants.</li> </ul> <p>Phenotypes that failed to improve:</p> <ul style="list-style-type: none"> <li>• While enrichment decreased the number of PND8 USVs in wildtype mice, mutants had decreased numbers of USVs compared to wildtype and this was not affected by enrichment.</li> </ul> <p>Exacerbations:</p> <ul style="list-style-type: none"> <li>• Not reported</li> </ul>
[343]	Male BTBR inbred mouse strain	The mice were placed in enriched housing in groups of 8 at 7 weeks of age for 30 days. The enrichment cage was a three floor dog kennel with various toys that were changed every 5 days.	<p>Positive effects:</p> <ul style="list-style-type: none"> <li>• BTBR mice self-groom significantly more than C57BL/6 mice and this phenotype was rescued by environmental enrichment</li> </ul> <p>Phenotypes that failed to improve:</p> <ul style="list-style-type: none"> <li>• Not reported</li> </ul> <p>Exacerbations:</p> <ul style="list-style-type: none"> <li>• Not reported</li> </ul>

Reference	Type of ASD Model	Enrichment Paradigm	Effect on Behavior
[347]	Male mice exposed prenatally to VPA	One week after weaning, mice were in enriched environments for four weeks. This consisted of a larger cage (65 x 35 x 30 cm) filled with toys that were repositioned twice per week.	<p>Positive effects:</p> <ul style="list-style-type: none"> <li>● VPA-exposed mice housed in standard conditions spent more time in the closed arms of the elevated plus maze compared to controls, but enriched VPA-exposed mice were similar to controls.</li> <li>● VPA-exposed mice housed in standard conditions spent less time sniffing a stimulus in a social interaction test compared to controls, but enriched VPA-exposed mice were similar to controls.</li> <li>● VPA-exposed mice housed in standard conditions showed deficits in novel object recognition, but enriched VPA-exposed mice were similar to controls.</li> </ul> <p>Phenotypes that failed to improve:</p> <ul style="list-style-type: none"> <li>● VPA-exposed mice were hypoactive, reared less, and had fewer center crossings in the open field irrespective of environmental condition.</li> </ul> <p>Exacerbations:</p> <ul style="list-style-type: none"> <li>● Not reported</li> </ul>

Reference	Type of ASD Model	Enrichment Paradigm	Effect on Behavior
[338]	Male rats prenatally exposed to valproic acid (VPA)	<p>Enriched rats underwent multisensory stimulation from PND 7-21 and further enriched housing from PND 22-35.</p> <p>Multisensory stimulation involved exposing pups to various temperatures and textures for approximately 25 minutes per day.</p> <p>Enriched housing consisted of 12 rats housed in a large aquarium (60 x 60 x 40 cm) filled with toys that were changed every 2 days.</p>	<p>Positive effects:</p> <ul style="list-style-type: none"> <li>● Increased thermal nociceptive threshold and reduced mechanical allodynia were prevented in enriched VPA rats</li> <li>● Diminished acoustic prepulse inhibition was prevented in enriched VPA rats</li> <li>● Hyperactivity and increased repetitive movements in open field were prevented in enriched VPA rats</li> <li>● Reduced exploratory activity (rearing, hole-poking) was prevented in enriched VPA rats</li> <li>● Enriched rearing increased pinning behavior during social play and social exploration in both VPA and control rats</li> <li>● Enriched rearing increased time spent in the open arms of the elevated plus maze in both VPA and control rats</li> </ul> <p>Phenotypes that failed to improve:</p> <ul style="list-style-type: none"> <li>● Not reported</li> </ul> <p>Exacerbations:</p> <ul style="list-style-type: none"> <li>● Not reported</li> </ul>

Reference	Type of ASD Model	Enrichment Paradigm	Effect on Behavior
[344]	Male rats prenatally exposed to valproic acid (VPA)	Rats were enriched from PND 23-123. Enriched rats were in larger cages in groups of 6 and were given access to various toys. Enriched environments were either “predictable” or “unpredictable,” which simply meant whether or not the toys were changed at all. In the “unpredictable” condition the toys were changed twice weekly.	<p>Positive effects:</p> <ul style="list-style-type: none"> <li>● VPA-exposed rats housed in standard conditions had increased fear conditioning responses, but VPA-exposed rats raised in “unpredictable” enriched environments were similar to controls. However, VPA-exposed rats raised in “predictable” enriched environments had an impairment in fear conditioning.</li> </ul> <p>Phenotypes that failed to improve:</p> <ul style="list-style-type: none"> <li>● VPA-exposed rats had increased repeated entries in the Y-maze task regardless of housing condition.</li> </ul> <p>Exacerbations:</p> <ul style="list-style-type: none"> <li>● VPA-exposed rats housed in the “predictable” enriched environments had higher sociability in the 3-chamber test compared to control rats housed in similar conditions. However, this appears to be mostly because of a decrease in sociability in the enriched controls compared to standard-housed controls.</li> <li>● VPA-exposed rats housed in “predictable” enriched environments spent more time in the open arms of the elevated plus maze compared to the other groups.</li> </ul>

Particularly striking was that although we modeled our enrichment paradigm after the one described in a previous study that found positive effects of enrichment on a mouse model of Rett syndrome [43], including increased time spent in the center of the open field and increased motor performance on the rotarod, we found that enrichment negatively impacted both of these measurements in our mouse model. This might suggest that a “one-size fits all” approach may not

work for behavioral intervention with patients with different genetic mutations, but the translational value of the findings in these studies are not immediately clear. One possible explanation for the conflicting findings in the two studies is the different clinical presentations of Rett syndrome and Phelan-McDermid syndrome in humans; while patients with *SHANK3* mutations typically display signs of neurological impairments at birth [358], patients with *MECP2* mutations typically present after 12-16 months [359]. Another possible explanation is that because in our attempt to remain blind to experimental condition we removed mice from the enriched environments prior to behavior testing and this may have had an anxiogenic effect. The previous study utilizing the mouse model of Rett syndrome kept the mice in enriched environments throughout testing. A potential follow-up experiment could specifically examine the effect of transferring mice back to standard cages following the enrichment paradigm.

However, there are many other possible explanations for the negative results presented here, including varying methods of enrichment and differences in genetic backgrounds used in previous studies, as well as different methods of assessing behavioral phenotypes. While the negative results presented do not exclude the possibility that a different form of enrichment would be beneficial to our mouse model, it would be unreasonably time consuming to try all the different variations of enrichment. Regardless, the lack of effect of environment suggests that *SHANK3* mutations are highly penetrant and underscores the need for molecularly targeted pharmaceutical intervention. Still, environmental enrichment remains promising for other forms of ASD and many other brain-related disorders (reviewed in [360]).

## **4. Incompletely disrupting Shank3 expression postnatally is insufficient to produce phenotypes associated with germline deficiency**

### ***4.1 Introduction***

It has been proposed that ASD results from disruptions to synaptic development during a critical period of brain plasticity. Patients are typically diagnosed within the first three years of life, corresponding to a period of rapid growth and refinement of neural connections. However, much remains to be discovered regarding the developmental pathogenesis of the disorder. The Shank3 mouse model of ASD is well-suited to determine whether disruptions to synaptic development contribute to ASD pathogenesis because *in vitro* studies have directly linked Shank3 to the formation of synapses [160] and *in vivo* studies utilizing conventional knockouts have presented multiple ASD-like and comorbid behavioral phenotypes [171, 318].

Conditional knockout technology has been developed for use in mice to manipulate gene expression over space and time. This technology has allowed researchers to identify brain regions and cell types involved in the manifestation of ASD-like behaviors in mouse models. It has also allowed for researchers to begin to study the developmental trajectory of the disorder and the reversibility of behavioral phenotypes through genetic rescue (reviewed in [319]). Although it has been demonstrated that a subset of phenotypes can be rescued in adulthood through restoring Shank3 expression [301], it has not yet been determined whether ASD-like behaviors can be induced by disrupting Shank3 expression in fully developed organisms, or whether there is a critical period in development for Shank3 expression. In other mouse models of ASD, such as with *Mecp2* mutants, it appears that some phenotypes can be induced in adult mice through conditional knockout and reversed in adult mutants by genetic rescue [295-298]. However, in other models, such as with *Ube3a* mutants, certain phenotypes cannot be reversed in adult mutants by genetic

rescue or induced through postnatal deletion [299, 361]. This suggests that different ASD-causing mutations may have varying consequences during development.

In the current study, we crossed the ubiquitously-expressed inducible Cre line, Tg(CAG-cre/Esr1\*)5Amc (CAGGS-CreER; JAX 004453) with our mice containing loxP sites surrounding *Shank3* exons 4-22 (*Shank3* e4-22<sup>flox</sup>). We then delivered tamoxifen to determine the effects of disrupting *Shank3* expression during two different time periods in development. We found that reducing *Shank3* expression in fully developed mice had minimal effects on behaviors that are characteristic of our conventional knockout mice. Similarly, disrupting *Shank3* expression during an earlier time period (postnatal day 10-21) did not induce behaviors associated with germline deficiency. This suggests that *Shank3* may play a role in development prior to synaptogenesis. However, limited efficiency of the disruption could have contributed to our negative results. For both groups of mice, we used conventional germline knockout littermates to act as positive controls and found that the behavioral phenotypes for these mice were consistent with what we previously observed.

## **4.2 Methods**

### **4.2.1 Animals**

*Shank3* e4-22<sup>flox</sup> and e4-22<sup>-/-</sup> mice were previously generated and characterized by our lab and were maintained on a C57BL/6J background after backcrossing for at least 8 generations [171]. We crossed our *Shank3* e4-22<sup>flox</sup> and e4-22<sup>-/-</sup> mice with the ubiquitously-expressed inducible Cre line, Tg(CAG-cre/Esr1\*)5Amc (CAGGS-CreER) [Stock No. 004453, Jackson Laboratories, Bar Harbor, ME], which we also backcrossed to a C57BL/6J background for at least 8 generations. This allowed us to create two groups of inducible knockout mice: one group with both *Shank3* alleles floxed (fl/fl) and one group with one *Shank3* allele floxed and one null *Shank3* allele (fl/-). Our

breeding scheme (female *Shank3* e4-22<sup>fl<sup>ox</sup>/-</sup> mice and male CAGGS-CreER+; *Shank3* e4-22<sup>fl<sup>ox</sup>/-</sup> mice) allowed us to generate germline knockout mice (-/-) as littermates and positive controls, as well as both groups of inducible knockout mice. For both adult knockout (AKO) and early postnatal knockout (EPKO) groups and for both types of inducible knockouts (fl/fl and fl/-) “control” groups were a combination of mice who either did not express the Cre transgene, did not receive tamoxifen, or both. The mice designated as AKO or EPKO were Cre<sup>+</sup> and were given tamoxifen during the corresponding developmental period. We observed some “leakiness” of the Cre (i.e. some recombination in offspring without tamoxifen administration) during pilot experiments using Cre<sup>+</sup> females as breeders, so we only used Cre<sup>+</sup> males as breeders for all experiments presented here. All experiments were conducted with protocols approved by the Institutional Animal Care and Use Committee at Duke University.

#### **4.2.2 Tamoxifen administration**

We first sought to develop a paradigm in which to deplete *Shank3* expression in adult and developing mice. We attempted to deliver tamoxifen dissolved in corn oil through both intraperitoneal injections, subcutaneous injections, and through oral gavage, which have all been previously reported in the literature. In all cases, we observed a high rate of mortality in the mice, regardless of genotype. We then switched to using a tamoxifen containing diet (Envigo Teklad 250 mg/kg diet, red color, Stock No. TD.130856), which allowed us to minimize toxicity and simultaneously reduce handling stress, which is particularly important for behavioral experiments.

For the AKO condition, we put the mice on the tamoxifen-containing diet for four weeks starting on postnatal day 60 (P60), allowed them to recover on a normal diet for two weeks, and then placed them on the tamoxifen-containing diet for an additional four weeks, culminating in 8 weeks total of exposure to the tamoxifen-containing diet. This reduced mortality to approximately 25% and maximized efficiency of eliminating the *Shank3* protein. During a pilot experiment, we placed

some mice on the tamoxifen-containing diet for a total of 16 weeks and this did not increase the efficiency compared to the 8 week condition. For the early postnatal knockout condition, we put nursing mothers (breeders, who were Cre negative) on the tamoxifen-containing diet and tamoxifen was delivered via the lactating dam to pups from postnatal day 10 (P10) to postnatal day 21 (P21). This resulted in similar mortality rates and *Shank3* deletion efficiency to the adult knockout condition.

#### **4.2.3 Isolation of striatal postsynaptic density fractions**

Isolation of crude postsynaptic densities (PSDs) was performed as previously described (Wang et al. 2016) to determine the deletion efficiency of our conditional knockout models. Protease and phosphatase inhibitors were used throughout at a concentration of 1:200 each and the entire process was done at 4°C. Striata from mice in each of the 10 groups (fl/fl control, fl/fl conditional knockout, fl/- control, fl/- conditional knockout, -/- for each developmental time point) were homogenized in HEPES-buffered sucrose (0.32 M sucrose, 4 mM HEPES, pH 7.4) and centrifuged at  $800 \times g$  for 10 min. The supernatants were transferred to a new set of tubes and centrifuged at  $12,000 \times g$  for 15 min. The supernatant from this step was discarded. The pellet was lysed using water, then buffered with HEPES (pH 7.4) to 4 mM, and the sample was mixed by rotation for 30 min, followed by centrifugation at  $20,500 \times g$  for 30 min to yield the synaptosomal membrane (SPM) fraction. The SPM was resuspended in a buffer containing 50 mM HEPES (pH 7.4), 2 mM EDTA, and 0.5% Triton-X 100. After 15 min of mixing by rotation, the crude PSD fraction was obtained by centrifugation at  $32,000 \times g$  for 20 min. The crude PSD pellet was dissolved in 1% SDS in PBS for further immunoblot analysis.

#### **4.2.4 Quantitative immunoblot analysis**

An equal amount of total protein from each striatal PSD fraction was loaded and separated by SDS-PAGE. Proteins were transferred to PVDF membranes (Bio-Rac, Hercules, CA). The

membranes were then blocked for 1 hr in 5% non-fat milk in TRIS-buffered saline (TBS, pH 7.4). Then they were incubated with the primary antibodies diluted in the same solution overnight at 4°C. The following day, the membranes were washed in TBS containing 0.1% Tween-20 (TBST) and then were incubated with HRP-conjugated secondary antibodies diluted in 5% non-fat milk in TBS for 1 hr at room temperature. Following 3 additional washes in TBST, the membranes were incubated with ECL reagent (Thermo Fisher Scientific, Waltham, MA) and then imaged on a ChemiDoc MP Imaging System (Bio-Rad). The gray values of Shank3 protein were measured using ImageJ software (NIH, Bethesda, MD) and normalized to a corresponding internal control ( $\beta$ -tubulin III).

#### **4.2.5 Antibodies**

The Shank3 antibody was a generous gift from YongQing Zhang from the Institute of Genetics and Development at Chinese Academy of Science. The  $\beta$ -tubulin III antibody (ab18207) was purchased from Abcam (Cambridge, MA) and was used at a 1:10,000 dilution. The HRP-conjugated secondary antibodies were purchased from Santa Cruz Biotechnology and were used at the same dilution as their respective primary antibodies.

#### **4.2.6 Behavioral phenotyping**

##### **4.2.6.1 Cohorts for behavioral assays**

Three cohorts containing mice from the five groups (fl/fl control, fl/fl conditional knockout, fl/- control, fl/- conditional knockout, -/-) in each of the AKO and EPKO conditions were run through a battery of behavioral tests, for a total of 6 behavioral cohorts for this study. The experimenter was blind to both genotype and rearing conditions until data analysis. The assays were performed in order they are described for all cohorts. Both male and female mice were used

for all experiments presented in this study, except for ultrasonic vocalizations, which is largely a sex-specific behavior.

#### **4.2.6.2 Open field locomotion**

Activity in the open field was measured for 1 hour in an automated Omnitech Digiscan apparatus (AccuScan Instruments, Columbus, OH). AccuScan software calculated the total distance traveled and time spent in the center of the arena.

#### **4.2.6.3 Self-grooming**

Individual animals were placed into clean home cages without bedding and acclimated for five minutes. Mice were filmed for 10 minutes and then videos were later manually scored for time spent grooming.

#### **4.2.6.4 Rotarod**

Performance on the rotarod (Med-Associates) was assessed over four trials lasting five minutes each. The intertrial interval was 30 minutes. The rod started at four rotations per minute (RPM) and slowly increased to 40 RPM over the five-minute trial.

#### **4.2.6.5 Operant conditioning**

Mice were food restricted until they reached approximately 85% of their original body weight. Individual operant conditioning chambers (Med-Associates) were equipped with a retractable lever and a liquid dipper that delivered a drop of sweetened condensed milk as a food reward. The Med-PC-IV program was used to create the reinforcement schedule and record the data. The paradigm consisted of seven days of continuous reinforcement (one lever press earned one drop of sweetened condensed milk every time). Each session began with illumination of the chamber and presentation of the lever and ended with extinguishing the light and retracting the

lever. Trials ended after either one of two conditions had been satisfied: 60 minutes had passed or the mouse had pressed the lever 100 times.

#### **4.2.6.6 Adult ultrasonic vocalizations**

Male mice were given breeding experience with an age-matched female mouse for at least four days (the duration of the estrous cycle) and then were individually housed for at least 24 hours. For testing, the male mice were placed in a sound-attenuating styrofoam chamber equipped with an externally polarized condenser CM16/CMPA microphone with a frequency range of 10-200 kHz (Avisoft Bioacoustics Inc.) suspended 20 cm above the floor of the chamber. After the test mouse acclimated for 10 minutes, an 8-10 week old virgin female C57BL/6J mouse (Jackson Labs) was added to the chamber and vocalizations were recorded for five minutes as waveform audio files using Avisoft-RECORDER. The files were analyzed later using Avisoft SASLab Pro software. Mice that did not call were excluded from analysis.

### **4.3 Results**

#### **4.3.1 Shank3 expression can be depleted in adult mice with limited efficiency**

First, we wanted to see whether there was any role of neurodevelopment in the manifestation of ASD-like behaviors of *Shank3* deficient mice. We therefore optimized a system to deplete Shank3 expression in fully developed mice and assessed their behavior to test whether *Shank3* mutations that are induced in adult mice can produce phenotypes that are consistent with germline deletion. CAGGS-CreER; *Shank3* e4-22<sup>fl<sub>ox</sub>/fl<sub>ox</sub></sup> mice develop with wildtype levels of Shank3 and then tamoxifen administration allows for recombination of the floxed DNA sequences. After putting the CAGGS-CreER; *Shank3* e4-22<sup>fl<sub>ox</sub>/fl<sub>ox</sub></sup> (fl/fl AKO) mice on a tamoxifen-containing diet for eight weeks, only a modest reduction of Shank3 protein was observed in the PSD fractions of the striatum compared to controls (Figure 26). We therefore took advantage of the fact that our

heterozygous *Shank3*  $\Delta e4-22^{+/-}$  mice show little to no phenotype (Hulbert et al. 2018, Wang et al. 2016). After eight weeks on a tamoxifen-containing diet, CAGS-CreER; *Shank3*  $e4-22^{flox/flox}$  (*fl/-* AKO) mice showed a reduction in *Shank3* protein in the PSD fractions of the striatum compared to their controls, but this disruption was still incomplete (Figure 26).

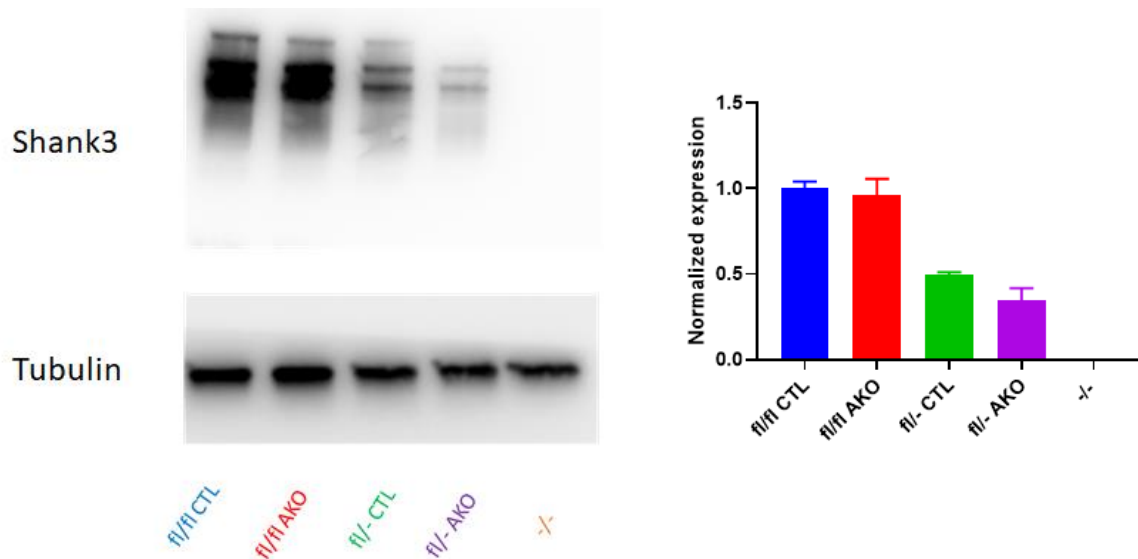


**Figure 26: Quantification of *Shank3* protein levels in adult knockout (AKO) mice.**

(left) Representative western blot of PSD fractions from striata in mice in each of the five groups (*fl/fl* CTL, *fl/fl* AKO, *fl/-* CTL, *fl/-* AKO, *-/-*) showing *Shank3* expression levels.  $\beta$ -tubulin was used as a loading control. (right) Quantification of *Shank3* expression normalized to *fl/fl* control levels ( $n = 3$  mice per group). Bar graphs represent means  $\pm$  SEM.

#### 4.3.2 Adult knockout mice do not present with behavioral phenotypes that have been observed in germline knockout mice

Self-grooming is often elevated in mouse models of ASD and is thought to represent a repetitive behavior. We previously reported that *Shank3*  $\Delta e4-22^{+/-}$  mice self-groom at significantly higher rates compared to wildtype and heterozygous mice. Our current study confirms this

phenotype in the germline knockout mice, but there were no differences between fl/fl AKO mice and their controls or fl/- AKO mice and their controls (Figure 27).

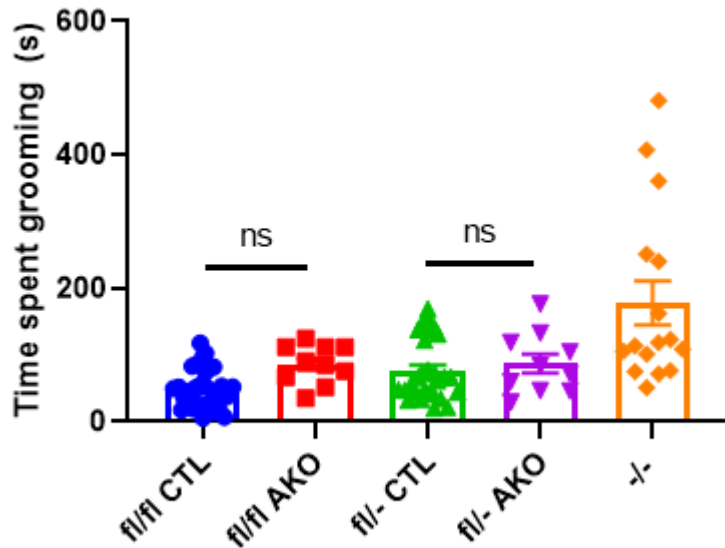


**Figure 27: Self-grooming rates of Shank3 adult knockout, germline knockout, and control groups**

**Neither group of adult knockout (AKO) mice, those who express two floxed Shank3 alleles (fl/fl) or those who express one floxed Shank3 allele and one null Shank3 allele (fl/-) groomed significantly more than their respective controls. Germline Shank3 knockout (-/-) mice groomed at a rate that is consistent with our previous observations. Data points are individual mice superimposed onto bar graphs representing means  $\pm$  SEM. “ns” indicates nonsignificant differences between conditional knockout groups and their controls.**

Ultrasonic vocalizations (USVs) are used to evaluate social communication in mouse models of ASD. We previously reported that Shank3  $\Delta e4-22^{-/-}$  mice call fewer times and their calls are significantly shorter in length compared to wildtype and heterozygous mice (Wang et al. 2016). The cumulative duration of calls takes both measurements into account. There were no significant differences in cumulative duration of USVs between either AKO group and their

controls (Figure 28). However, there was a trend for longer cumulative duration in both groups of AKO mice compared to their controls, which is the opposite direction of what is observed in the germline knockout mice (Figure 28).

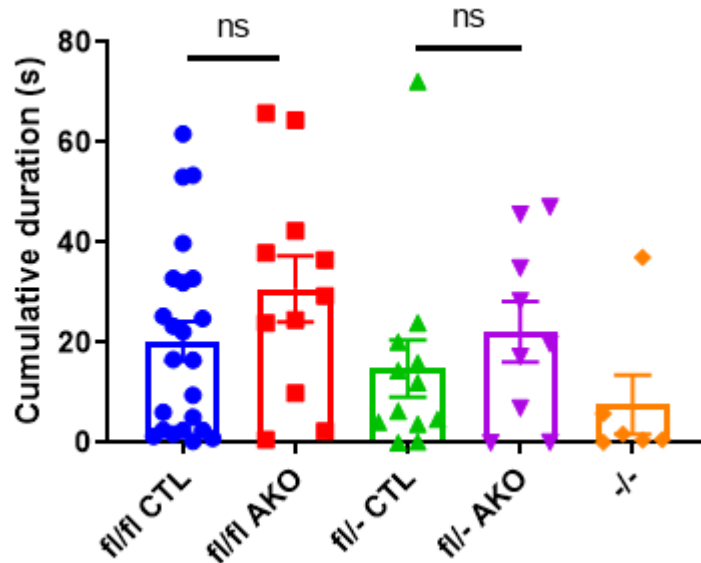


**Figure 28: Cumulative duration of ultrasonic vocalizations in Shank3 adult knockout, germline knockout, and control groups**

**Neither group of adult knockout (AKO) mice, those who express two floxed Shank3 alleles (fl/fl) or those who express one floxed Shank3 allele and one null Shank3 allele (fl/-) showed significant differences in cumulative duration of ultrasonic vocalizations compared to their respective controls. Data points are individual mice superimposed onto bar graphs representing means  $\pm$  SEM. “ns” indicates nonsignificant differences between conditional knockout groups and their controls.**

The open field test is used to measure spontaneous activity as well as anxiety-like behavior, as indicated by decreased time spent in the center of the arena. We previously reported that Shank3  $\Delta e4-22^{-/-}$  mice are hypoactive and spend less time in the center of the chambers compared to wildtype and heterozygous mice [171]. In the current study, disrupting Shank3 expression in adult mice had no significant effect on either activity (Figure 29) or on time spent in the center of the open field apparatus (Figure 30).

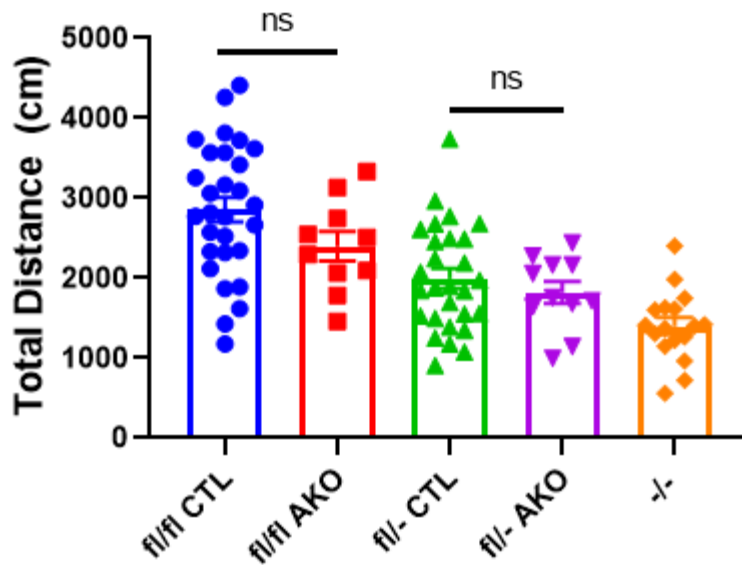


**Figure 29: Total distance traveled in the open field in Shank3 adult knockout, germline knockout, and control groups**

Neither group of adult knockout (AKO) mice, those who express two floxed Shank3 alleles (fl/fl) or those who express one floxed Shank3 allele and one null Shank3 allele (fl/-) showed significant differences in activity in the open field compared to their respective controls. Data points are individual mice superimposed onto bar graphs representing means  $\pm$  SEM. “ns” indicates nonsignificant differences between conditional knockout groups and their controls.

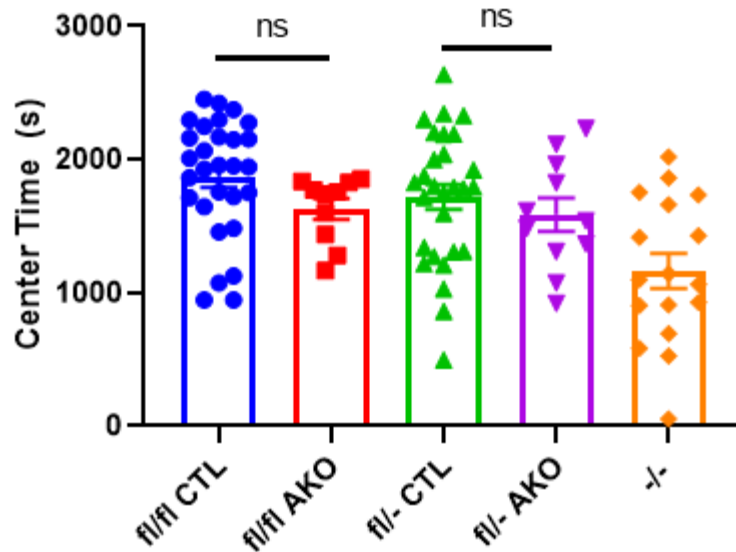


**Figure 30: Time spent in the center of the open field in Shank3 adult knockout, germline knockout, and control groups**

Neither group of adult knockout (AKO) mice, those who express two floxed Shank3 alleles (fl/fl) or those who express one floxed Shank3 allele and one null Shank3 allele (fl/-) showed significant differences in activity in the open field compared to their respective controls. Data points are individual mice superimposed onto bar graphs representing means  $\pm$  SEM. “ns” indicates nonsignificant differences between conditional knockout groups and their controls.

Patients with ASD often have comorbid difficulties with motor coordination. The accelerating rotarod task is one way to measure motor coordination in mice. Our Shank3  $\Delta e4-22^{-/-}$  mice fall off the rotarod more quickly than wildtype or heterozygous mice (Wang et al. 2016). However, disrupting Shank3 expression in adult mice did not have any significant effect on rotarod performance (Figures 31 and 32).

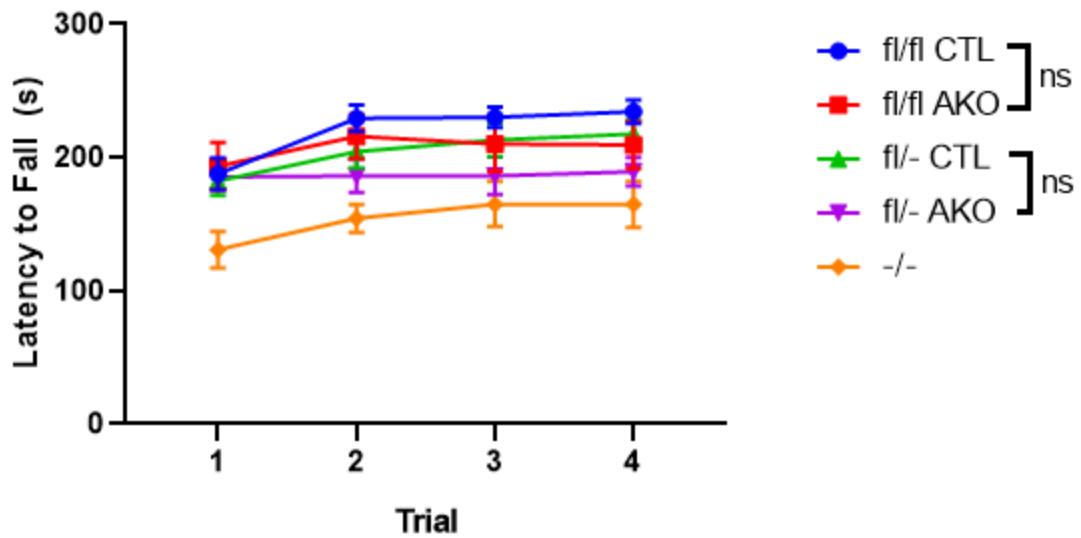


**Figure 31: Latency to fall off of the accelerating rotarod over four trials for Shank3 adult knockout, germline knockout, and control groups**

Neither group of adult knockout (AKO) mice, those who express two floxed Shank3 alleles (fl/fl) or those who express one floxed Shank3 allele and one null Shank3 allele (fl/-) showed significant differences in performance on the rotarod compared to their respective controls. Data represents means  $\pm$  SEM for each of the five groups in four consecutive trials. “ns” indicates nonsignificant differences between conditional knockout groups and their controls.

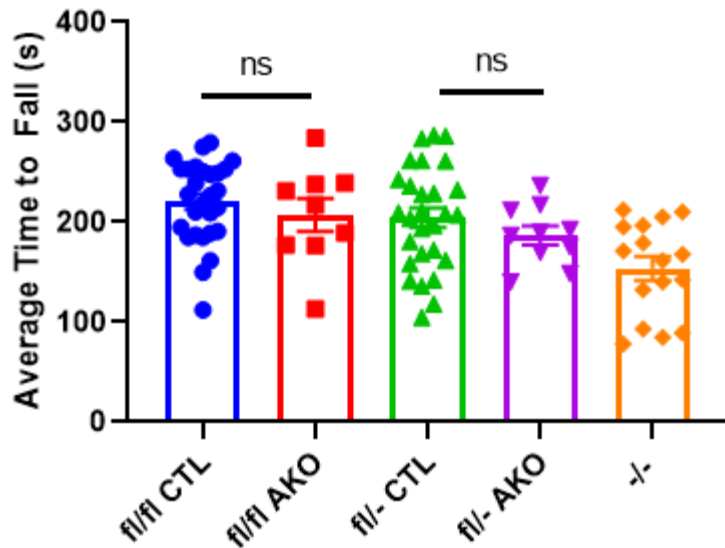


**Figure 32: Average latency to fall off of the accelerating rotarod over four trials for Shank3 adult knockout, germline knockout, and control groups**

Neither group of adult knockout (AKO) mice, those who express two floxed Shank3 alleles (fl/fl) or those who express one floxed Shank3 allele and one null Shank3 allele (fl/-) showed significant differences in performance on the rotarod compared to their respective controls.

Data points are the average performance of individual mice over the four trials superimposed onto bar graphs representing means  $\pm$  SEM. “ns” indicates nonsignificant differences between conditional knockout groups and their controls.

Intellectual disability also commonly presents with ASD. Operant conditioning is one way to assess learning and memory impairments in mice. We previously reported a robust deficit on a reward learning task in Shank3  $\Delta e4-22^{-/-}$  mice (Wang et al. 2016). We repeated the protocol in the current study and found that disrupting Shank3 in adult mice does not impair performance on this task. In fact, the fl/fl AKO mice actually performed better on this task compared to their control group (Figures 33 and 34). There were no significant differences between fl/- AKO mice and their controls on this operant conditioning task (Figures 33 and 34).

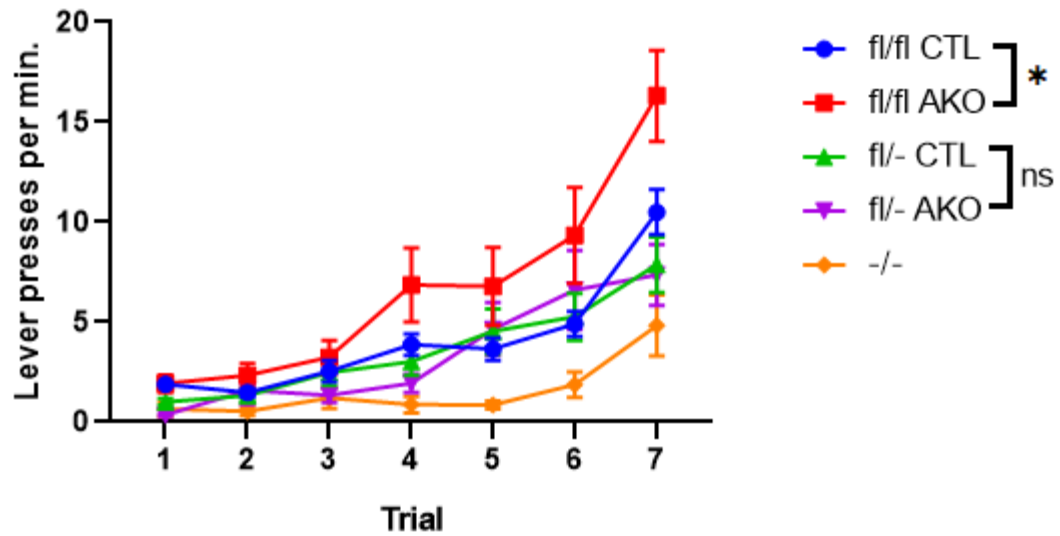


**Figure 33: Lever presses per minute during a reward learning task over seven trials for Shank3 adult knockout, germline knockout, and control groups**

The adult knockout (AKO) mice that express two floxed Shank3 alleles (fl/fl) press significantly more than their controls (RMANOVA,  $p < 0.05$ , main effect of genotype). There is no significant difference in performance between fl/- AKO mice and their controls. Data represents means  $\pm$  SEM for each of the five groups in seven consecutive trials. “ns” indicates nonsignificant differences between conditional knockout groups and their controls. \* represents  $p < 0.05$  between conditional knockout groups and their controls.

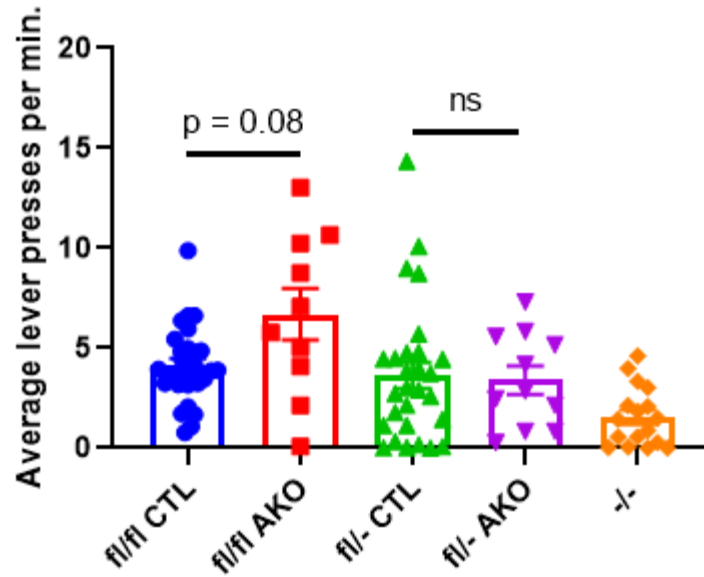


**Figure 34: Average lever presses per minute during a reward learning task over seven trials for Shank3 adult knockout, germline knockout, and control groups**

The adult knockout (AKO) mice that express two floxed Shank3 alleles (fl/fl) tend to press more than their controls, although this difference is not quite significant when comparing average performance across the seven trials ( $p = 0.08$ , unpaired two-tailed student's t-test). There is no significant difference in performance between fl/- AKO mice and their controls.

Data points are the average performance of individual mice over the seven trials superimposed onto bar graphs representing means  $\pm$  SEM. "ns" indicates nonsignificant differences between conditional knockout groups and their controls. Borderline significant differences are indicated with exact p values.

### 4.3.3 Shank3 expression can be disrupted in developing mice with variable efficiency

Overall, we observed that disrupting Shank3 expression in adult mice was insufficient to produce behavioral phenotypes associated with germline deficiency. This could indicate that Shank3 has a particular role in development that causes ASD-like behaviors to present in adulthood when this developmental process goes awry. To further explore this possibility, we then optimized the conditional knockout system to disrupt Shank3 expression earlier in development. We again used both CAGGS-Cre; Shank3 e4-22<sup>fllox/fllox</sup> mice and CAGGS-Cre;

Shank3  $e4-22^{fllox/-}$  mice in an attempt to maximize the efficiency of the deletion. We found that that administering tamoxifen from P10-P21 was more efficient than the eight weeks during adulthood. After the CAGGS-CreER; Shank3  $e4-22^{fllox/fllox}$  (fl/fl EPKO) mice received tamoxifen via the milk of their nursing mother, which was placed on a tamoxifen containing diet while the pups were P10-P21, many of these mice showed reduced Shank3 expression in the PSD of the striatum compared to their controls, resembling expression levels of germline heterozygous mice (Figure 35). Likewise, CAGGS-CreER; Shank3  $e4-22^{fllox/-}$  mice that were exposed to tamoxifen from P10-P21 showed a reduction in Shank3 expression compared to their control mice, often resembling expression levels of germline knockout mice (Figure 35). However, the Shank3 expression levels in these groups of mice were variable.

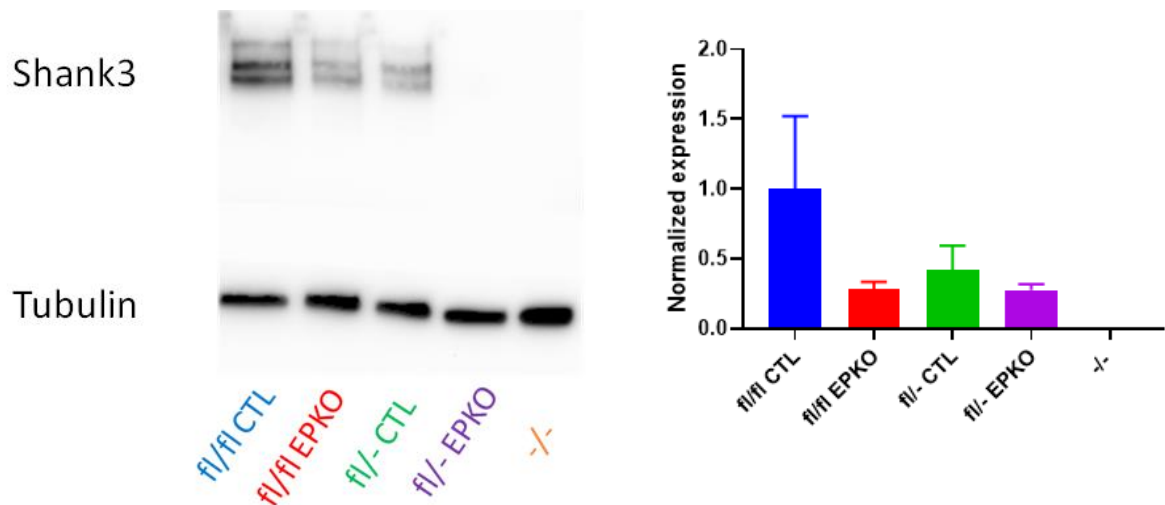


**Figure 35: Quantification of Shank3 protein levels in early postnatal knockout (EPKO) mice.**

(left) Example western blot of PSD fractions from striata in mice in each of the five groups (fl/fl CTL, fl/fl EPKO, fl/- CTL, fl/- EPKO, -/-) showing Shank3 expression levels.  $\beta$ -tubulin was used as a loading control. (right) Quantification of Shank3 expression normalized to fl/fl control levels (n = 3 mice per group). Bar graphs represent means  $\pm$  SEM.

#### 4.3.4 Disrupting Shank3 expression during an earlier period in development has minimal effects on behaviors associated with germline deficiency

Similar to the AKO mice, our EPKO mice did not display significantly different rates of self-grooming compared to their controls (Figure 36). Although the difference was not quite significant, fl/- EPKO mice tended to groom more than their controls ( $p = 0.09$ , student's t-test).

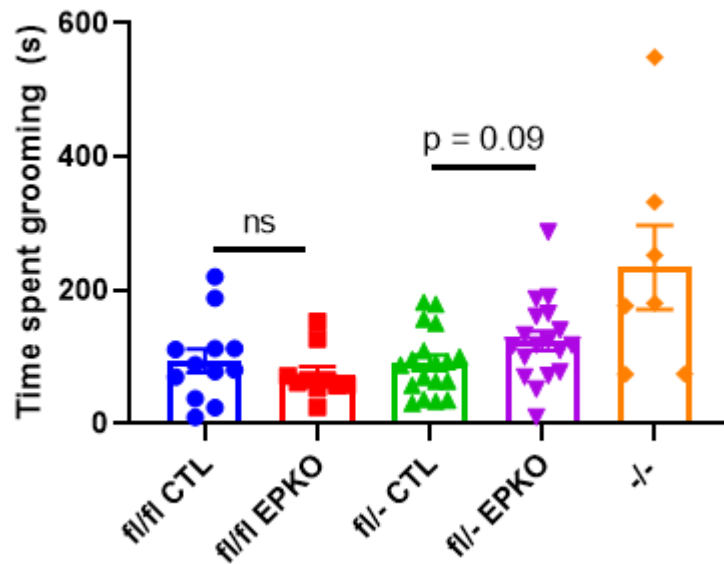


**Figure 36: Self-grooming rates of Shank3 early postnatal knockout, germline knockout, and control groups**

Neither group of early postnatal knockout (EPKO) mice, those who express two floxed Shank3 alleles (fl/fl) or those who express one floxed Shank3 allele and one null Shank3 allele (fl/-) groomed significantly more than their respective controls. However, fl/- EPKO mice tended to groom more than their controls ( $p = 0.09$ , student's t-test). Germline Shank3 knockout (-/-) mice groomed at a rate that is consistent with our previous observations. Data points are individual mice superimposed onto bar graphs representing means  $\pm$  SEM. “ns” indicates nonsignificant differences between conditional knockout groups and their controls. Borderline significant differences are indicated with exact p-values.

Ultrasonic vocalizations were also not significantly altered in either of the EPKO groups (Figure 37). Notably, similar to AKO mice, EPKO mice tended to have longer cumulative

durations of calls compared to their controls. However, these differences were once again not significant.

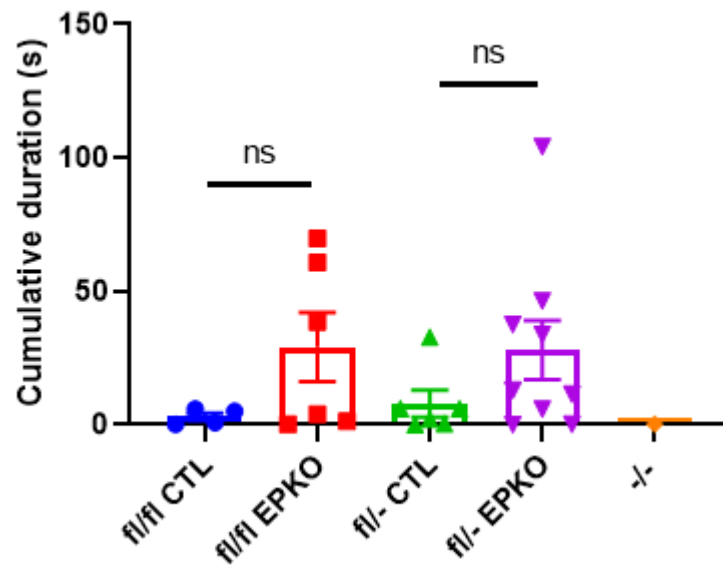


**Figure 37: Cumulative duration of ultrasonic vocalizations in Shank3 early postnatal knockout, germline knockout, and control groups**

Neither group of early postnatal knockout (EPKO) mice, those who express two floxed Shank3 alleles (fl/fl) or those who express one floxed Shank3 allele and one null Shank3 allele (fl/-) showed significant differences in cumulative duration of ultrasonic vocalizations compared to their respective controls. Data points are individual mice superimposed onto bar graphs representing means  $\pm$  SEM. “ns” indicates nonsignificant differences between conditional knockout groups and their controls.

In the open field, neither group of EPKO mice were hypoactive compared to their controls (Figure 38). In fact, each group tended to travel more distance in the open field than their

controls, but these differences were not significant. In terms of time spent in the center of the open field, neither group of EPKO performed significantly differently than their controls (Figure 39).

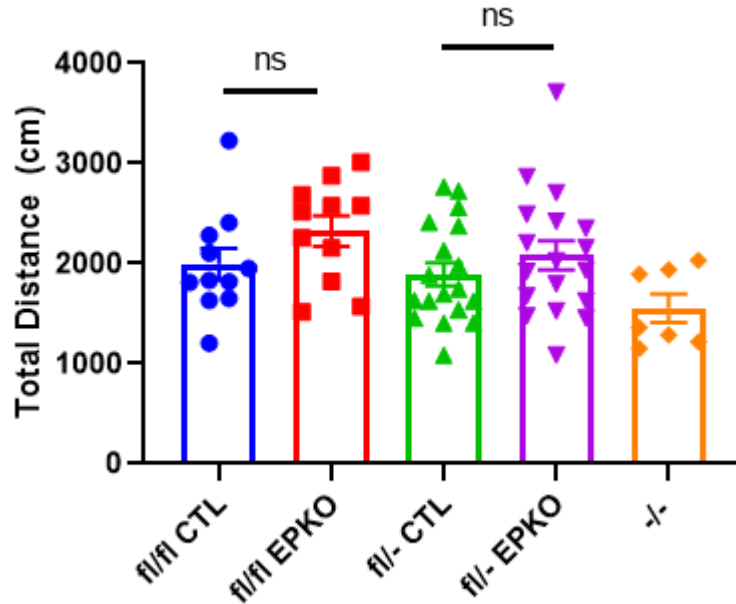


**Figure 38: Total distance traveled in the open field in Shank3 early postnatal knockout, germline knockout, and control groups**

Neither group of early postnatal knockout (EPKO) mice, those who express two floxed Shank3 alleles (fl/fl) or those who express one floxed Shank3 allele and one null Shank3 allele (fl/-) showed significant differences in activity in the open field compared to their respective controls. Data points are individual mice superimposed onto bar graphs representing means  $\pm$  SEM. “ns” indicates nonsignificant differences between conditional knockout groups and their controls.

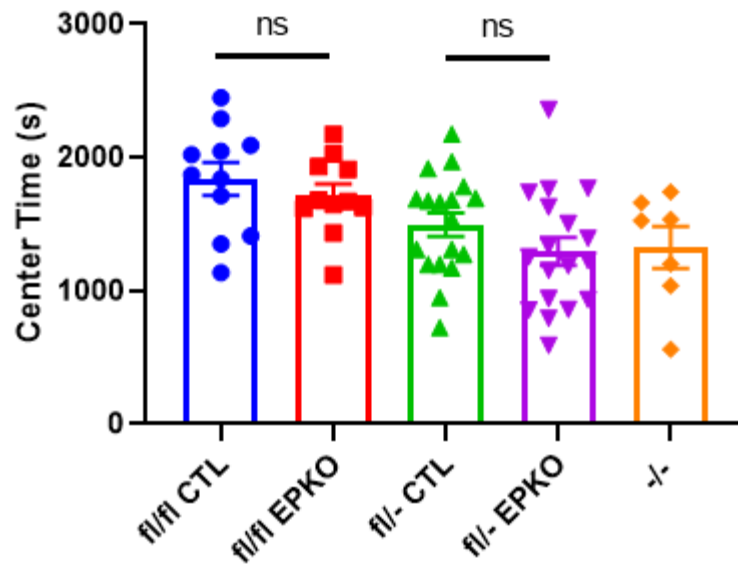


**Figure 39: Time spent in the center of the open field in Shank3 early postnatal knockout, germline knockout, and control groups**

Neither group of early postnatal knockout (EPKO) mice, those who express two floxed Shank3 alleles (fl/fl) or those who express one floxed Shank3 allele and one null Shank3 allele (fl/-) showed significant differences in activity in the open field compared to their respective controls. Data points are individual mice superimposed onto bar graphs representing means  $\pm$  SEM. “ns” indicates nonsignificant differences between conditional knockout groups and their controls.

Motor coordination was also not affected following disruption of Shank3 expression during the early postnatal period. The EPKO mice performed statistically the same as their control groups on the accelerating rotarod task (Figure 40). In fact, when each mouse’s average performance across the four trials was examined, fl/- EPKO mice tended to perform better than their controls, but this difference was not quite significant ( $p = 0.078$ , student’s t-test; Figure 41).

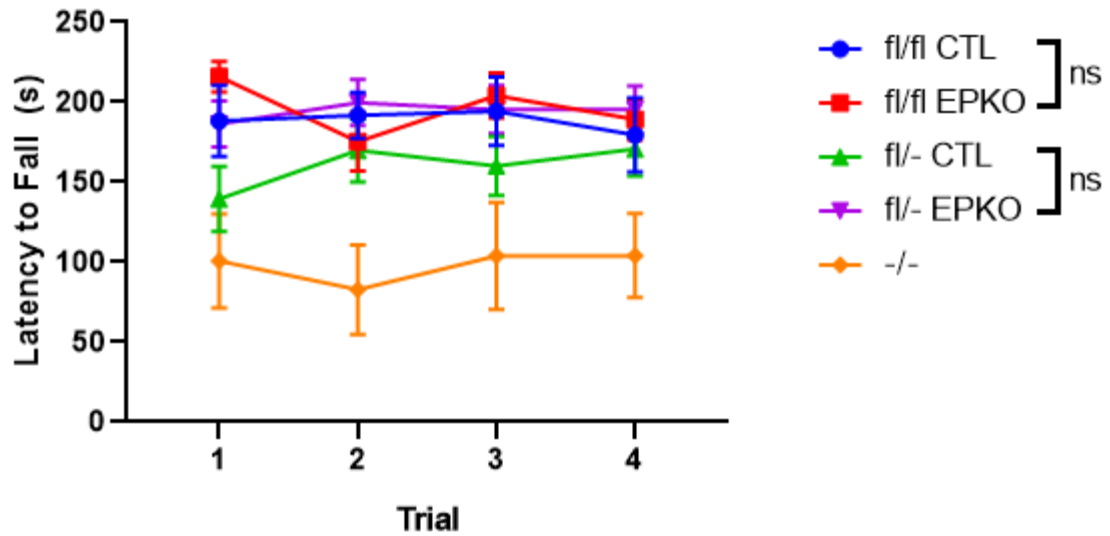


**Figure 40: Latency to fall off of the accelerating rotarod over four trials for Shank3 early postnatal knockout, germline knockout, and control groups**

Neither group of early postnatal knockout (EPKO) mice, those who express two floxed Shank3 alleles (fl/fl) or those who express one floxed Shank3 allele and one null Shank3 allele (fl/-) showed significant differences in performance on the rotarod compared to their respective controls. Data represents means  $\pm$  SEM for each of the five groups in four consecutive trials. “ns” indicates nonsignificant differences between conditional knockout groups and their controls.

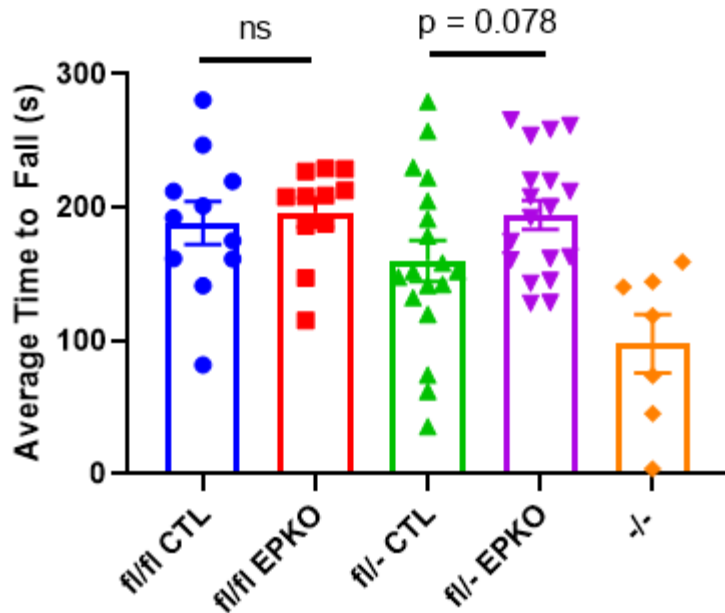


**Figure 41: Average latency to fall off of the accelerating rotarod over four trials for Shank3 early postnatal knockout, germline knockout, and control groups**

Neither group of early postnatal knockout (EPKO) mice, those who express two floxed Shank3 alleles (fl/fl) or those who express one floxed Shank3 allele and one null Shank3 allele (fl/-) showed significant differences in performance on the rotarod compared to their respective controls. fl/- EPKO mice had a tendency to last longer on the accelerating rotarod compared to their controls, but this difference was not quite significant ( $p = 0.078$ , student's t-test). Data points are the average performance of individual mice over the four trials superimposed onto bar graphs representing means  $\pm$  SEM. "ns" indicates nonsignificant differences between conditional knockout groups and their controls. Borderline significant differences are indicated with exact p-values.

Finally, like the adult knockouts, EPKO mice did not display impairments on the operant conditioning task (Figures 42 and 43). However, it is worth noting that all mice in the EPKO cohorts, including control mice, performed worse than what is typically observed on this task, for unknown reasons.

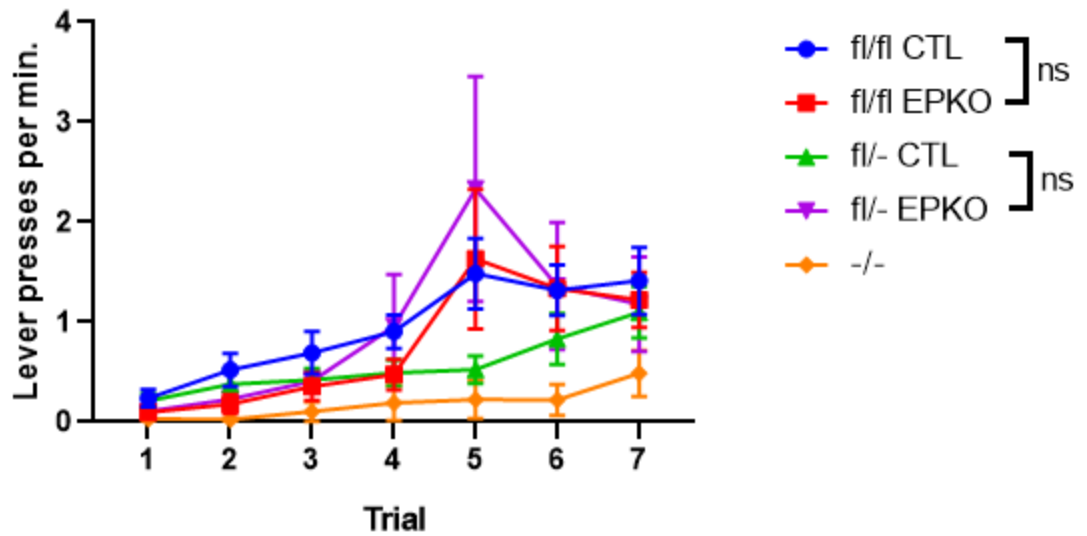


**Figure 42: Lever presses per minute during a reward learning task over seven trials for Shank3 early postnatal knockout, germline knockout, and control groups**

**Neither group of early postnatal knockout (EPKO) mice perform any differently than their controls on the operant conditioning task. Data represents means  $\pm$  SEM for each of the five groups in seven consecutive trials. “ns” indicates nonsignificant differences between conditional knockout groups and their controls.**

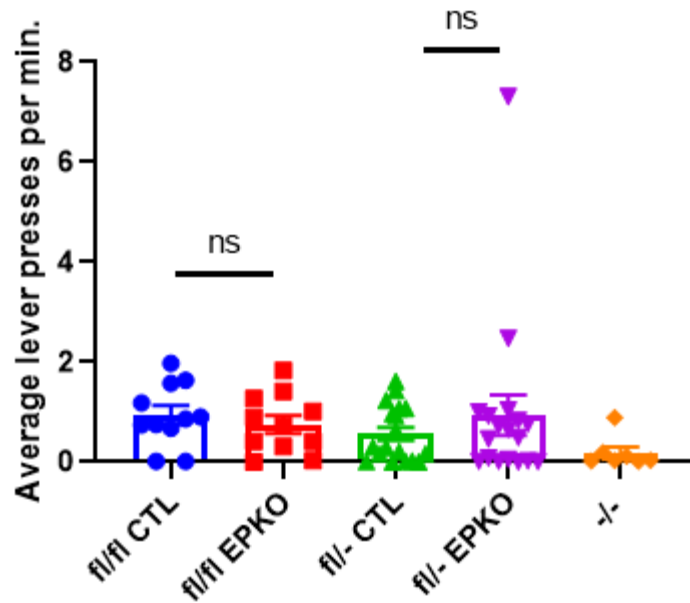


**Figure 43: Average lever presses per minute during a reward learning task over seven trials for Shank3 early postnatal knockout, germline knockout, and control groups**

**Neither group of early postnatal knockout (EPKO) mice perform significantly differently than their control group on the operant conditioning task. Data points are the average performance of individual mice over the seven trials superimposed onto bar graphs representing means  $\pm$  SEM. “ns” indicates nonsignificant differences between conditional knockout groups and their controls.**

#### **4.4 Conclusions**

We first wanted to determine whether disrupting Shank3 expression in fully developed mice could lead to the expression of behavioral phenotypes we have observed in Shank3 germline deficient mice. Our inability to induce these behavioral phenotypes in adult mice suggests that the behavioral phenotypes caused by Shank3 deficiency may be due to disrupted neurodevelopment, rather than ongoing neuronal dysfunction. However, the relative inefficiency of the protein depletion makes it difficult to make any definitive conclusions. This raises questions concerning what level of Shank3 suppression is sufficient to produce these phenotypes. In human patients, missing one copy of the *SHANK3* gene is typically sufficient to produce a fairly severe diagnosis

of ASD. However, across multiple studies in our laboratory and others, mice heterozygous for *Shank3* have a mild or no phenotype. It remains to be determined why humans are more sensitive to gene dosage for *SHANK3*.

After observing no phenotype in the adult knockout mice that resembled phenotypes in the germline deficient mice, we optimized the system to deplete *Shank3* expression earlier in development. We did observe some greater efficiency when working with this earlier time period, but it was still insufficient to reliably produce any phenotypes associated with germline deficiency. There was a trend of increased self-grooming in EPKO mice, but the differences did not reach statistical significance, and no other behavioral phenotypes that are present in our conventional knockout mice were observed in the EPKO mice. This suggests that there may be roles for *Shank3* in development prior to the peak in synapse formation and elimination that is occurring during the time period chosen. However, again, the variability in efficiency we observed limits our interpretation.

Relatively few studies have attempted to examine the inducibility or reversibility of ASD-like behaviors in mice through conditional knockout or genetic rescue [199, 295-299, 301, 361, 362]. Among those that have, not all of the studies specifically examined repetitive behaviors or social communication deficits, the core symptoms of ASD. However, in general, these studies have indicated that certain phenotypes can be induced or reversed by manipulating gene expression, while other phenotypes are unchangeable (reviewed in [319]). In particular, one study demonstrated that elevated self-grooming could be rescued (i.e. reduced to wildtype levels) by restoring *Shank3* expression in mice that developed with a *Shank3* mutation that disrupted most isoforms [301]. Taken together with our results, this suggests that *Shank3* may be required for certain developmental processes, such as synapse formation, that can be triggered later by

restoring its expression, but are not lost by disrupting *Shank3* expression after development has already occurred.

Previous studies utilizing the same system we attempted to use in the current study reported much more success regarding the efficiency of the deletion. We attempted to delete a relatively large portion of DNA, spanning 18 exons, which may have contributed to our limited efficiency. Previous studies also do not mention any adverse effects of tamoxifen, but mortality was a major problem in the current study across multiple routes of administration. In designing future experiments, researchers should be aware of the limitations that exist in using inducible knockout technology and should keep in mind that tamoxifen treatment may have some off-target effects. Not only are cryptic *loxP* sites present in the mouse genome that may result in recombination of other genes, but tamoxifen is far from an inert drug, with a host of side effects [259, 363].

Our findings add to the growing concern regarding the interpretation of studies utilizing conditional knockout technology to study the plasticity of behavioral phenotypes associated with ASD. Another recent study reported apparent rescue of behavioral phenotypes in vehicle-treated CAGGs-CreER expressing *Shank3* mutants, implicating some baseline behavioral effects produced by the Cre transgene [364]. An alternative potential reason for the negative results presented in the current study is our inclusion of the appropriate Cre-positive mice that did not receive tamoxifen in our control groups, whereas previous studies did not implement all necessary controls. Although the conclusions we are able to draw about the developmental pathophysiology of ASD are limited due to technical constraints, our study does confirm that mice with germline deficiency of *Shank3* have robust, repeatable phenotypes.

## 5. Conclusion: Discussion and future directions

### 5.1 Different mouse models of ASD present with widely varying behavioral phenotypes

The *Shank3* e4-22<sup>-/-</sup> and *Chd8*<sup>+/-</sup> mouse models of ASD both have strong construct validity for the human disorder, as mutations with the same presumed molecular consequences have been observed repeatedly in the clinical population. However, the two models present with exclusively non-overlapping behavioral phenotypes. In particular, some of the most robust and repeatable findings from the *Shank3* e4-22<sup>-/-</sup> model across multiple studies presented in this dissertation are elevated self-grooming, decreased number and length of ultrasonic vocalizations, hypoactivity in the open field, increased thigmotaxis in the open field, impaired performance on the rotarod, and impaired performance on a reward learning paradigm. Our *Chd8*<sup>+/-</sup> model, on the other hand, displays no differences in self-grooming, shows *increased* number and length of ultrasonic vocalizations, normal activity in the open field, no thigmotaxis in the open field, *improved* performance on the rotarod, and no impairment in reward learning.

Even across studies that examine different *Chd8* models, there is a wide variety of behavioral phenotypes reported. One potential explanation for this variability is that the models involve deletions of different parts of the *Chd8* gene. Our lab has extensively characterized the transcriptional complexity of *Shank3*, which revealed multiple intragenic promoters and alternatively spliced exons, and demonstrated that different exonic deletions disrupted different sets of many different possible isoforms. However, no such work has been done on the *Chd8* gene and this is one potential avenue for future research.

Another question that remains is why the heterozygous *Shank3* animals continue to present no real phenotype. Perhaps future studies using other model organisms, such as non-human primates, will help shed light on this issue. At least two different non-human primate

models of *SHANK3*-related ASD have been produced and reported in the literature already [365, 366].

## ***5.2 Environmental enrichment can improve behavioral phenotypes in some, but not all, mouse models of ASD***

Previous studies have reported that exposing mouse models of ASD to enriched environments can help ameliorate some of the behavioral phenotypes in these models. However, our study was the first to report little to no benefit of such non-pharmacological interventions. It may be that other laboratories have produced similar findings, but did not report them due to bias against negative results. It is also possible that previous studies utilizing environmental enrichment were subject to experimental bias if they did not take proper precautions to blind themselves to housing conditions. Moreover, it is possible we used the incorrect enrichment paradigm for our model, but many variations in methods make it difficult to assess this possibility.

More likely, some mouse models of ASD are more responsive to environmental enrichment than others. As ASD has many different etiologies and symptom severity, it is important to create individualized treatment plans for patients with different genetic mutations. Our findings underscore the necessity for alternative approaches to treating *SHANK3*-related ASD.

## ***5.3 Limitations inherent in conditional knockout technology caution its future use***

Our inability to reliably deplete Shank3 expression postnatally using available conditional knockout technology cautions the use of such methods in future studies. We also observed a significant amount of toxicity associated with tamoxifen treatment, which has not been reported by previous studies. These findings add to a growing concern about the

interpretability of studies that utilize such methods. Of course, alternative approaches also carry their own sets of limitations.

## References

1. American Psychiatric Association. and American Psychiatric Association. DSM-5 Task Force., *Diagnostic and statistical manual of mental disorders : DSM-5*. 5th ed. 2013, Washington, D.C.: American Psychiatric Association. xlv, 947 p.
2. Argyropoulos, A., K.L. Gilby, and E.L. Hill-Yardin, *Studying autism in rodent models: reconciling endophenotypes with comorbidities*. *Front Hum Neurosci*, 2013. **7**: p. 417.
3. Lord, C., et al., *Autism spectrum disorders*. *Neuron*, 2000. **28**(2): p. 355-63.
4. Howlin, P., et al., *Adult outcome for children with autism*. *J Child Psychol Psychiatry*, 2004. **45**(2): p. 212-29.
5. Jeremy Willsey, A. and M.W. State, *Autism spectrum disorders: from genes to neurobiology*. *Curr Opin Neurobiol*, 2015. **30C**: p. 92-99.
6. Persico, A.M. and V. Napolioni, *Autism genetics*. *Behav Brain Res*, 2013. **251**: p. 95-112.
7. Chang, J., et al., *Genotype to phenotype relationships in autism spectrum disorders*. *Nat Neurosci*, 2015. **18**(2): p. 191-8.
8. Chaste, P., et al., *A genome-wide association study of autism using the Simons Simplex Collection: Does reducing phenotypic heterogeneity in autism increase genetic homogeneity?* *Biol Psychiatry*, 2015. **77**(9): p. 775-84.
9. Hallmayer, J., et al., *Genetic heritability and shared environmental factors among twin pairs with autism*. *Arch Gen Psychiatry*, 2011. **68**(11): p. 1095-102.
10. *Prevalence of autism spectrum disorder among children aged 8 years - autism and developmental disabilities monitoring network, 11 sites, United States, 2010*. *MMWR Surveill Summ*, 2014. **63**(2): p. 1-21.
11. King, M. and P. Bearman, *Diagnostic change and the increased prevalence of autism*. *Int J Epidemiol*, 2009. **38**(5): p. 1224-34.
12. Liu, K.Y., M. King, and P.S. Bearman, *Social influence and the autism epidemic*. *AJS*, 2010. **115**(5): p. 1387-434.

13. Nevison, C.D., *A comparison of temporal trends in United States autism prevalence to trends in suspected environmental factors*. Environ Health, 2014. **13**: p. 73.
14. Buescher, A.V., et al., *Costs of autism spectrum disorders in the United Kingdom and the United States*. JAMA Pediatr, 2014. **168**(8): p. 721-8.
15. Karten, A. and J. Hirsch, *Brief report: Anomalous neural deactivations and functional connectivity during receptive language in autism spectrum disorder: a functional MRI study*. J Autism Dev Disord, 2015. **45**(6): p. 1905-14.
16. Devlin, B. and S.W. Scherer, *Genetic architecture in autism spectrum disorder*. Curr Opin Genet Dev, 2012. **22**(3): p. 229-37.
17. Willner, P., *The validity of animal models of depression*. Psychopharmacology (Berl), 1984. **83**(1): p. 1-16.
18. Belzung, C. and M. Lemoine, *Criteria of validity for animal models of psychiatric disorders: focus on anxiety disorders and depression*. Biol Mood Anxiety Disord, 2011. **1**(1): p. 9.
19. Silverman, J.L., et al., *Behavioural phenotyping assays for mouse models of autism*. Nat Rev Neurosci, 2010. **11**(7): p. 490-502.
20. *Psychiatric genome-wide association study analyses implicate neuronal, immune and histone pathways*. Nat Neurosci, 2015. **18**(2): p. 199-209.
21. Amir, R.E., et al., *Rett syndrome is caused by mutations in X-linked MECP2, encoding methyl-CpG-binding protein 2*. Nat Genet, 1999. **23**(2): p. 185-8.
22. Lyst, M.J. and A. Bird, *Rett syndrome: a complex disorder with simple roots*. Nat Rev Genet, 2015. **16**(5): p. 261-75.
23. Nan, X., F.J. Campoy, and A. Bird, *MeCP2 is a transcriptional repressor with abundant binding sites in genomic chromatin*. Cell, 1997. **88**(4): p. 471-81.
24. Chahrouh, M., et al., *MeCP2, a key contributor to neurological disease, activates and represses transcription*. Science, 2008. **320**(5880): p. 1224-9.

25. Ben-Shachar, S., et al., *Mouse models of MeCP2 disorders share gene expression changes in the cerebellum and hypothalamus*. Hum Mol Genet, 2009. **18**(13): p. 2431-42.
26. Young, J.I., et al., *Regulation of RNA splicing by the methylation-dependent transcriptional repressor methyl-CpG binding protein 2*. Proc Natl Acad Sci U S A, 2005. **102**(49): p. 17551-8.
27. Maunakea, A.K., et al., *Intragenic DNA methylation modulates alternative splicing by recruiting MeCP2 to promote exon recognition*. Cell Res, 2013. **23**(11): p. 1256-69.
28. Chen, R.Z., et al., *Deficiency of methyl-CpG binding protein-2 in CNS neurons results in a Rett-like phenotype in mice*. Nat Genet, 2001. **27**(3): p. 327-31.
29. Guy, J., et al., *A mouse Mecp2-null mutation causes neurological symptoms that mimic Rett syndrome*. Nat Genet, 2001. **27**(3): p. 322-6.
30. Shahbazian, M., et al., *Mice with truncated MeCP2 recapitulate many Rett syndrome features and display hyperacetylation of histone H3*. Neuron, 2002. **35**(2): p. 243-54.
31. Belichenko, P.V., et al., *Widespread changes in dendritic and axonal morphology in Mecp2-mutant mouse models of Rett syndrome: evidence for disruption of neuronal networks*. J Comp Neurol, 2009. **514**(3): p. 240-58.
32. Fukuda, T., et al., *Delayed maturation of neuronal architecture and synaptogenesis in cerebral cortex of Mecp2-deficient mice*. J Neuropathol Exp Neurol, 2005. **64**(6): p. 537-44.
33. Smrt, R.D., et al., *Mecp2 deficiency leads to delayed maturation and altered gene expression in hippocampal neurons*. Neurobiol Dis, 2007. **27**(1): p. 77-89.
34. Chapleau, C.A., et al., *Hippocampal CA1 pyramidal neurons of Mecp2 mutant mice show a dendritic spine phenotype only in the presymptomatic stage*. Neural Plast, 2012. **2012**: p. 976164.
35. Moretti, P., et al., *Learning and memory and synaptic plasticity are impaired in a mouse model of Rett syndrome*. J Neurosci, 2006. **26**(1): p. 319-27.
36. Landi, S., et al., *The short-time structural plasticity of dendritic spines is altered in a model of Rett syndrome*. Sci Rep, 2011. **1**: p. 45.

37. Asaka, Y., et al., *Hippocampal synaptic plasticity is impaired in the Mecp2-null mouse model of Rett syndrome*. *Neurobiol Dis*, 2006. **21**(1): p. 217-27.
38. Dani, V.S., et al., *Reduced cortical activity due to a shift in the balance between excitation and inhibition in a mouse model of Rett syndrome*. *Proc Natl Acad Sci U S A*, 2005. **102**(35): p. 12560-5.
39. Chao, H.T., H.Y. Zoghbi, and C. Rosenmund, *MeCP2 controls excitatory synaptic strength by regulating glutamatergic synapse number*. *Neuron*, 2007. **56**(1): p. 58-65.
40. Chang, Q., et al., *The disease progression of Mecp2 mutant mice is affected by the level of BDNF expression*. *Neuron*, 2006. **49**(3): p. 341-8.
41. Ogier, M., et al., *Brain-derived neurotrophic factor expression and respiratory function improve after ampakine treatment in a mouse model of Rett syndrome*. *J Neurosci*, 2007. **27**(40): p. 10912-7.
42. Kline, D.D., et al., *Exogenous brain-derived neurotrophic factor rescues synaptic dysfunction in Mecp2-null mice*. *J Neurosci*, 2010. **30**(15): p. 5303-10.
43. Lonetti, G., et al., *Early environmental enrichment moderates the behavioral and synaptic phenotype of MeCP2 null mice*. *Biol Psychiatry*, 2010. **67**(7): p. 657-65.
44. Marfella, C.G. and A.N. Imbalzano, *The Chd family of chromatin remodelers*. *Mutat Res*, 2007. **618**(1-2): p. 30-40.
45. Sakamoto, I., et al., *A novel beta-catenin-binding protein inhibits beta-catenin-dependent Tcf activation and axis formation*. *J Biol Chem*, 2000. **275**(42): p. 32871-8.
46. Okerlund, N.D. and B.N. Cheyette, *Synaptic Wnt signaling-a contributor to major psychiatric disorders?* *J Neurodev Disord*, 2011. **3**(2): p. 162-74.
47. Durak, O., et al., *Chd8 mediates cortical neurogenesis via transcriptional regulation of cell cycle and Wnt signaling*. *Nat Neurosci*, 2016. **19**(11): p. 1477-1488.
48. Nishiyama, M., et al., *Early embryonic death in mice lacking the beta-catenin-binding protein Duplin*. *Mol Cell Biol*, 2004. **24**(19): p. 8386-94.

49. Nishiyama, M., et al., *CHD8 suppresses p53-mediated apoptosis through histone H1 recruitment during early embryogenesis*. Nat Cell Biol, 2009. **11**(2): p. 172-82.
50. Xu, Q., et al., *Autism-associated CHD8 deficiency impairs axon development and migration of cortical neurons*. Mol Autism, 2018. **9**: p. 65.
51. Platt, R.J., et al., *Chd8 Mutation Leads to Autistic-like Behaviors and Impaired Striatal Circuits*. Cell Rep, 2017. **19**(2): p. 335-350.
52. Jung, H., et al., *Sexually dimorphic behavior, neuronal activity, and gene expression in Chd8-mutant mice*. Nat Neurosci, 2018. **21**(9): p. 1218-1228.
53. Verkerk, A.J., et al., *Identification of a gene (FMR-1) containing a CGG repeat coincident with a breakpoint cluster region exhibiting length variation in fragile X syndrome*. Cell, 1991. **65**(5): p. 905-14.
54. Pieretti, M., et al., *Absence of expression of the FMR-1 gene in fragile X syndrome*. Cell, 1991. **66**(4): p. 817-22.
55. Darnell, J.C., et al., *FMRP stalls ribosomal translocation on mRNAs linked to synaptic function and autism*. Cell, 2011. **146**(2): p. 247-61.
56. Bassell, G.J. and S.T. Warren, *Fragile X syndrome: loss of local mRNA regulation alters synaptic development and function*. Neuron, 2008. **60**(2): p. 201-14.
57. Brouwer, J.R., et al., *Elevated Fmr1 mRNA levels and reduced protein expression in a mouse model with an unmethylated Fragile X full mutation*. Exp Cell Res, 2007. **313**(2): p. 244-53.
58. *Fmr1 knockout mice: a model to study fragile X mental retardation*. The Dutch-Belgian Fragile X Consortium. Cell, 1994. **78**(1): p. 23-33.
59. Mientjes, E.J., et al., *The generation of a conditional Fmr1 knock out mouse model to study Fmrp function in vivo*. Neurobiol Dis, 2006. **21**(3): p. 549-55.
60. Comery, T.A., et al., *Abnormal dendritic spines in fragile X knockout mice: maturation and pruning deficits*. Proc Natl Acad Sci U S A, 1997. **94**(10): p. 5401-4.

61. He, C.X. and C. Portera-Cailliau, *The trouble with spines in fragile X syndrome: density, maturity and plasticity*. Neuroscience, 2013. **251**: p. 120-8.
62. Cruz-Martin, A., M. Crespo, and C. Portera-Cailliau, *Delayed stabilization of dendritic spines in fragile X mice*. J Neurosci, 2010. **30**(23): p. 7793-803.
63. Pan, F., et al., *Dendritic spine instability and insensitivity to modulation by sensory experience in a mouse model of fragile X syndrome*. Proc Natl Acad Sci U S A, 2010. **107**(41): p. 17768-73.
64. Chung, L., A.L. Bey, and Y.H. Jiang, *Synaptic plasticity in mouse models of autism spectrum disorders*. Korean J Physiol Pharmacol, 2012. **16**(6): p. 369-78.
65. Sidorov, M.S., B.D. Auerbach, and M.F. Bear, *Fragile X mental retardation protein and synaptic plasticity*. Mol Brain, 2013. **6**: p. 15.
66. Godfraind, J.M., et al., *Long-term potentiation in the hippocampus of fragile X knockout mice*. Am J Med Genet, 1996. **64**(2): p. 246-51.
67. Paradee, W., et al., *Fragile X mouse: strain effects of knockout phenotype and evidence suggesting deficient amygdala function*. Neuroscience, 1999. **94**(1): p. 185-92.
68. Huber, K.M., et al., *Altered synaptic plasticity in a mouse model of fragile X mental retardation*. Proc Natl Acad Sci U S A, 2002. **99**(11): p. 7746-50.
69. Lauterborn, J.C., et al., *Brain-derived neurotrophic factor rescues synaptic plasticity in a mouse model of fragile X syndrome*. J Neurosci, 2007. **27**(40): p. 10685-94.
70. Lee, H.Y., et al., *Bidirectional regulation of dendritic voltage-gated potassium channels by the fragile X mental retardation protein*. Neuron, 2011. **72**(4): p. 630-42.
71. Pilpel, Y., et al., *Synaptic ionotropic glutamate receptors and plasticity are developmentally altered in the CA1 field of Fmr1 knockout mice*. J Physiol, 2009. **587**(Pt 4): p. 787-804.
72. Li, J., et al., *Reduced cortical synaptic plasticity and GluR1 expression associated with fragile X mental retardation protein deficiency*. Mol Cell Neurosci, 2002. **19**(2): p. 138-51.

73. Koekkoek, S.K., et al., *Deletion of FMR1 in Purkinje cells enhances parallel fiber LTD, enlarges spines, and attenuates cerebellar eyelid conditioning in Fragile X syndrome*. *Neuron*, 2005. **47**(3): p. 339-52.
74. Bear, M.F., K.M. Huber, and S.T. Warren, *The mGluR theory of fragile X mental retardation*. *Trends Neurosci*, 2004. **27**(7): p. 370-7.
75. Dolen, G., et al., *Correction of fragile X syndrome in mice*. *Neuron*, 2007. **56**(6): p. 955-62.
76. Michalon, A., et al., *Chronic pharmacological mGlu5 inhibition corrects fragile X in adult mice*. *Neuron*, 2012. **74**(1): p. 49-56.
77. Silverman, J.L., et al., *Negative allosteric modulation of the mGluR5 receptor reduces repetitive behaviors and rescues social deficits in mouse models of autism*. *Sci Transl Med*, 2012. **4**(131): p. 131ra51.
78. Castren, M.L. and E. Castren, *BDNF in fragile X syndrome*. *Neuropharmacology*, 2014. **76 Pt C**: p. 729-36.
79. Dahlhaus, R. and A. El-Husseini, *Altered neuroligin expression is involved in social deficits in a mouse model of the fragile X syndrome*. *Behav Brain Res*, 2010. **208**(1): p. 96-105.
80. Schutt, J., et al., *Fragile X mental retardation protein regulates the levels of scaffold proteins and glutamate receptors in postsynaptic densities*. *J Biol Chem*, 2009. **284**(38): p. 25479-87.
81. Smalley, S.L., et al., *Autism and tuberous sclerosis*. *J Autism Dev Disord*, 1992. **22**(3): p. 339-55.
82. *Identification and characterization of the tuberous sclerosis gene on chromosome 16*. *Cell*, 1993. **75**(7): p. 1305-15.
83. van Slegtenhorst, M., et al., *Identification of the tuberous sclerosis gene TSC1 on chromosome 9q34*. *Science*, 1997. **277**(5327): p. 805-8.
84. Tee, A.R., et al., *Tuberous sclerosis complex gene products, Tuberin and Hamartin, control mTOR signaling by acting as a GTPase-activating protein complex toward Rheb*. *Curr Biol*, 2003. **13**(15): p. 1259-68.

85. Fingar, D.C., et al., *Mammalian cell size is controlled by mTOR and its downstream targets S6K1 and 4EBP1/eIF4E*. *Genes Dev*, 2002. **16**(12): p. 1472-87.
86. Hoeffler, C.A. and E. Klann, *mTOR signaling: at the crossroads of plasticity, memory and disease*. *Trends Neurosci*, 2010. **33**(2): p. 67-75.
87. Kobayashi, T., et al., *A germ-line Tsc1 mutation causes tumor development and embryonic lethality that are similar, but not identical to, those caused by Tsc2 mutation in mice*. *Proc Natl Acad Sci U S A*, 2001. **98**(15): p. 8762-7.
88. Kwiatkowski, D.J., et al., *A mouse model of TSC1 reveals sex-dependent lethality from liver hemangiomas, and up-regulation of p70S6 kinase activity in Tsc1 null cells*. *Hum Mol Genet*, 2002. **11**(5): p. 525-34.
89. Wilson, C., et al., *A mouse model of tuberous sclerosis 1 showing background specific early post-natal mortality and metastatic renal cell carcinoma*. *Hum Mol Genet*, 2005. **14**(13): p. 1839-50.
90. Onda, H., et al., *Tsc2(+/-) mice develop tumors in multiple sites that express gelsolin and are influenced by genetic background*. *J Clin Invest*, 1999. **104**(6): p. 687-95.
91. Kobayashi, T., et al., *Renal carcinogenesis, hepatic hemangiomas, and embryonic lethality caused by a germ-line Tsc2 mutation in mice*. *Cancer Res*, 1999. **59**(6): p. 1206-11.
92. Bey, A.L. and Y.H. Jiang, *Overview of mouse models of autism spectrum disorders*. *Curr Protoc Pharmacol*, 2014. **66**: p. 5.66.1-26.
93. Tavazoie, S.F., et al., *Regulation of neuronal morphology and function by the tumor suppressors Tsc1 and Tsc2*. *Nat Neurosci*, 2005. **8**(12): p. 1727-34.
94. Bateup, H.S., et al., *Loss of Tsc1 in vivo impairs hippocampal mGluR-LTD and increases excitatory synaptic function*. *J Neurosci*, 2011. **31**(24): p. 8862-9.
95. Tang, G., et al., *Loss of mTOR-dependent macroautophagy causes autistic-like synaptic pruning deficits*. *Neuron*, 2014. **83**(5): p. 1131-43.
96. Auerbach, B.D., E.K. Osterweil, and M.F. Bear, *Mutations causing syndromic autism define an axis of synaptic pathophysiology*. *Nature*, 2011. **480**(7375): p. 63-8.

97. Weston, M.C., H. Chen, and J.W. Swann, *Loss of mTOR repressors Tsc1 or Pten has divergent effects on excitatory and inhibitory synaptic transmission in single hippocampal neuron cultures*. *Front Mol Neurosci*, 2014. **7**: p. 1.
98. Crino, P.B., *Evolving neurobiology of tuberous sclerosis complex*. *Acta Neuropathol*, 2013. **125**(3): p. 317-32.
99. Tang, S.J., et al., *A rapamycin-sensitive signaling pathway contributes to long-term synaptic plasticity in the hippocampus*. *Proc Natl Acad Sci U S A*, 2002. **99**(1): p. 467-72.
100. Sharma, A., et al., *Dysregulation of mTOR signaling in fragile X syndrome*. *J Neurosci*, 2010. **30**(2): p. 694-702.
101. Yasuda, S., et al., *Activation of Rheb, but not of mTORC1, impairs spine synapse morphogenesis in tuberous sclerosis complex*. *Sci Rep*, 2014. **4**: p. 5155.
102. Eng, C., *PTEN: one gene, many syndromes*. *Hum Mutat*, 2003. **22**(3): p. 183-98.
103. Butler, M.G., et al., *Subset of individuals with autism spectrum disorders and extreme macrocephaly associated with germline PTEN tumour suppressor gene mutations*. *J Med Genet*, 2005. **42**(4): p. 318-21.
104. Buxbaum, J.D., et al., *Mutation screening of the PTEN gene in patients with autism spectrum disorders and macrocephaly*. *Am J Med Genet B Neuropsychiatr Genet*, 2007. **144b**(4): p. 484-91.
105. Courchesne, E., R. Carper, and N. Akshoomoff, *Evidence of brain overgrowth in the first year of life in autism*. *Jama*, 2003. **290**(3): p. 337-44.
106. Fombonne, E., et al., *Microcephaly and macrocephaly in autism*. *J Autism Dev Disord*, 1999. **29**(2): p. 113-9.
107. Maehama, T. and J.E. Dixon, *The tumor suppressor, PTEN/MMAC1, dephosphorylates the lipid second messenger, phosphatidylinositol 3,4,5-trisphosphate*. *J Biol Chem*, 1998. **273**(22): p. 13375-8.
108. Potter, C.J., L.G. Pedraza, and T. Xu, *Akt regulates growth by directly phosphorylating Tsc2*. *Nat Cell Biol*, 2002. **4**(9): p. 658-65.

109. Inoki, K., et al., *TSC2 is phosphorylated and inhibited by Akt and suppresses mTOR signalling*. Nat Cell Biol, 2002. **4**(9): p. 648-57.
110. Di Cristofano, A., et al., *Pten is essential for embryonic development and tumour suppression*. Nat Genet, 1998. **19**(4): p. 348-55.
111. Suzuki, A., et al., *High cancer susceptibility and embryonic lethality associated with mutation of the PTEN tumor suppressor gene in mice*. Curr Biol, 1998. **8**(21): p. 1169-78.
112. Kwon, C.H., et al., *Pten regulates neuronal arborization and social interaction in mice*. Neuron, 2006. **50**(3): p. 377-88.
113. Napoli, E., et al., *Mitochondrial dysfunction in Pten haplo-insufficient mice with social deficits and repetitive behavior: interplay between Pten and p53*. PLoS One, 2012. **7**(8): p. e42504.
114. Lugo, J.N., et al., *Deletion of PTEN produces autism-like behavioral deficits and alterations in synaptic proteins*. Front Mol Neurosci, 2014. **7**: p. 27.
115. Tilot, A.K., et al., *Germline disruption of Pten localization causes enhanced sex-dependent social motivation and increased glial production*. Hum Mol Genet, 2014. **23**(12): p. 3212-27.
116. Fraser, M.M., et al., *Phosphatase and tensin homolog, deleted on chromosome 10 deficiency in brain causes defects in synaptic structure, transmission and plasticity, and myelination abnormalities*. Neuroscience, 2008. **151**(2): p. 476-88.
117. Luikart, B.W., et al., *Pten knockdown in vivo increases excitatory drive onto dentate granule cells*. J Neurosci, 2011. **31**(11): p. 4345-54.
118. Williams, M.R., et al., *Hyperactivity of newborn Pten knock-out neurons results from increased excitatory synaptic drive*. J Neurosci, 2015. **35**(3): p. 943-59.
119. Haws, M.E., et al., *PTEN knockdown alters dendritic spine/protrusion morphology, not density*. J Comp Neurol, 2014. **522**(5): p. 1171-90.
120. Wang, Y., A. Cheng, and M.P. Mattson, *The PTEN phosphatase is essential for long-term depression of hippocampal synapses*. Neuromolecular Med, 2006. **8**(3): p. 329-36.

121. Takeuchi, K., et al., *Dysregulation of synaptic plasticity precedes appearance of morphological defects in a Pten conditional knockout mouse model of autism*. Proc Natl Acad Sci U S A, 2013. **110**(12): p. 4738-43.
122. Sperow, M., et al., *Phosphatase and tensin homologue (PTEN) regulates synaptic plasticity independently of its effect on neuronal morphology and migration*. J Physiol, 2012. **590**(4): p. 777-92.
123. Peters, S.U., et al., *Autism in Angelman syndrome: implications for autism research*. Clin Genet, 2004. **66**(6): p. 530-6.
124. Kishino, T., M. Lalonde, and J. Wagstaff, *UBE3A/E6-AP mutations cause Angelman syndrome*. Nat Genet, 1997. **15**(1): p. 70-3.
125. Matsuura, T., et al., *De novo truncating mutations in E6-AP ubiquitin-protein ligase gene (UBE3A) in Angelman syndrome*. Nat Genet, 1997. **15**(1): p. 74-7.
126. Albrecht, U., et al., *Imprinted expression of the murine Angelman syndrome gene, Ube3a, in hippocampal and Purkinje neurons*. Nat Genet, 1997. **17**(1): p. 75-8.
127. Rougeulle, C., H. Glatt, and M. Lalonde, *The Angelman syndrome candidate gene, UBE3A/E6-AP, is imprinted in brain*. Nat Genet, 1997. **17**(1): p. 14-5.
128. Yamasaki, K., et al., *Neurons but not glial cells show reciprocal imprinting of sense and antisense transcripts of Ube3a*. Hum Mol Genet, 2003. **12**(8): p. 837-47.
129. Cook, E.H., Jr., et al., *Autism or atypical autism in maternally but not paternally derived proximal 15q duplication*. Am J Hum Genet, 1997. **60**(4): p. 928-34.
130. Glessner, J.T., et al., *Autism genome-wide copy number variation reveals ubiquitin and neuronal genes*. Nature, 2009. **459**(7246): p. 569-73.
131. Hogart, A., et al., *The comorbidity of autism with the genomic disorders of chromosome 15q11.2-q13*. Neurobiol Dis, 2010. **38**(2): p. 181-91.
132. Huibregtse, J.M., M. Scheffner, and P.M. Howley, *Cloning and expression of the cDNA for E6-AP, a protein that mediates the interaction of the human papillomavirus E6 oncoprotein with p53*. Mol Cell Biol, 1993. **13**(2): p. 775-84.

133. Mabb, A.M. and M.D. Ehlers, *Ubiquitination in postsynaptic function and plasticity*. *Annu Rev Cell Dev Biol*, 2010. **26**: p. 179-210.
134. Jiang, Y.H., et al., *Mutation of the Angelman ubiquitin ligase in mice causes increased cytoplasmic p53 and deficits of contextual learning and long-term potentiation*. *Neuron*, 1998. **21**(4): p. 799-811.
135. Miura, K., et al., *Neurobehavioral and electroencephalographic abnormalities in Ube3a maternal-deficient mice*. *Neurobiol Dis*, 2002. **9**(2): p. 149-59.
136. Smith, S.E., et al., *Increased gene dosage of Ube3a results in autism traits and decreased glutamate synaptic transmission in mice*. *Sci Transl Med*, 2011. **3**(103): p. 103ra97.
137. Dindot, S.V., et al., *The Angelman syndrome ubiquitin ligase localizes to the synapse and nucleus, and maternal deficiency results in abnormal dendritic spine morphology*. *Hum Mol Genet*, 2008. **17**(1): p. 111-8.
138. Yashiro, K., et al., *Ube3a is required for experience-dependent maturation of the neocortex*. *Nat Neurosci*, 2009. **12**(6): p. 777-83.
139. Miao, S., et al., *The Angelman syndrome protein Ube3a is required for polarized dendrite morphogenesis in pyramidal neurons*. *J Neurosci*, 2013. **33**(1): p. 327-33.
140. Weeber, E.J., et al., *Derangements of hippocampal calcium/calmodulin-dependent protein kinase II in a mouse model for Angelman mental retardation syndrome*. *J Neurosci*, 2003. **23**(7): p. 2634-44.
141. Sato, M. and M.P. Stryker, *Genomic imprinting of experience-dependent cortical plasticity by the ubiquitin ligase gene Ube3a*. *Proc Natl Acad Sci U S A*, 2010. **107**(12): p. 5611-6.
142. Pignatelli, M., et al., *Changes in mGlu5 receptor-dependent synaptic plasticity and coupling to homer proteins in the hippocampus of Ube3A hemizygous mice modeling angelman syndrome*. *J Neurosci*, 2014. **34**(13): p. 4558-66.
143. Greer, P.L., et al., *The Angelman Syndrome protein Ube3A regulates synapse development by ubiquitinating arc*. *Cell*, 2010. **140**(5): p. 704-16.

144. Hayrapetyan, V., et al., *Region-specific impairments in striatal synaptic transmission and impaired instrumental learning in a mouse model of Angelman syndrome*. Eur J Neurosci, 2014. **39**(6): p. 1018-25.
145. Kumar, S., A.L. Talis, and P.M. Howley, *Identification of HHR23A as a substrate for E6-associated protein-mediated ubiquitination*. J Biol Chem, 1999. **274**(26): p. 18785-92.
146. Mani, A., et al., *E6AP mediates regulated proteasomal degradation of the nuclear receptor coactivator amplified in breast cancer 1 in immortalized cells*. Cancer Res, 2006. **66**(17): p. 8680-6.
147. Mulherkar, S.A., J. Sharma, and N.R. Jana, *The ubiquitin ligase E6-AP promotes degradation of alpha-synuclein*. J Neurochem, 2009. **110**(6): p. 1955-64.
148. Louria-Hayon, I., et al., *E6AP promotes the degradation of the PML tumor suppressor*. Cell Death Differ, 2009. **16**(8): p. 1156-66.
149. Zaaroor-Regev, D., et al., *Regulation of the polycomb protein Ring1B by self-ubiquitination or by E6-AP may have implications to the pathogenesis of Angelman syndrome*. Proc Natl Acad Sci U S A, 2010. **107**(15): p. 6788-93.
150. Kuhnle, S., et al., *Role of the ubiquitin ligase E6AP/UBE3A in controlling levels of the synaptic protein Arc*. Proc Natl Acad Sci U S A, 2013. **110**(22): p. 8888-93.
151. Kim, S., et al., *Ube3a/E6AP is involved in a subset of MeCP2 functions*. Biochem Biophys Res Commun, 2013. **437**(1): p. 67-73.
152. Cao, C., et al., *Impairment of TrkB-PSD-95 signaling in Angelman syndrome*. PLoS Biol, 2013. **11**(2): p. e1001478.
153. Wallace, M.L., et al., *Maternal loss of Ube3a produces an excitatory/inhibitory imbalance through neuron type-specific synaptic defects*. Neuron, 2012. **74**(5): p. 793-800.
154. Durand, C.M., et al., *Mutations in the gene encoding the synaptic scaffolding protein SHANK3 are associated with autism spectrum disorders*. Nat Genet, 2007. **39**(1): p. 25-7.
155. Berkel, S., et al., *Mutations in the SHANK2 synaptic scaffolding gene in autism spectrum disorder and mental retardation*. Nat Genet, 2010. **42**(6): p. 489-91.

156. Sato, D., et al., *SHANK1 Deletions in Males with Autism Spectrum Disorder*. Am J Hum Genet, 2012. **90**(5): p. 879-87.
157. Bonaglia, M.C., et al., *Disruption of the ProSAP2 gene in a t(12;22)(q24.1;q13.3) is associated with the 22q13.3 deletion syndrome*. Am J Hum Genet, 2001. **69**(2): p. 261-8.
158. Wilson, H.L., et al., *Molecular characterisation of the 22q13 deletion syndrome supports the role of haploinsufficiency of SHANK3/PROSAP2 in the major neurological symptoms*. J Med Genet, 2003. **40**(8): p. 575-84.
159. Sheng, M. and E. Kim, *The Shank family of scaffold proteins*. J Cell Sci, 2000. **113** ( Pt 11): p. 1851-6.
160. Roussignol, G., et al., *Shank expression is sufficient to induce functional dendritic spine synapses in aspiny neurons*. J Neurosci, 2005. **25**(14): p. 3560-70.
161. Grabrucker, A.M., et al., *Concerted action of zinc and ProSAP/Shank in synaptogenesis and synapse maturation*. Embo j, 2011. **30**(3): p. 569-81.
162. Hung, A.Y., et al., *Smaller dendritic spines, weaker synaptic transmission, but enhanced spatial learning in mice lacking Shank1*. J Neurosci, 2008. **28**(7): p. 1697-708.
163. Silverman, J.L., et al., *Sociability and motor functions in Shank1 mutant mice*. Brain Res, 2011. **1380**: p. 120-37.
164. Wohr, M., et al., *Communication impairments in mice lacking Shank1: reduced levels of ultrasonic vocalizations and scent marking behavior*. PLoS One, 2011. **6**(6): p. e20631.
165. Sungur, A.O., et al., *Repetitive behaviors in the Shank1 knockout mouse model for autism spectrum disorder: developmental aspects and effects of social context*. J Neurosci Methods, 2014. **234**: p. 92-100.
166. Schmeisser, M.J., et al., *Autistic-like behaviours and hyperactivity in mice lacking ProSAP1/Shank2*. Nature, 2012. **486**(7402): p. 256-60.
167. Won, H., et al., *Autistic-like social behaviour in Shank2-mutant mice improved by restoring NMDA receptor function*. Nature, 2012. **486**(7402): p. 261-5.

168. Jiang, Y.H. and M.D. Ehlers, *Modeling autism by SHANK gene mutations in mice*. *Neuron*, 2013. **78**(1): p. 8-27.
169. Ey, E., et al., *The Autism ProSAP1/Shank2 mouse model displays quantitative and structural abnormalities in ultrasonic vocalisations*. *Behav Brain Res*, 2013. **256**: p. 677-89.
170. Wang, X., et al., *Transcriptional and functional complexity of Shank3 provides a molecular framework to understand the phenotypic heterogeneity of SHANK3 causing autism and Shank3 mutant mice*. *Mol Autism*, 2014. **5**: p. 30.
171. Wang, X., et al., *Altered mGluR5-Homer scaffolds and corticostriatal connectivity in a Shank3 complete knockout model of autism*. *Nat Commun*, 2016. **7**: p. 11459.
172. Drapeau, E., et al., *Behavioral Phenotyping of an Improved Mouse Model of Phelan-McDermid Syndrome with a Complete Deletion of the Shank3 Gene*. *eNeuro*, 2018. **5**(3).
173. Peça, J., et al., *Shank3 mutant mice display autistic-like behaviours and striatal dysfunction*. *Nature*, 2011. **472**(7344): p. 437-42.
174. Bozdagi, O., et al., *Haploinsufficiency of the autism-associated Shank3 gene leads to deficits in synaptic function, social interaction, and social communication*. *Mol Autism*, 2010. **1**(1): p. 15.
175. Wang, X., et al., *Synaptic dysfunction and abnormal behaviors in mice lacking major isoforms of Shank3*. *Hum Mol Genet*, 2011. **20**(15): p. 3093-108.
176. Jaramillo, T.C., et al., *Altered Striatal Synaptic Function and Abnormal Behaviour in Shank3 Exon4-9 Deletion Mouse Model of Autism*. *Autism Res*, 2016. **9**(3): p. 350-75.
177. Lee, J., et al., *Shank3-mutant mice lacking exon 9 show altered excitation/inhibition balance, enhanced rearing, and spatial memory deficit*. *Front Cell Neurosci*, 2015. **9**: p. 94.
178. Kouser, M., et al., *Loss of predominant Shank3 isoforms results in hippocampus-dependent impairments in behavior and synaptic transmission*. *J Neurosci*, 2013. **33**(47): p. 18448-68.
179. Duffney, L.J., et al., *Autism-like Deficits in Shank3-Deficient Mice Are Rescued by Targeting Actin Regulators*. *Cell Rep*, 2015. **11**(9): p. 1400-13.

180. Speed, H.E., et al., *Autism-Associated Insertion Mutation (InsG) of Shank3 Exon 21 Causes Impaired Synaptic Transmission and Behavioral Deficits*. J Neurosci, 2015. **35**(26): p. 9648-65.
181. Duffney, L.J., et al., *Shank3 deficiency induces NMDA receptor hypofunction via an actin-dependent mechanism*. J Neurosci, 2013. **33**(40): p. 15767-78.
182. Gauthier, J., et al., *Truncating mutations in NRXN2 and NRXN1 in autism spectrum disorders and schizophrenia*. Hum Genet, 2011. **130**(4): p. 563-73.
183. Camacho-Garcia, R.J., et al., *Rare variants analysis of neurexin-1beta in autism reveals a novel start codon mutation affecting protein levels at synapses*. Psychiatr Genet, 2013. **23**(6): p. 262-6.
184. Vaags, A.K., et al., *Rare deletions at the neurexin 3 locus in autism spectrum disorder*. Am J Hum Genet, 2012. **90**(1): p. 133-41.
185. Steinberg, K.M., et al., *Identification of rare X-linked neuroligin variants by massively parallel sequencing in males with autism spectrum disorder*. Mol Autism, 2012. **3**(1): p. 8.
186. Jamain, S., et al., *Mutations of the X-linked genes encoding neuroligins NLGN3 and NLGN4 are associated with autism*. Nat Genet, 2003. **34**(1): p. 27-9.
187. Feng, J., et al., *High frequency of neurexin 1beta signal peptide structural variants in patients with autism*. Neurosci Lett, 2006. **409**(1): p. 10-3.
188. Alarcon, M., et al., *Linkage, association, and gene-expression analyses identify CNTNAP2 as an autism-susceptibility gene*. Am J Hum Genet, 2008. **82**(1): p. 150-9.
189. Arking, D.E., et al., *A common genetic variant in the neurexin superfamily member CNTNAP2 increases familial risk of autism*. Am J Hum Genet, 2008. **82**(1): p. 160-4.
190. Karayannis, T., et al., *Cntnap4 differentially contributes to GABAergic and dopaminergic synaptic transmission*. Nature, 2014. **511**(7508): p. 236-40.
191. Tabuchi, K. and T.C. Sudhof, *Structure and evolution of neurexin genes: insight into the mechanism of alternative splicing*. Genomics, 2002. **79**(6): p. 849-59.

192. Ullrich, B., Y.A. Ushkaryov, and T.C. Sudhof, *Cartography of neuexins: more than 1000 isoforms generated by alternative splicing and expressed in distinct subsets of neurons*. *Neuron*, 1995. **14**(3): p. 497-507.
193. Treutlein, B., et al., *Cartography of neuexin alternative splicing mapped by single-molecule long-read mRNA sequencing*. *Proc Natl Acad Sci U S A*, 2014. **111**(13): p. E1291-9.
194. Ichtchenko, K., T. Nguyen, and T.C. Sudhof, *Structures, alternative splicing, and neuexin binding of multiple neuroligins*. *J Biol Chem*, 1996. **271**(5): p. 2676-82.
195. Bang, M.L. and S. Owczarek, *A matter of balance: role of neuexin and neuroligin at the synapse*. *Neurochem Res*, 2013. **38**(6): p. 1174-89.
196. Etherton, M.R., et al., *Mouse neuexin-1alpha deletion causes correlated electrophysiological and behavioral changes consistent with cognitive impairments*. *Proc Natl Acad Sci U S A*, 2009. **106**(42): p. 17998-8003.
197. Grayton, H.M., et al., *Altered social behaviours in neuexin 1alpha knockout mice resemble core symptoms in neurodevelopmental disorders*. *PLoS One*, 2013. **8**(6): p. e67114.
198. Dachtler, J., et al., *Deletion of alpha-neuexin II results in autism-related behaviors in mice*. *Transl Psychiatry*, 2014. **4**: p. e484.
199. Rabaneda, L.G., et al., *Neuexin dysfunction in adult neurons results in autistic-like behavior in mice*. *Cell Rep*, 2014. **8**(2): p. 338-46.
200. Penagarikano, O., et al., *Absence of CNTNAP2 leads to epilepsy, neuronal migration abnormalities, and core autism-related deficits*. *Cell*, 2011. **147**(1): p. 235-46.
201. Blundell, J., et al., *Neuroligin-1 deletion results in impaired spatial memory and increased repetitive behavior*. *J Neurosci*, 2010. **30**(6): p. 2115-29.
202. Blundell, J., et al., *Increased anxiety-like behavior in mice lacking the inhibitory synapse cell adhesion molecule neuroligin 2*. *Genes Brain Behav*, 2009. **8**(1): p. 114-26.
203. Wohr, M., et al., *Developmental delays and reduced pup ultrasonic vocalizations but normal sociability in mice lacking the postsynaptic cell adhesion protein neuroligin2*. *Behav Brain Res*, 2013. **251**: p. 50-64.

204. Radyushkin, K., et al., *Neuroigin-3-deficient mice: model of a monogenic heritable form of autism with an olfactory deficit*. Genes Brain Behav, 2009. **8**(4): p. 416-25.
205. Rothwell, P.E., et al., *Autism-associated neuroigin-3 mutations commonly impair striatal circuits to boost repetitive behaviors*. Cell, 2014. **158**(1): p. 198-212.
206. Jamain, S., et al., *Reduced social interaction and ultrasonic communication in a mouse model of monogenic heritable autism*. Proc Natl Acad Sci U S A, 2008. **105**(5): p. 1710-5.
207. El-Kordi, A., et al., *Development of an autism severity score for mice using Nlgn4 null mutants as a construct-valid model of heritable monogenic autism*. Behav Brain Res, 2013. **251**: p. 41-9.
208. Ju, A., et al., *Juvenile manifestation of ultrasound communication deficits in the neuroigin-4 null mutant mouse model of autism*. Behav Brain Res, 2014. **270**: p. 159-64.
209. Tabuchi, K., et al., *A neuroigin-3 mutation implicated in autism increases inhibitory synaptic transmission in mice*. Science, 2007. **318**(5847): p. 71-6.
210. Jaramillo, T.C., et al., *Autism-related neuroigin-3 mutation alters social behavior and spatial learning*. Autism Res, 2014. **7**(2): p. 264-72.
211. Graf, E.R., et al., *Neurexins induce differentiation of GABA and glutamate postsynaptic specializations via neuroigins*. Cell, 2004. **119**(7): p. 1013-26.
212. Scheiffele, P., et al., *Neuroigin expressed in nonneuronal cells triggers presynaptic development in contacting axons*. Cell, 2000. **101**(6): p. 657-69.
213. Chih, B., H. Engelman, and P. Scheiffele, *Control of excitatory and inhibitory synapse formation by neuroigins*. Science, 2005. **307**(5713): p. 1324-8.
214. Missler, M., et al., *Alpha-neurexins couple Ca<sup>2+</sup> channels to synaptic vesicle exocytosis*. Nature, 2003. **423**(6943): p. 939-48.
215. Varoqueaux, F., et al., *Neuroigins determine synapse maturation and function*. Neuron, 2006. **51**(6): p. 741-54.
216. Kwon, H.B., et al., *Neuroigin-1-dependent competition regulates cortical synaptogenesis and synapse number*. Nat Neurosci, 2012. **15**(12): p. 1667-74.

217. Etherton, M., et al., *Autism-linked neuroligin-3 R451C mutation differentially alters hippocampal and cortical synaptic function*. Proc Natl Acad Sci U S A, 2011. **108**(33): p. 13764-9.
218. Isshiki, M., et al., *Enhanced synapse remodelling as a common phenotype in mouse models of autism*. Nat Commun, 2014. **5**: p. 4742.
219. Budreck, E.C., et al., *Neuroligin-1 controls synaptic abundance of NMDA-type glutamate receptors through extracellular coupling*. Proc Natl Acad Sci U S A, 2013. **110**(2): p. 725-30.
220. Jung, S.Y., et al., *Input-specific synaptic plasticity in the amygdala is regulated by neuroligin-1 via postsynaptic NMDA receptors*. Proc Natl Acad Sci U S A, 2010. **107**(10): p. 4710-5.
221. Jedlicka, P., et al., *Neuroligin-1 regulates excitatory synaptic transmission, LTP and EPSP-spike coupling in the dentate gyrus in vivo*. Brain Struct Funct, 2015. **220**(1): p. 47-58.
222. Delattre, V., et al., *Nlgn4 knockout induces network hypo-excitability in juvenile mouse somatosensory cortex in vitro*. Sci Rep, 2013. **3**: p. 2897.
223. Cellot, G. and E. Cherubini, *Reduced inhibitory gate in the barrel cortex of Neuroligin3R451C knock-in mice, an animal model of autism spectrum disorders*. Physiol Rep, 2014. **2**(7).
224. Pizzarelli, R. and E. Cherubini, *Developmental regulation of GABAergic signalling in the hippocampus of neuroligin 3 R451C knock-in mice: an animal model of Autism*. Front Cell Neurosci, 2013. **7**: p. 85.
225. Foldy, C., R.C. Malenka, and T.C. Sudhof, *Autism-associated neuroligin-3 mutations commonly disrupt tonic endocannabinoid signaling*. Neuron, 2013. **78**(3): p. 498-509.
226. Meyer, G., et al., *The complexity of PDZ domain-mediated interactions at glutamatergic synapses: a case study on neuroligin*. Neuropharmacology, 2004. **47**(5): p. 724-33.

227. Arons, M.H., et al., *Autism-associated mutations in ProSAP2/Shank3 impair synaptic transmission and neurexin-neuroigin-mediated transsynaptic signaling*. J Neurosci, 2012. **32**(43): p. 14966-78.
228. Belmonte, M.K., et al., *Autism and abnormal development of brain connectivity*. J Neurosci, 2004. **24**(42): p. 9228-31.
229. Geschwind, D.H. and P. Levitt, *Autism spectrum disorders: developmental disconnection syndromes*. Curr Opin Neurobiol, 2007. **17**(1): p. 103-11.
230. Kana, R.K., et al., *Brain connectivity in autism*. Front Hum Neurosci, 2014. **8**: p. 349.
231. Minschew, N.J. and T.A. Keller, *The nature of brain dysfunction in autism: functional brain imaging studies*. Curr Opin Neurol, 2010. **23**(2): p. 124-30.
232. Vissers, M.E., M.X. Cohen, and H.M. Geurts, *Brain connectivity and high functioning autism: a promising path of research that needs refined models, methodological convergence, and stronger behavioral links*. Neurosci Biobehav Rev, 2012. **36**(1): p. 604-25.
233. Di Martino, A., et al., *The autism brain imaging data exchange: towards a large-scale evaluation of the intrinsic brain architecture in autism*. Mol Psychiatry, 2014. **19**(6): p. 659-67.
234. Uddin, L.Q., K. Supekar, and V. Menon, *Reconceptualizing functional brain connectivity in autism from a developmental perspective*. Front Hum Neurosci, 2013. **7**: p. 458.
235. Just, M.A., et al., *Cortical activation and synchronization during sentence comprehension in high-functioning autism: evidence of underconnectivity*. Brain, 2004. **127**(Pt 8): p. 1811-21.
236. Keown, C.L., et al., *Local functional overconnectivity in posterior brain regions is associated with symptom severity in autism spectrum disorders*. Cell Rep, 2013. **5**(3): p. 567-72.
237. Supekar, K., et al., *Brain hyperconnectivity in children with autism and its links to social deficits*. Cell Rep, 2013. **5**(3): p. 738-47.
238. Gunaydin, L.A., et al., *Natural neural projection dynamics underlying social behavior*. Cell, 2014. **157**(7): p. 1535-51.

239. Felix-Ortiz, A.C. and K.M. Tye, *Amygdala inputs to the ventral hippocampus bidirectionally modulate social behavior*. J Neurosci, 2014. **34**(2): p. 586-95.
240. Hulbert, S.W. and Y.H. Jiang, *Monogenic mouse models of autism spectrum disorders: Common mechanisms and missing links*. Neuroscience, 2016. **321**: p. 3-23.
241. Alexander, A.L., et al., *Diffusion tensor imaging of the corpus callosum in Autism*. Neuroimage, 2007. **34**(1): p. 61-73.
242. Sztainberg, Y. and H.Y. Zoghbi, *Lessons learned from studying syndromic autism spectrum disorders*. Nat Neurosci, 2016. **19**(11): p. 1408-1417.
243. Nadler, J.J., et al., *Automated apparatus for quantitation of social approach behaviors in mice*. Genes Brain Behav, 2004. **3**(5): p. 303-14.
244. Choleris, E., et al., *Microparticle-based delivery of oxytocin receptor antisense DNA in the medial amygdala blocks social recognition in female mice*. Proc Natl Acad Sci U S A, 2007. **104**(11): p. 4670-5.
245. Kudryavtseva, N.N., *Use of the "partition" test in behavioral and pharmacological experiments*. Neurosci Behav Physiol, 2003. **33**(5): p. 461-71.
246. Moretti, P., et al., *Abnormalities of social interactions and home-cage behavior in a mouse model of Rett syndrome*. Hum Mol Genet, 2005. **14**(2): p. 205-20.
247. Terranova, M.L. and G. Laviola, *Scoring of social interactions and play in mice during adolescence*. Curr Protoc Toxicol, 2005. **Chapter 13**: p. Unit13.10.
248. Winslow, J.T. and K.A. Miczek, *Habituation of aggression in mice: pharmacological evidence of catecholaminergic and serotonergic mediation*. Psychopharmacology (Berl), 1983. **81**(4): p. 286-91.
249. Scattoni, M.L., J. Crawley, and L. Ricceri, *Ultrasonic vocalizations: a tool for behavioural phenotyping of mouse models of neurodevelopmental disorders*. Neurosci Biobehav Rev, 2009. **33**(4): p. 508-15.
250. Deacon, R.M., *Assessing nest building in mice*. Nat Protoc, 2006. **1**(3): p. 1117-9.

251. Crawley, J.N., *Translational animal models of autism and neurodevelopmental disorders*. Dialogues Clin Neurosci, 2012. **14**(3): p. 293-305.
252. Moy, S.S., et al., *Development of a mouse test for repetitive, restricted behaviors: relevance to autism*. Behav Brain Res, 2008. **188**(1): p. 178-94.
253. Thomas, A., et al., *Marble burying reflects a repetitive and perseverative behavior more than novelty-induced anxiety*. Psychopharmacology (Berl), 2009. **204**(2): p. 361-73.
254. Gierut, J.J., T.E. Jacks, and K.M. Haigis, *Strategies to achieve conditional gene mutation in mice*. Cold Spring Harb Protoc, 2014. **2014**(4): p. 339-49.
255. Tsien, J.Z., et al., *Subregion- and cell type-restricted gene knockout in mouse brain*. Cell, 1996. **87**(7): p. 1317-26.
256. Metzger, D., et al., *Conditional site-specific recombination in mammalian cells using a ligand-dependent chimeric Cre recombinase*. Proc Natl Acad Sci U S A, 1995. **92**(15): p. 6991-5.
257. Sprengel, R. and M.T. Hasan, *Tetracycline-controlled genetic switches*. Handb Exp Pharmacol, 2007(178): p. 49-72.
258. Heldt, S.A. and K.J. Ressler, *The Use of Lentiviral Vectors and Cre/loxP to Investigate the Function of Genes in Complex Behaviors*. Front Mol Neurosci, 2009. **2**: p. 22.
259. Semprini, S., et al., *Cryptic loxP sites in mammalian genomes: genome-wide distribution and relevance for the efficiency of BAC/PAC recombineering techniques*. Nucleic Acids Res, 2007. **35**(5): p. 1402-10.
260. Yin, H., et al., *Genome editing with Cas9 in adult mice corrects a disease mutation and phenotype*. Nat Biotechnol, 2014. **32**(6): p. 551-3.
261. Wang, J., et al., *Generation of cell-type-specific gene mutations by expressing the sgRNA of the CRISPR system from the RNA polymerase II promoters*. Protein Cell, 2015. **6**(9): p. 689-92.
262. Fu, Y., et al., *High-frequency off-target mutagenesis induced by CRISPR-Cas nucleases in human cells*. Nat Biotechnol, 2013. **31**(9): p. 822-6.

263. Rubenstein, J.L. and M.M. Merzenich, *Model of autism: increased ratio of excitation/inhibition in key neural systems*. Genes Brain Behav, 2003. **2**(5): p. 255-67.
264. Gemelli, T., et al., *Postnatal loss of methyl-CpG binding protein 2 in the forebrain is sufficient to mediate behavioral aspects of Rett syndrome in mice*. Biol Psychiatry, 2006. **59**(5): p. 468-76.
265. Goffin, D., et al., *Cellular origins of auditory event-related potential deficits in Rett syndrome*. Nat Neurosci, 2014. **17**(6): p. 804-6.
266. Meng, X., et al., *Manipulations of MeCP2 in glutamatergic neurons highlight their contributions to Rett and other neurological disorders*. Elife, 2016. **5**.
267. Harrington, A.J., et al., *MEF2C regulates cortical inhibitory and excitatory synapses and behaviors relevant to neurodevelopmental disorders*. Elife, 2016. **5**.
268. Oaks, A.W., et al., *Cc2d1a Loss of Function Disrupts Functional and Morphological Development in Forebrain Neurons Leading to Cognitive and Social Deficits*. Cereb Cortex, 2016.
269. McMahon, J.J., et al., *Seizure-dependent mTOR activation in 5-HT neurons promotes autism-like behaviors in mice*. Neurobiol Dis, 2015. **73**: p. 296-306.
270. Bey, A.L., et al., *Brain region-specific disruption of Shank3 in mice reveals a dissociation for cortical and striatal circuits in autism-related behaviors*. Transl Psychiatry, 2018. **8**(1): p. 94.
271. Chao, H.T., et al., *Dysfunction in GABA signalling mediates autism-like stereotypies and Rett syndrome phenotypes*. Nature, 2010. **468**(7321): p. 263-9.
272. Ure, K., et al., *Restoration of Mecp2 expression in GABAergic neurons is sufficient to rescue multiple disease features in a mouse model of Rett syndrome*. Elife, 2016. **5**.
273. Yoo, T., et al., *GABA Neuronal Deletion of Shank3 Exons 14-16 in Mice Suppresses Striatal Excitatory Synaptic Input and Induces Social and Locomotor Abnormalities*. Front Cell Neurosci, 2018. **12**: p. 341.
274. Rudy, B., et al., *Three groups of interneurons account for nearly 100% of neocortical GABAergic neurons*. Dev Neurobiol, 2011. **71**(1): p. 45-61.

275. Ito-Ishida, A., et al., *Loss of MeCP2 in Parvalbumin-and Somatostatin-Expressing Neurons in Mice Leads to Distinct Rett Syndrome-like Phenotypes*. *Neuron*, 2015. **88**(4): p. 651-8.
276. He, L.J., et al., *Conditional deletion of Mecp2 in parvalbumin-expressing GABAergic cells results in the absence of critical period plasticity*. *Nat Commun*, 2014. **5**: p. 5036.
277. Rubinstein, M., et al., *Dissecting the phenotypes of Dravet syndrome by gene deletion*. *Brain*, 2015. **138**(Pt 8): p. 2219-33.
278. Samaco, R.C., et al., *Loss of MeCP2 in aminergic neurons causes cell-autonomous defects in neurotransmitter synthesis and specific behavioral abnormalities*. *Proc Natl Acad Sci U S A*, 2009. **106**(51): p. 21966-71.
279. Riday, T.T., et al., *Pathway-specific dopaminergic deficits in a mouse model of Angelman syndrome*. *J Clin Invest*, 2012. **122**(12): p. 4544-54.
280. Mulherkar, S.A. and N.R. Jana, *Loss of dopaminergic neurons and resulting behavioural deficits in mouse model of Angelman syndrome*. *Neurobiol Dis*, 2010. **40**(3): p. 586-92.
281. Rothwell, P.E., et al., *Autism-associated neuroligin-3 mutations commonly impair striatal circuits to boost repetitive behaviors*. *Cell*, 2014. **158**(1): p. 198-212.
282. Zhang, Y., et al., *Loss of MeCP2 in cholinergic neurons causes part of RTT-like phenotypes via  $\alpha 7$  receptor in hippocampus*. *Cell Res*, 2016. **26**(6): p. 728-42.
283. Clipperton-Allen, A.E., Y. Chen, and D.T. Page, *Autism-relevant behaviors are minimally impacted by conditional deletion of Pten in oxytocinergic neurons*. *Autism Res*, 2016. **9**(12): p. 1248-1262.
284. Ferguson, J.N., et al., *Social amnesia in mice lacking the oxytocin gene*. *Nat Genet*, 2000. **25**(3): p. 284-8.
285. Pobbe, R.L., et al., *Oxytocin receptor knockout mice display deficits in the expression of autism-related behaviors*. *Horm Behav*, 2012. **61**(3): p. 436-44.

286. Lazzari, V.M., et al., *Oxytocin modulates social interaction but is not essential for sexual behavior in male mice*. Behav Brain Res, 2013. **244**: p. 130-6.
287. Clipperton-Allen, A.E. and D.T. Page, *Pten haploinsufficient mice show broad brain overgrowth but selective impairments in autism-relevant behavioral tests*. Hum Mol Genet, 2014. **23**(13): p. 3490-505.
288. Mittleman, G., et al., *Cerebellar modulation of frontal cortex dopamine efflux in mice: relevance to autism and schizophrenia*. Synapse, 2008. **62**(7): p. 544-50.
289. Tsai, P.T., et al., *Autistic-like behaviour and cerebellar dysfunction in Purkinje cell Tsc1 mutant mice*. Nature, 2012. **488**(7413): p. 647-51.
290. Reith, R.M., et al., *Loss of Tsc2 in Purkinje cells is associated with autistic-like behavior in a mouse model of tuberous sclerosis complex*. Neurobiol Dis, 2013. **51**: p. 93-103.
291. Cupolillo, D., et al., *Autistic-Like Traits and Cerebellar Dysfunction in Purkinje Cell PTEN Knock-Out Mice*. Neuropsychopharmacology, 2016. **41**(6): p. 1457-66.
292. Peter, S., et al., *Dysfunctional cerebellar Purkinje cells contribute to autism-like behaviour in Shank2-deficient mice*. Nat Commun, 2016. **7**: p. 12627.
293. Ha, S., et al., *Cerebellar Shank2 Regulates Excitatory Synapse Density, Motor Coordination, and Specific Repetitive and Anxiety-Like Behaviors*. J Neurosci, 2016. **36**(48): p. 12129-12143.
294. Berger, J.M., T.T. Rohn, and J.T. Oxford, *Autism as the Early Closure of a Neuroplastic Critical Period Normally Seen in Adolescence*. Biol Syst Open Access, 2013. **1**.
295. McGraw, C.M., R.C. Samaco, and H.Y. Zoghbi, *Adult neural function requires MeCP2*. Science, 2011. **333**(6039): p. 186.
296. Lang, M., et al., *Rescue of behavioral and EEG deficits in male and female Mecp2-deficient mice by delayed Mecp2 gene reactivation*. Hum Mol Genet, 2014. **23**(2): p. 303-18.
297. Guy, J., et al., *Reversal of neurological defects in a mouse model of Rett syndrome*. Science, 2007. **315**(5815): p. 1143-7.
298. Robinson, L., et al., *Morphological and functional reversal of phenotypes in a mouse model of Rett syndrome*. Brain, 2012. **135**(Pt 9): p. 2699-710.

299. Silva-Santos, S., et al., *Ube3a reinstatement identifies distinct developmental windows in a murine Angelman syndrome model*. J Clin Invest, 2015. **125**(5): p. 2069-76.
300. Rabaneda, L.G., et al., *Neurexin dysfunction in adult neurons results in autistic-like behavior in mice*. Cell Rep, 2014. **8**(2): p. 338-46.
301. Mei, Y., et al., *Adult restoration of Shank3 expression rescues selective autistic-like phenotypes*. Nature, 2016. **530**(7591): p. 481-4.
302. Minichiello, L., et al., *Essential role for TrkB receptors in hippocampus-mediated learning*. Neuron, 1999. **24**(2): p. 401-14.
303. Gorski, J.A., et al., *Cortical excitatory neurons and glia, but not GABAergic neurons, are produced in the Emx1-expressing lineage*. J Neurosci, 2002. **22**(15): p. 6309-14.
304. Goebbels, S., et al., *Genetic targeting of principal neurons in neocortex and hippocampus of NEX-Cre mice*. Genesis, 2006. **44**(12): p. 611-21.
305. Vong, L., et al., *Leptin action on GABAergic neurons prevents obesity and reduces inhibitory tone to POMC neurons*. Neuron, 2011. **71**(1): p. 142-54.
306. Monory, K., et al., *The endocannabinoid system controls key epileptogenic circuits in the hippocampus*. Neuron, 2006. **51**(4): p. 455-66.
307. Hippenmeyer, S., et al., *A developmental switch in the response of DRG neurons to ETS transcription factor signaling*. PLoS Biol, 2005. **3**(5): p. e159.
308. Taniguchi, H., et al., *A resource of Cre driver lines for genetic targeting of GABAergic neurons in cerebral cortex*. Neuron, 2011. **71**(6): p. 995-1013.
309. Gong, S., et al., *Targeting Cre recombinase to specific neuron populations with bacterial artificial chromosome constructs*. J Neurosci, 2007. **27**(37): p. 9817-23.
310. Lindeberg, J., et al., *Transgenic expression of Cre recombinase from the tyrosine hydroxylase locus*. Genesis, 2004. **40**(2): p. 67-73.
311. Rossi, J., et al., *Melanocortin-4 receptors expressed by cholinergic neurons regulate energy balance and glucose homeostasis*. Cell Metab, 2011. **13**(2): p. 195-204.

312. Wu, Z., et al., *An obligate role of oxytocin neurons in diet induced energy expenditure*. PLoS One, 2012. 7(9): p. e45167.
313. Barski, J.J., K. Dethleffsen, and M. Meyer, *Cre recombinase expression in cerebellar Purkinje cells*. Genesis, 2000. 28(3-4): p. 93-8.
314. Zhang, X.M., et al., *Highly restricted expression of Cre recombinase in cerebellar Purkinje cells*. Genesis, 2004. 40(1): p. 45-51.
315. Kwon, C.H., et al., *Pten regulates neuronal soma size: a mouse model of Lhermitte-Duclos disease*. Nat Genet, 2001. 29(4): p. 404-11.
316. Hayashi, S. and A.P. McMahon, *Efficient recombination in diverse tissues by a tamoxifen-inducible form of Cre: a tool for temporally regulated gene activation/inactivation in the mouse*. Dev Biol, 2002. 244(2): p. 305-18.
317. Mayford, M., et al., *Control of memory formation through regulated expression of a CaMKII transgene*. Science, 1996. 274(5293): p. 1678-83.
318. Hulbert, S.W., A.L. Bey, and Y.H. Jiang, *Environmental enrichment has minimal effects on behavior in the Shank3 complete knockout model of autism spectrum disorder*. Brain Behav, 2018. 8(11): p. e01107.
319. Hulbert, S.W. and Y.H. Jiang, *Cellular and Circuitry Bases of Autism: Lessons Learned from the Temporospatial Manipulation of Autism Genes in the Brain*. Neurosci Bull, 2017. 33(2): p. 205-218.
320. Leblond, C.S., et al., *Meta-analysis of SHANK Mutations in Autism Spectrum Disorders: a gradient of severity in cognitive impairments*. PLoS Genet, 2014. 10(9): p. e1004580.
321. Moessner, R., et al., *Contribution of SHANK3 mutations to autism spectrum disorder*. Am J Hum Genet, 2007. 81(6): p. 1289-97.
322. Neale, B.M., et al., *Patterns and rates of exonic de novo mutations in autism spectrum disorders*. Nature, 2012. 485(7397): p. 242-5.

323. Sanders, S.J., et al., *De novo mutations revealed by whole-exome sequencing are strongly associated with autism*. *Nature*, 2012. **485**(7397): p. 237-41.
324. Bernier, R., et al., *Disruptive CHD8 mutations define a subtype of autism early in development*. *Cell*, 2014. **158**(2): p. 263-276.
325. O'Roak, B.J., et al., *Multiplex targeted sequencing identifies recurrently mutated genes in autism spectrum disorders*. *Science*, 2012. **338**(6114): p. 1619-22.
326. Soorya, L., et al., *Prospective investigation of autism and genotype-phenotype correlations in 22q13 deletion syndrome and SHANK3 deficiency*. *Mol Autism*, 2013. **4**(1): p. 18.
327. Sarasua, S.M., et al., *Clinical and genomic evaluation of 201 patients with Phelan-McDermid syndrome*. *Hum Genet*, 2014. **133**(7): p. 847-59.
328. Moy, S.S., et al., *Sociability and preference for social novelty in five inbred strains: an approach to assess autistic-like behavior in mice*. *Genes Brain Behav*, 2004. **3**(5): p. 287-302.
329. Constancia, M., G. Kelsey, and W. Reik, *Resourceful imprinting*. *Nature*, 2004. **432**(7013): p. 53-7.
330. Suetterlin, P., et al., *Altered Neocortical Gene Expression, Brain Overgrowth and Functional Over-Connectivity in Chd8 Haploinsufficient Mice*. *Cereb Cortex*, 2018. **28**(6): p. 2192-2206.
331. Gompers, A.L., et al., *Germline Chd8 haploinsufficiency alters brain development in mouse*. *Nat Neurosci*, 2017. **20**(8): p. 1062-1073.
332. Katayama, Y., et al., *CHD8 haploinsufficiency results in autistic-like phenotypes in mice*. *Nature*, 2016. **537**(7622): p. 675-679.
333. Estes, A., et al., *Long-Term Outcomes of Early Intervention in 6-Year-Old Children With Autism Spectrum Disorder*. *J Am Acad Child Adolesc Psychiatry*, 2015. **54**(7): p. 580-7.
334. Rogers, S.J., et al., *Effects of a brief Early Start Denver model (ESDM)-based parent intervention on toddlers at risk for autism spectrum disorders: a randomized controlled trial*. *J Am Acad Child Adolesc Psychiatry*, 2012. **51**(10): p. 1052-65.

335. Woo, C.C. and M. Leon, *Environmental enrichment as an effective treatment for autism: a randomized controlled trial*. Behav Neurosci, 2013. **127**(4): p. 487-97.
336. Woo, C.C., et al., *Environmental enrichment as a therapy for autism: A clinical trial replication and extension*. Behav Neurosci, 2015. **129**(4): p. 412-22.
337. Restivo, L., et al., *Enriched environment promotes behavioral and morphological recovery in a mouse model for the fragile X syndrome*. Proc Natl Acad Sci U S A, 2005. **102**(32): p. 11557-62.
338. Schneider, T., J. Turczak, and R. Przewłocki, *Environmental enrichment reverses behavioral alterations in rats prenatally exposed to valproic acid: issues for a therapeutic approach in autism*. Neuropsychopharmacology, 2006. **31**(1): p. 36-46.
339. Kondo, M., et al., *Environmental enrichment ameliorates a motor coordination deficit in a mouse model of Rett syndrome--Mecp2 gene dosage effects and BDNF expression*. Eur J Neurosci, 2008. **27**(12): p. 3342-50.
340. Nag, N., et al., *Environmental enrichment alters locomotor behaviour and ventricular volume in Mecp2 1lox mice*. Behav Brain Res, 2009. **196**(1): p. 44-8.
341. Kerr, B., et al., *Unconventional transcriptional response to environmental enrichment in a mouse model of Rett syndrome*. PLoS One, 2010. **5**(7): p. e11534.
342. Lacaria, M., et al., *Enriched rearing improves behavioral responses of an animal model for CNV-based autistic-like traits*. Hum Mol Genet, 2012. **21**(14): p. 3083-96.
343. Reynolds, S., M. Urruela, and D.P. Devine, *Effects of environmental enrichment on repetitive behaviors in the BTBR T+tf/J mouse model of autism*. Autism Res, 2013. **6**(5): p. 337-43.
344. Favre, M.R., et al., *Predictable enriched environment prevents development of hyper-emotionality in the VPA rat model of autism*. Front Neurosci, 2015. **9**: p. 127.
345. Oddi, D., et al., *Early social enrichment rescues adult behavioral and brain abnormalities in a mouse model of fragile X syndrome*. Neuropsychopharmacology, 2015. **40**(5): p. 1113-22.

346. Garbugino, L., E. Centofante, and F.R. D'Amato, *Early Social Enrichment Improves Social Motivation and Skills in a Monogenic Mouse Model of Autism, the Oprm1 (-/-) Mouse*. *Neural Plast*, 2016. **2016**: p. 5346161.
347. Yamaguchi, H., et al., *Environmental enrichment attenuates behavioral abnormalities in valproic acid-exposed autism model mice*. *Behav Brain Res*, 2017. **333**: p. 67-73.
348. Boccuto, L., et al., *Prevalence of SHANK3 variants in patients with different subtypes of autism spectrum disorders*. *Eur J Hum Genet*, 2013. **21**(3): p. 310-6.
349. Zhou, Y., et al., *Mice with Shank3 Mutations Associated with ASD and Schizophrenia Display Both Shared and Distinct Defects*. *Neuron*, 2016. **89**(1): p. 147-62.
350. Jaramillo, T.C., et al., *Novel Shank3 mutant exhibits behaviors with face validity for autism and altered striatal and hippocampal function*. *Autism Res*, 2017. **10**(1): p. 42-65.
351. Drapeau, E., et al., *Absence of strong strain effects in behavioral analyses of Shank3-deficient mice*. *Dis Model Mech*, 2014. **7**(6): p. 667-81.
352. Baker, K.B., et al., *Male and female Fmr1 knockout mice on C57 albino background exhibit spatial learning and memory impairments*. *Genes Brain Behav*, 2010. **9**(6): p. 562-74.
353. Dobkin, C., et al., *Fmr1 knockout mouse has a distinctive strain-specific learning impairment*. *Neuroscience*, 2000. **100**(2): p. 423-9.
354. Errijgers, V., et al., *Effect of genetic background on acoustic startle response in fragile X knockout mice*. *Genet Res (Camb)*, 2008. **90**(4): p. 341-5.
355. Pietropaolo, S., et al., *Genetic-background modulation of core and variable autistic-like symptoms in Fmr1 knock-out mice*. *PLoS One*, 2011. **6**(2): p. e17073.
356. Spencer, C.M., et al., *Modifying behavioral phenotypes in Fmr1KO mice: genetic background differences reveal autistic-like responses*. *Autism Res*, 2011. **4**(1): p. 40-56.
357. Laviola, G., et al., *Effects of enriched environment on animal models of neurodegenerative diseases and psychiatric disorders*. *Neurobiol Dis*, 2008. **31**(2): p. 159-68.
358. Phelan, K. and H.E. McDermid, *The 22q13.3 Deletion Syndrome (Phelan-McDermid Syndrome)*. *Mol Syndromol*, 2012. **2**(3-5): p. 186-201.

359. Neul, J.L., et al., *Rett syndrome: revised diagnostic criteria and nomenclature*. *Ann Neurol*, 2010. **68**(6): p. 944-50.
360. Nithianantharajah, J. and A.J. Hannan, *Enriched environments, experience-dependent plasticity and disorders of the nervous system*. *Nat Rev Neurosci*, 2006. **7**(9): p. 697-709.
361. Sonzogni, M., et al., *Delayed loss of UBE3A reduces the expression of Angelman syndrome-associated phenotypes*. *Mol Autism*, 2019. **10**: p. 23.
362. Gu, B., et al., *Ube3a reinstatement mitigates epileptogenesis in Angelman syndrome model mice*. *J Clin Invest*, 2019. **129**(1): p. 163-168.
363. Patel, S.H., et al., *Low-dose tamoxifen treatment in juvenile males has long-term adverse effects on the reproductive system: implications for inducible transgenics*. *Sci Rep*, 2017. **7**(1): p. 8991.
364. Speed, H.E., et al., *Apparent Genetic Rescue of Adult Shank3 Exon 21 Insertion Mutation Mice Tempered by Appropriate Control Experiments*. *eNeuro*, 2019.
365. Tu, Z., et al., *CRISPR/Cas9-mediated disruption of SHANK3 in monkey leads to drug-treatable autism-like symptoms*. *Hum Mol Genet*, 2019. **28**(4): p. 561-571.
366. Zhou, Y., et al., *Atypical behaviour and connectivity in SHANK3-mutant macaques*. *Nature*, 2019. **570**(7761): p. 326-331.

## Biography

Samuel William Hulbert earned a Bachelor's of Science in Neuroscience from Furman University in 2013. Samuel was awarded a Dennis Weatherstone Predoctoral Fellowship from Autism Speaks in 2015 for this research. Samuel is proud of all of the work he has done during his time in graduate school, despite dealing with cancer and significant side effects from treatment. After graduation, he hopes to become a physician scientist and continue to help advance science and medicine. So far, Samuel has contributed to the following publications:

Xu Q, Liu YY, Wang X, Tan GH, Li HP, **Hulbert SW**, Li CY, Hu CC, Xiong ZQ, Xu X, Jiang YH. Autism-associated CHD8 deficiency impairs axon development and migration of cortical neurons. *Mol Autism*. 2018 Dec 19; 9:65.

**Hulbert SW**, Bey AL, Jiang YH. Environmental enrichment has minimal effects on behavior in the Shank3 complete knockout model of autism spectrum disorder. *Brain Behav*. 2018 Nov; 8(11):e01107.

Bey AL, Wang X, Yan H, Kim N, Passman RL, Yang Y, Cao X, Towers AJ, **Hulbert SW**, Duffney LJ, Gaidis E, Rodriguiz RM, Wetsel WC, Yin HH, Jiang YH. Brain region-specific disruption of Shank3 in mice reveals a dissociation for cortical and striatal circuits in autism-related behaviors. *Transl Psychiatry*. 2018 Apr 27; 8(1):94.

Ray TA, Roy S, Kozlowski C, Wang J, Cafaro J, **Hulbert SW**, Wright CV, Field GD, Kay JN. Formation of retinal direction-selective circuitry initiated by starburst amacrine cell homotypic contact. *Elife*. 2018 Apr 3; 7.

**Hulbert SW**, Jiang YH. Cellular and Circuitry Bases of Autism: Lessons Learned from the Temporospatial Manipulation of Autism Genes in the Brain. *Neurosci Bull*. 2017 Apr; 33(2):205-218.

Kim Y, Lee HM, Xiong Y, Sciaky N, Hulbert SW, Cao X, Everitt JI, Jin J, Roth BL, Jiang YH. Targeting the histone methyltransferase G9a activates imprinted genes and improves survival of a mouse model of Prader-Willi syndrome. *Nat Med*. 2017 Feb; 23(2):213-222.

Wang X, Bey AL, Katz BM, Badea A, Kim N, David LK, Duffney LJ, Kumar S, Mague SD, **Hulbert SW**, Dutta N, Hayrapetyan V, Yu C, Gaidis E, Zhao S, Ding JD, Xu Q, Chung L, Rodriguiz RM, Wang F, Weinberg RJ, Wetsel WC, Dzirasa K, Yin H, Jiang YH. Altered mGluR5-Homer scaffolds and corticostriatal connectivity in a Shank3 complete knockout model of autism. *Nat Commun*. 2016 May 10; 7:11459.

**Hulbert SW**, Jiang YH. Monogenic mouse models of autism spectrum disorders: Common mechanisms and missing links. *Neuroscience*. 2016 May 3; 321:3-23.